LOW TEMPERATURE OZONATION OF CANADIAN ATHABASCA BITUMEN

by

Sima Hendessi

A thesis submitted in partial fulfillment of the requirements for the degree of

Master of Science

in

Chemical Engineering

Department of Chemical and Materials Engineering
University of Alberta

ABSTRACT

In this work, low temperature ozonation of Canadian Athabasca bitumen with ozone-enriched air in the temperature range of 140 to 160°C was investigated. Due to the resonance hybrid structure of ozone, it reacts directly and indirectly with the hydrocarbon molecules. Indirect ozone reaction mechanism involves free radical addition reactions similar to oxidation and leads to the observed increase in the viscosity and hardness of the ozonized bitumen. However, direct reaction mechanism of ozone involves possible ring-opening of cyclic hydrocarbons during ozonation. Of particular interest were the ring-cleavage reactions taking place during ozonation. A model compound ozonation study at 130°C showed that although ozonation of naphthenic-aromatic and heterocyclic compound classes present in oil sands bitumen resulted in moderate conversion of parent compounds to the ozonation products (except indene which had the highest ozonation conversion), these compound classes are primarily responsible for free radical addition reactions during ozonation. Ozonation of aromatic and acyclic paraffinic hydrocarbons resulted in relatively low ozonation conversion and no addition products were formed. Naphthenic and alkylaromatic compounds had relatively high ozonation conversion, and very low tendency to form addition reaction products. Ring-cleavage reaction products were formed during ozonation of aromatic, naphthenic-aromatic and heterocyclic compound classes. The aforementioned results of model compound classes ozonation could be applied to explain the bitumen ozonation results. A comparison between viscosity of ozonized and oxidized bitumen revealed that the increase in the bitumen viscosity and hardness in ozonation was relatively lower than oxidation using pure oxygen under the same reaction condition which might be due to the higher partial pressure of the oxidant leading to an increased rate of oxidation. In bitumen ozonation, ring-cleavage reactions happened as a result of direct reaction mechanism of ozone.

Keywords: Oil sands bitumen, ozonation, hardness, free radical addition reaction, ring-cleavage reaction.

ACKNOWLEDGMENT

TABLE OF CONTENTS

LIST OF TABLES

LIST OF FIGURES

1. INTRODUCTION

1.1 Background

The largest reserves of oil sands bitumen, which is a potential source of crude oil, are located in Alberta province, Canada. [1][2] Three major deposits of oil sands are located in the Athabasca, Cold Lake and Peace River deposits. [3][4] Oil sands bitumen is a very complex combination of various organic compounds consisting large number of high molecular weight hydrocarbons. [2][5] Due to high viscosity (10,000 mPa s to over 1,000,000 mPa s), high density and low fluidity properties, it is difficult to transport bitumen and it tends to cause problems such as blockage of extraction and transport pipes. [2][6][7][8][9][10] Bitumen contains mostly residue boiling material which can be upgraded and converted to high-value products after production. [7][11][12][13] There is a growing interest in the utilization of heavy oil and bitumen resources to produce refined fuels and petrochemicals by upgrading. [14][15][16]

Currently, the high viscosity of bitumen requires the addition of a solvent in order to allow their production and transportation through pipelines over a significant distance. The present commercial upgrading methods, such as thermal conversion or coking, catalytic conversion, distillation and hydrotreating have been found to be less effective when applied to small-scale field operations. They also require considerable energy input. [7][15][17][18][19][20][21] Alternatively field operations have to rely on solvents to facilitate heavy oil and bitumen flow through pipeline. Recovery and upgrading of bitumen must involve a minimum of expense to be economically attractive. [7][17][21][22][23] The cost of suitable solvents and expected increased production of heavy crude oil has led to the investigation of new methods for field upgrading. [24]

Upgrading of heavy oil and bitumen at the production site (*in-situ* upgrading) will significantly save on the costs, including diluents. [7][25]
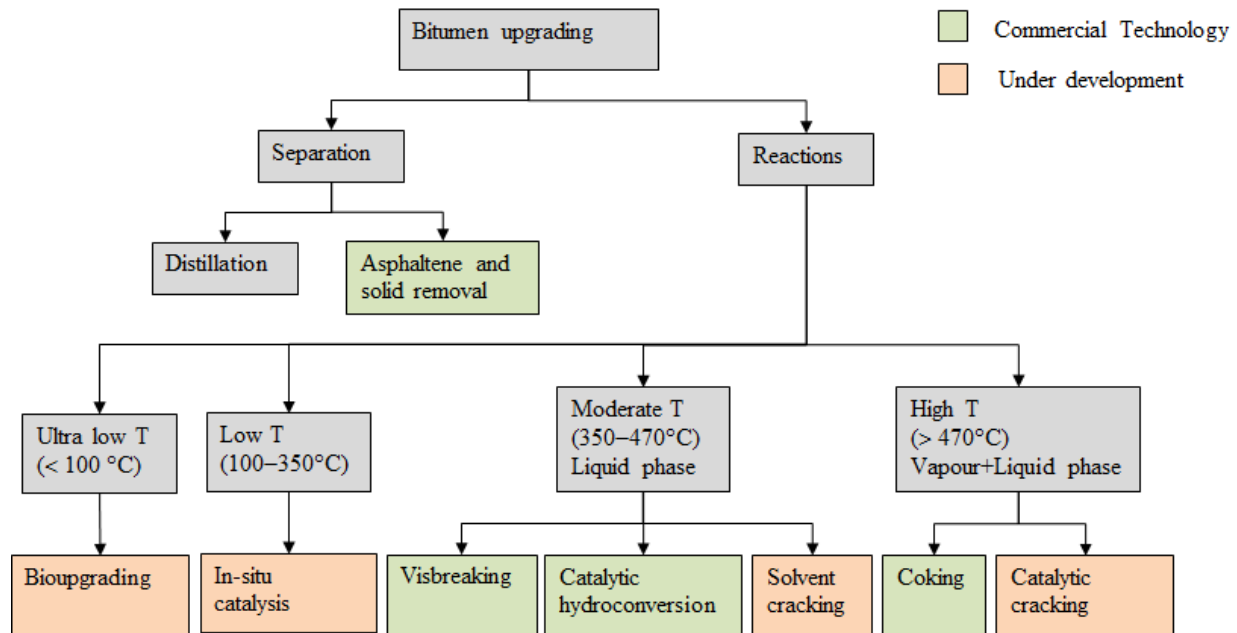
Figure 1.1. Commercial and under development upgrading technologies for heavy oil and bitumen [26]

The present methods used for reducing viscosity and upgrading of heavy oil and bitumen are cost intensive. As mentioned earlier, an upgrading method using inexpensive chemicals and involving simple chemical reactions to modify bitumen is highly desirable. [3]

One of the upgrading methods of heavy oil and bitumen is microbial oil upgrading which relies on microorganisms called methanogens. The methanogens can convert the bitumen into methane, which does not have poor fluidity and can be readily recovered and transported by pipeline. The reason for selecting this method over the other ones is its associated advantages, including that microorganisms do not consume large amount of energy, they are independent of the price of crude oil compared to other methods, and also the produced methane using this method can be more easily recovered and transported compared to bitumen. [1] This is not likely to be a profitable approach when gas prices are low (as it currently is). The research has a longer term vision.

Several studies have been conducted on the conversion of hydrocarbon compounds using methanogens. [27][28][29] Majority of them concluded that direct degradation of heavy fractions is a slow process under anaerobic condition.

In the process that is the topic of the present investigation, bitumen is converted to methane in two steps. [1] The first step is the *in-situ* oxidation of bitumen to convert large molecules into smaller fragments, which are more suitable for methanogenic conversion. [24] The second step is the introduction of methanogens into bitumen and conversion of the biodegradable fragments formed in the previous step into methane and carbon dioxide using microorganisms under anaerobic conversion. Methanogens can only consume a very limited range of substances, i.e., simple compounds with one or two carbons such as methanol, dissolved carbon dioxide and dissolved hydrogen gas, to grow and produce methane. [30][31] The purpose of oxidation in the first step is to overcome some of the limitations of the microorganisms regarding their attack on large molecules of bitumen by converting the bitumen into smaller oxidized fragments. This study deals only with the first step of the methanogenic conversion method which is conversion of bitumen into lighter biodegradable fragments using an oxidizing agent.

Oxidation of the bitumen components by air or oxygen as an oxidizing agent is feasible, yet the required temperature for conversion of bitumen to significant amounts of water-soluble low molecular weight substrates is high. [23][32][33] Of more concern are reports of oxidative hardening even at moderate to low temperatures of oxidation. Moschopedis claimed that bitumen oxidation reactions with air or oxygen at elevated temperatures (150-250 °C) had an adverse effect and led to formation of more complex compounds with higher molecular weight. [23] According to previous work done in our research group, oxidation using air as oxidant formed addition products by cross-linking the cyclic hydrocarbons and caused an increase in the bitumen viscosity which led to bitumen hardening. [33] Bitumen hardening is one of the major obstacles in achieving the purpose of the oxidation step in the process, which is microbial digestion of the oxidized products.

Recently, ozone application in different industries such as air, water and wastewater treatment; in food industry; and chemical and pharmaceutical industries has extremely increased because it is a powerful oxidizing agent with a rapid reaction rate. Due to high reactivity of ozone, it is a very well-known oxidizing agent for a variety of applications. [9][34] However, converting heavy

hydrocarbons like heavy oil and bitumen to more useful products by ozonation has not been extensively studied. [1][20][35][36][37] Currently, ozonation is being considered as one possible way for conversion of large molecules of oil sands bitumen to smaller fragments. Ozonation of bitumen generates smaller compounds containing oxygenate functional groups such as carboxyl (R-(C=O)-OH) and carbonyl (R-(C=O)-R′) groups. [11][35][38] Due to the resonance hybrid structure of ozone and its molecular electronic configuration, it reacts directly and indirectly with the hydrocarbon molecules. Indirect ozone reaction mechanism involves free radical addition reactions similar to oxidation and leads to the observed increase in the viscosity and hardness of the ozonized bitumen. However, direct reaction mechanism of ozone involves possible ring-opening of cyclic hydrocarbons during ozonation, which leads to formation of smaller molecules.

In this research, the feasibility of converting heavy hydrocarbons in Athabasca bitumen to lighter useful products through ozonation has been investigated. The main objective of the project was to develop a feasible and economical oxidative pathway to convert oil sands bitumen to water soluble products with lower viscosity which afterwards can be converted by microbial degradation.

1.2 Objective and scope of work

1.2.1 Objectives

- Investigating the possibility of ring-cleavage reactions in ring-containing hydrocarbons, e.g., aromatic and naphthenic class compounds, which are dominant in bitumen, by treatment using ozone-enriched air as an oxidizing agent at relatively mild temperature and low gas flow rate.

- Establishing the nature of the reactions happening during low temperature ozonation of ring-containing model compounds and get an insight into the ring-cleavage reactions as well as hardening mechanism of bitumen due to ozonation.

- Determining whether or not the hypothesis that the high viscosity observed after 6 h ozonation of bitumen at low temperatures (140, 150 and 160 °C) is caused by free radical addition or polymerization reactions.

- Comparing the extent of hardening phenomenon and increase in the bitumen viscosity in low temperature ozonation, oxidation using air as the oxidant, and oxidation using pure oxygen as the oxidant.

- Getting a better understanding of the causes of bitumen hardening due to low temperature ozonation and to suggest a way to overcome this problem.

1.2.2 Scope of work

The low temperature oxidation of Alberta oil sands bitumen using air as an oxidant was previously investigated in our research group, which did not have the desired outcome, and analyses showed a negligible conversion of large and heavy molecules of bitumen into smaller fragments due to oxidation. [33] In the current work, the feasibility of converting heavy hydrocarbons to lighter useful products through ozonation has been investigated. For this purpose, this study is divided into two parts. The first part of the study deals with low temperature ozonation of selected hydrocarbon compound classes found in oil sands bitumen, at low ozone-enriched air flow rate as the oxidizing agent. Then it goes through analyses of the ozonation products utilizing different techniques and instruments including gas chromatography-mass spectroscopy (GC-MS), gas chromatography equipped with flame ionization detector (GC-FID), Fourier transform infrared (FTIR) spectroscopy, refractometer, density meter, thermogravimetric analyzer (TGA), differential scanning calorimeter (DSC), and comparison of the results obtained for different hydrocarbon classes. Afterward, calculations of ozonation conversion and selectivity of the process toward ozonation reaction products, and comparison of the results for different hydrocarbon classes are presented.

The second part of the study evaluates oxidation using air, oxidation using pure oxygen and ozonation of Athabasca bitumen at low temperatures (140, 150 and 160 °C) and low oxidizing gas flow rate. Then it goes through comparison of the measured viscosity, penetration and refractive index for the products. Then the results obtained by FTIR and DSC for the bitumen feed as well as ozonized bitumen samples after 6 h ozonation at different temperatures are presented. Finally, the results obtained by hydrogen nuclear magnetic resonance (^{1}H NMR) spectroscopy for the ozonized bitumen samples are presented.

2. LITERATURE REVIEW AND THEORY

2.1   Introduction

This chapter provides an overview of the basics of bitumen ozonation. For this purpose, it has been divided into four sections. The first section discusses the efforts made so far in determining the composition of Athabasca bitumen with the focus of getting an insight into the types of hydrocarbon class compounds in Athabasca bitumen and their approximate relative abundance. The second section gives a brief description on bitumen oxidation, bitumen hardening phenomenon caused by oxidation and the probable causes of hardening. The third section goes through a brief description of the ozonation chemistry. In this section, chemical reactions of different classes of compounds taking place in the ozonation process are addressed. Finally the forth section describes how ozonation is a preferred process to alternative processes in order to improve the current technologies. It also presents the previous research attempts to perform ozonation on Alberta oil sands bitumen (AOSB).

In general, this chapter intends to give a better understanding of the complicated molecular structure of bitumen, bitumen oxidation and ozonation, and the nature of the reactions happening during ozonation.

2.2   Bitumen: composition and structure of its molecular compounds

The Alberta oil sands contain bitumen, which is semi-solid at ambient temperature, and it is one of the most complex compounds, which is known to consist of a large number of organic molecules. [39][40]

Solubility characterization of bitumen categorizes the compounds in two groups: asphaltenes and maltenes. Maltenes is the deasphalted part of bitumen, which can in turn be structurally sub-classified into paraffinic, naphthenic and aromatic compounds. [41]

On average, bitumen is composed of 83.2% C, 10.4% H, 0.94% O, 0.36% N and 4.8% S. [42] The elemental composition of three major deposits of Alberta oil sands bitumen is presented in **Table 2.1**.

Table 2.1. Elemental composition of three major sources of Alberta oil sands bitumen [43]

Source	Weight % of bitumen				
	C	H	N	O	S
Athabasca	83.98	10.22	0.65	1.97	4.57
Peace River	81.68	9.98	0.14	2.08	5.60
Cold Lake	83.98	10.46	0.23	0.94	4.70

In another categorization of bitumen compounds based on chemical characterization and affinity, it can be divided into four classes of compounds, i.e., asphaltenes, saturates, aromatics and resins. This classification is based on a specific analytical separation involving column chromatography. The relative amount of these groups varies in different bitumens. [44][45] Deviation of the different categories in bitumen from three major source of bitumen deposits in Alberta are shown in **Table 2.2**.

Table 2.2. SARA analysis of three major sources of Alberta oil sands bitumen [46]

Source	Weight % of bitumen			
	Saturates	Aromatics	Resins	Asphaltenes
Athabasca	16.3	39.8	28.5	15.4
Peace River	20.8	41.1	22.1	16.0
Cold Lake	19.4	38.1	26.7	15.8

Although the number and the size of rings in a single fused ring system in bitumen is not known with certainty yet, NMR studies on Athabasca bitumen showed that 43% of the carbon is aromatic, 31% is aliphatic, and 26% is naphthenic. [44][47] Aromatic content of three major sources of Alberta oil sand bitumens are presented in **Table 2.3**.

Table 2.3. Aromatic contents of three major sources of Alberta oil sands bitumen, separated by USBM API-60 procedure [48][49][50]

Source	Weight % of bitumen			
	Monoaromatic	Diaromatic	Polyaromatic	Total
Athabasca	8.3	3.8	23.8	35.9
Peace River	8.1	3.6	24.4	36.1
Cold Lake	8.6	3.3	30.2	42.1

2.3   Bitumen oxidation and hardening phenomenon

Although conversion of the large molecules of bitumen feedstock to higher value smaller fragments is desirable, it is very difficult to achieve by oxidation. One of the major obstacles in achieving this purpose is bitumen hardening due to oxidation, which is accompanied by a significant increase in bitumen viscosity and a decrease in its penetration. Hardness or consistency of bitumen is defined in terms of penetration value and it is a vertical distance penetrated by a standard needle into the bitumen under specific conditions of load, time and temperature.

At temperatures below 250 °C, low temperature oxidation reactions are dominant in bitumen and the products are mainly oxygenated hydrocarbons. [51] Low temperature oxidation of bitumen (oxidation by air or oxygen as oxidizing agent) was considered as a potential and economical technique to make the process of converting bitumen to water soluble and biodegradable products viable. However, previous work performed on Cold Lake bitumen in our research group concluded that prolonged oxidation of oil sands bitumen at low temperatures (in the range of 130 to 160 °C) resulted in undesirable increase in the viscosity of bitumen. It was proposed that bitumen hardening and increase in the bitumen viscosity is caused by free radical addition reactions. [52]

During bitumen oxidation using air or oxygen as an oxidizing agent, the molecular weight of bitumen and its C:H ratio increases with the degree of oxidation, which is an indication of oxidative polymerization occurring during oxidation. [53] A study by Glozman and Akhmetova showed that the aromatic content of bitumen increases during oxidation and the number of aromatic rings in the molecule increases, which indicates that condensation and polymerization

occur in bitumen during oxidation. This result is consistent with the results obtained by [1] H NMR for oxidized bitumen samples after 6 h oxidation using air with the flow rate of 120 ml min^{-1} at 140, 150 and 160 °C in our research group. [53][54][55] Rudenskaya also claimed that with increasing oxidation and the accompanying increase of the molecular weight and degree of polymerization in bitumen, plasticity of bitumen will decrease, penetration will decrease and viscosity will increase. In general, oxidation of bitumen leads to an increase in the degree of condensation, aromatic content, molecular weight and bitumen density. [53][54][56]

Various surface and *in-situ* upgrading methods have been proposed for Athabasca bitumen involving reaction of bitumen with an oxygen containing gas. [57][58] The main products of bitumen oxidation are water and oxygenated hydrocarbons such as carboxylic acids, aldehydes, ketones, alcohols and organic peroxides. [57] But usually the products have heavy molecular weight and they are not desirable since the purpose of oxidation is to produce lower molecular weight oxidized compounds which are also biodegradable. [47][59]

It has clearly been shown in the literature over the past 40 years that low temperature oxidation of bitumen leads to a significant increase in the viscosity of bitumen when oxidized by air or oxygen as an oxidant. It has been reported that oxidation reactions with air or oxygen, resulted in the formation of more complex compounds with higher molecular weights. [60][61][62][63] It has also been reported that the chemistry that leads to hardening at low temperature oxidation is the same as the ones at higher temperatures, except the fact that it is much slower at lower temperatures. [64][65] The hardening of bitumen is caused by free radical addition reactions. [52] The free radical addition reactions form even heavier molecules than those present in the bitumen feed. Viscosity is usually positively correlated with molecular weight, thus increase in molecular weight is likely to lead to an increase in viscosity. [64]

2.4   Ozonation

Ozone is a molecule composed of three oxygen atoms, which is a highly reactive and powerful oxidizing agent. The structure of ozone molecule can be described as a resonance hybrid that functions in chemical reactions as if the terminal oxygen atoms carry the positive and negative charge. [65][66][67][68][69] The four canonical forms of its structure are represented in **Figure 2.1**.
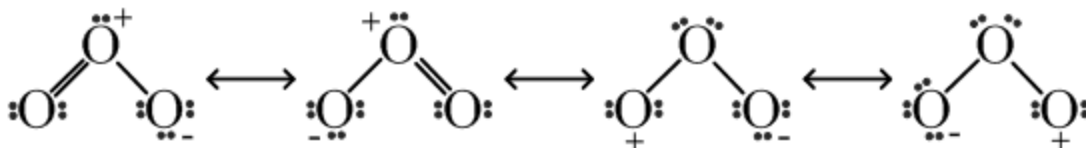
Figure 2.1. Structure of the ozone molecule as a resonance hybrid of the four canonical forms

Ozonation is the process of treating and converting organic compounds to more useable products, and it was invented by Christian Friedrich Schonbein in 1840. [70][71][72] The use of ozone in bitumen upgrading has sporadically appeared in the literature over the years, in which ozone has been used in conversion of oil sands bitumen into water-soluble derivatives. [73]

Ozone is highly reactive toward aliphatic multiple bonds and reacts only somewhat less readily with aromatic rings, degrading them eventually to low-molecular weight products, including glycolic, oxalic, and formic acids. The accepted reaction mechanism shown in **Figure 2.2** is that suggested by Criegee (1975) and Bailey (1978). [67][74] In this research, the feasibility of converting heavy hydrocarbons to lighter useful products through low temperature (below 250 °C) ozonation was of interest. Practically, ozone is generated from oxygen using the electrical discharge produced between two electrodes in a corona lamp. The process is described in **Equation 2.1** and **Equation 2.2**.

$$O_2 + e^-(high\ energy) \rightarrow 2O^\bullet + e^-(low\ energy) \hspace{3cm} \textbf{Equation 2.1}$$

$$O^\bullet + O_2 \rightarrow O_3 \hspace{5cm} \textbf{Equation 2.2}$$
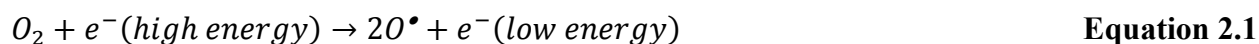
One of the disadvantages of ozonation using ozone-enriched air produced by an ozone-generator is that the yield of the ozone generator is low (0.02 to 3 wt % depending on corona lamp type and dry air feed flow rate) which leads to low concentration of ozone that can be used as oxidizing agent.
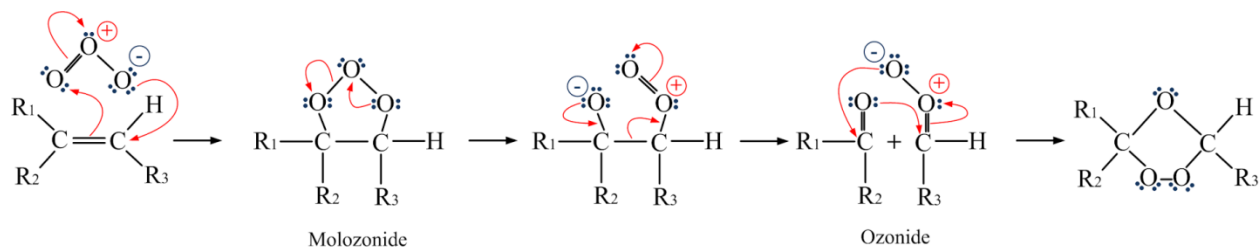
Figure 2.2. Criegee mechanism; 1,3-dipolar cycloaddition of ozone on unsaturated bonds and formation of highly reactive ozonide

Ozone oxidizes numerous hydrocarbon compounds through two reaction pathways: [69][70][74][75][76]

1. **Indirect reaction of ozone**, in which ozone breaks down to an oxygen molecule and an oxygen atom. This mechanism involves radical oxidation with atomic and molecular oxygen, to yield hydroxyl radical (free OH-radicals). Hydroxyl radicals are the species mainly responsible for the indirect reactions of ozone and it reacts fast and less selective than the direct reaction of ozone. [76][77] The reaction of saturated petroleum hydrocarbons with ozone, such as paraffins, aromatics and heteroatomic compounds with saturated fragments, undergoes free-radical chain oxidative transformations and forms carboxylic acids, carbonyl compounds, alcohols, and peroxides. [74][76][77][78] It is difficult or not possible to distinguish these products from normal autoxidation products.

2. **Direct reaction of ozone**, in which ozone reacts directly as molecular ozone with the hydrocarbon molecules. This mechanism is slow and selective. This reaction mechanism involves possible cleavage of the aromatic rings and heterocycles via ozonides. The direct ozone reaction mechanism is a quite selective mechanism, during which ozone reacts with double bonds and activated aromatic groups or amines. [67][68][76] The structure of the ozone molecule presented in **Figure 2.1** earlier in this chapter reveals that the ozone molecule can act as a 1,3-dipole, as an electrophilic agent, and as a nucleophilic agent. The following is a brief discussion of the three different types of direct reaction mechanisms of ozone.

   a) **1,3-Dipolar cyclo-addition:**

   As mentioned earlier in this chapter, as a result of dipolar structure of ozone, the ozone molecule may lead to 1,3-dipolar cyclo-addition on unsaturated π-bonds. The accepted reaction mechanism is that suggested by Criegee (1975) and Bailey (1978). Similar to

11

ozonation of double bonds of alkenes, ozonation of aromatic compounds also can be described by the Criegee mechanism in both gas-phase and liquid-phase. [67][74] It has been reported that if ozonation is carried out over a sufficient time, it leads to ring-cleavage in aromatics. Reaction of ozone with aromatics is a three step process. The first step follows Criegee mechanism and corresponds to a 1,3-dipolar cycloaddition of ozone to the aromatic ring on unsaturated π-bonds. This step is relatively fast with significant ozone consumption and eventually leads to opening of the aromatic ring and formation of a very unstable five-membered ring ozonide (1,2,3-trioxolane) as the reaction intermediate product. [79][80][81][82][83] The second step of the reaction is the quick rearrangement of the ozonide and formation of highly reactive initial reaction peroxidic products of ozonation through cyclo-conversion. This step probably consumes a little amount of ozone. [75][84][85][86][87][88] In the third step, the produced hydroperoxides reacts in different ways depending on experimental conditions and the nature of the hydrocarbon to yield more stable products, such as ketone, catechols, phenols, and etc.

An example of three step process of ozone reaction with aromatics is shown in **Figure 2.3**.
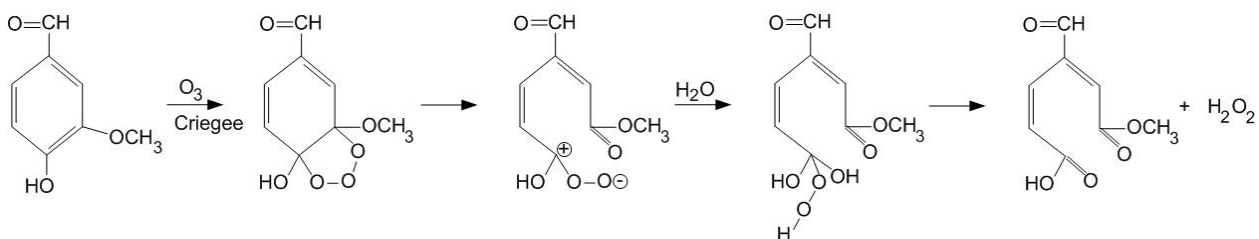
Figure 2.3. Three step process of ozone reaction with an aromatic compound [89]

b) **Electrophilic reactions:**

This type of reaction mechanism occurs in molecular solutions with strong electronic density. Aromatic compounds preferably undergo electrophilic reactions rather than cyclo-addition reactions because of the stability of the aromatic ring. Another important consideration is the presence of electron donor groups, e.g., OH and NH_2 in the aromatic group. Ozone is an electrophile and will remove electrons from electron rich positions on aromatic rings, and electron rich-donating groups promote degradation. [65][69][75] The aromatic compound bearing the electron donor group react quickly with the ozone molecule due to their tendency to donate electrons, which leads to formation of ortho- and para-hydroxylated by-products.

12

These hydroxylated compounds are highly reactive to ozone and undergo further ozonation which leads to cleavage of the aromatic ring and formation of aliphatic products with carbonyl and carboxyl functional groups. [67][68][77][90][91]

c) **Nucleophilic reactions:**

Nucleophilic reactions mainly take place where there is an electron deficiency and particularly on carbons containing electron-withdrawing groups, such as carboxyl group. [67][68][77][91]

The reaction between ozone and isonitriles to form isocynates could proceed via either an electrophilic or a nucleophilic reaction pathway, as shown in **Figure 2.4** and **Figure 2.5** respectively. [92]
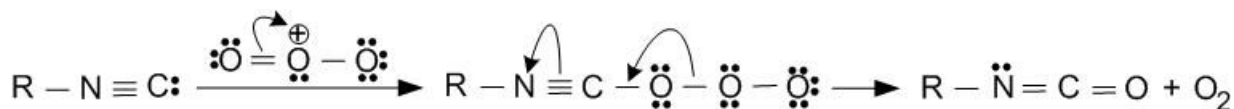
Figure 2.4. Electrophilic attack of ozone to isonitrile in order to produce isocyanates
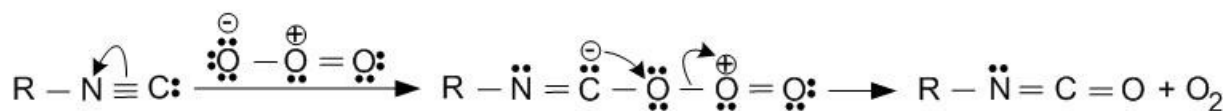
Figure 2.5. Nucleophilic attack of ozone to isonitrile in order to produce isocyanates

Both direct and indirect reactions of ozone are proceeding simultaneously. The rate of the reactions depends on different factors, such as reaction temperature and quantity of ozone. [76][93] The rate of direct and indirect ozone reactions is a function of the oil composition. If bitumen does not contain the hydrocarbon compounds that initiate the hydroxyl radical chain reaction (initiators), or if it contains many compounds that terminate the chain reaction very quickly (scavengers), direct ozonation will be the prevalent mechanism. However, if the bitumen contains compounds that promote the formation of hydroxyl radical, then indirect reaction will be the dominant mechanism.

The influence of the reaction temperature on the rate constant for any reaction can be described by Arrhenius equation, as described in **Equation 2.3**.

$$K = A\, e^{-E_a/(RT)}$$ **Equation 2.3**

Where,

K is the rate constant at temperature T [S⁻¹],

T is the reaction temperature [Kelvin],

E_a is the activation energy [kJ mol⁻¹],

R is the ideal gas constant; 0.008314 kJ mol⁻¹ K⁻¹,

A is the frequency factor.

The free radical oxidation pathway in ozone reactions is much faster than direct oxidation of ozone. Direct reactions of ozone are very selective and show a wide range of activation energy as a function of the bitumen composition. While the energy of activation of free radical reactions are typically in a narrow range. Therefore, temperature affects direct ozone reactions significantly more than reactions involving hydroxyl radical. [94][95][96][97]

The reaction of oxygen molecule with hydrocarbon compounds only takes place via free-radical reaction mechanism, just like the indirect reaction mechanism of ozone. Free radicals of oxygen have a natural tendency to participate in radical chain reactions. In the first step of free-radical chain reactions which is called initiation, the formation of radical species takes place. The faster this step occurs, the higher the degree of oxidation. Next, chain propagation part of the chain reactions takes place. Once a reactive free radical is generated, it can react with stable hydrocarbon and oxygen molecules to form new free radical species. Propagation step often involves hydrogen elimination or addition of the oxygen free radical to double bonds. The last step is the chain termination which occurs when two free radicals react with each other to form a non-radical substance. Due to low concentration of free radical species and the small likelihood of two radicals colliding with one another, occurrence of this step is rare. [57][58][98]

2.5   Bitumen ozonation

The use of ozone as oxidizing agent in upgrading bitumen has appeared on many occasions in the literature over the years. [67][68][74][76][77] The temperature required to convert bitumen components to more useful water-soluble products using oxygen is quite high. [99] In order to avoid high temperatures, ozone which is a stronger oxidant than oxygen can be used due to its ability to cleave olefinic double bonds. Ozonation can be performed at significantly lower temperatures and higher reaction rates than oxidation to produce lower molecular weight

components which are also suitable for microbial digestion. [100][101][102][103] Another advantage of ozonation is regarding the safety point of the view. Despite its high reactivity and instability, ozone can be generated on-site during its application from air. So it is not required to maintain an oxidizing agent stock. [104]

It has been reported that ozone preferentially attacks part of the bitumen with highest molecular weight and viscosity, i.e. asphaltene and resin fractions, and it converts this part into water-soluble or more hydrophilic materials. The saturates and aromatics are affected to a lesser degree. [105] Direct reaction of ozone with organic compounds is a quite selective reaction, during which ozone reacts quickly with the compounds containing double bonds, activated aromatic groups or amines. [160][107] Because of the high amount of aromatic, naphthenic and heteroatom containing compounds in bitumen with high reactivity, and considering low reactivity of oxygen, ozone seems to be more efficient oxidizing agent than oxygen. Ozone reacts with aromatic compounds leading to either a substitution (atom attack) or to a ring opening (bond attack). [90][108] As it can be seen in **Figure 2.6**, pyrene underwent exclusive bond attack by ozone; however benzopyrene as shown in **Figure 2.7** underwent exclusive atom attack by ozone. [68]
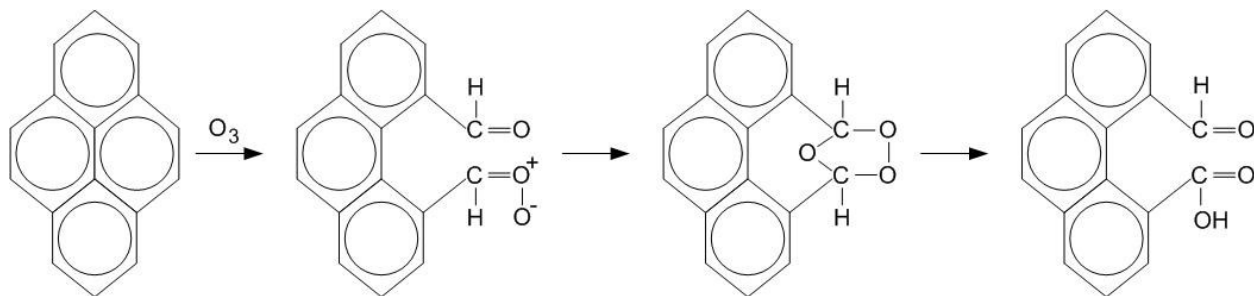
Figure 2.6. Ozonation of pyrene is an example of bond attack by ozone
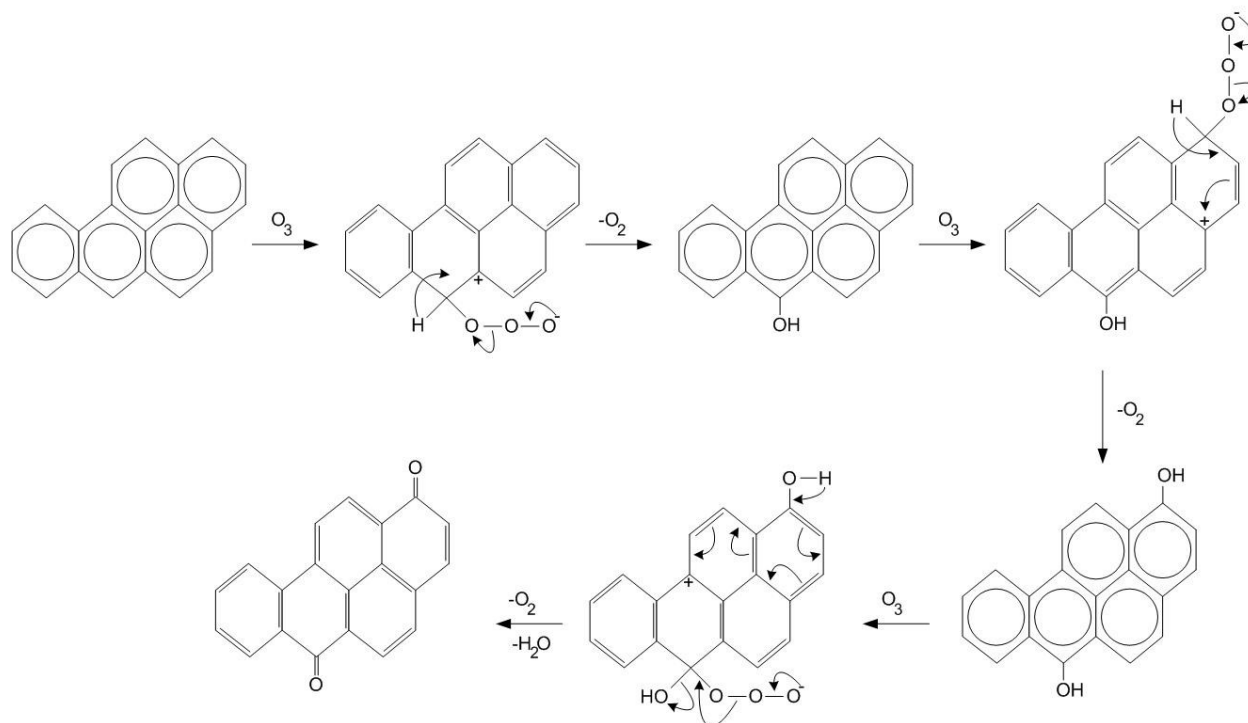
Figure 2.7. Ozonation of benzo[α]pyrene is an example of atom attack by ozone

Ozonation of organic compounds contains a series of complex reactions, involving reaction between ozone and parent compound as well as reaction between ozone and intermediates. With the progress of ozonation, the reactions of ozone and intermediate products become more dominant compared to the reaction of ozone and parent compound.[93][109]

3. LOW TEMPERATURE OZONATION OF SELECTED COMPOUND CLASSES AT LOW GAS FLOW RATE

3.1 Introduction

In this chapter, ozonation reactions of the hydrocarbon classes and heteroatom-containing classes, which are the dominant compounds in bitumen, at low temperatures (below 250 °C) will be discussed.

Due to the complexity of bitumen composition, analysis of the ozonized bitumen in order to fully understand the effects of ozone on bitumen samples is not an easy task. Although the molecular structure of bitumen has not been fully understood yet, it has been found that most of the molecules present in bitumen are combinations of paraffins, naphthenes, aromatics and heteromolecules containing sulphur, oxygen, nitrogen and heavy metals. In this thesis, the investigation is focused on cyclic hydrocarbon and heterocyclic compound classes.

The ozonation studies were performed at 130 °C to find the ozonation products of the selected model compounds, and to identify and estimate the sequences of the products from ozonation reactions using their mass spectra. The importance of this study is to understand the nature of the reactions happening during low temperature ozonation of the selected model compounds, which will provide essential guidelines to perform ozonation reactions in actual samples of bitumen.

The objective of the project is to investigate the possibility of ring-cleavage reactions of ring containing and cyclic hydrocarbons (e.g., aromatic compounds, naphthenic compounds, etc.) in

17

bitumen and the possibility of an increase in the biodegradability of bitumen by treatment with ozone-enriched air at relatively mild temperature and low gas flow rates.

3.2   Experimental

3.2.1   Materials

In order to simplify the analysis and comparison of the ozonation products, the model compounds were selected to be within a narrow carbon number range (C_8 to C_{10}) and boiling points (113 to 254 °C). Model compounds including naphthalene (as representative of aromatic compounds), tetralin, indane and indene (as representatives of naphthenic-aromatic compounds), decalin (as representative of naphthenic compounds), *p*-cymene (as representative of alkyl-aromatic compounds), *n*-decane (as representative of acyclic-paraffinic compounds) and also few heteroatom-containing compound classes including thianaphthene (as representative of heterocyclic sulphur-containing compounds), indoline, indole and quinoline (as representatives of heterocyclic nitrogen-containing compounds), 2,3-dihydrobenzofuran and 2,3-benzofuran (as representatives of heterocyclic oxygen-containing compounds) were considered for low temperature ozonation study. A brief summary of the properties of the model compounds used for the ozonation study is listed in **Table 3.1**, and structural formula of these compounds is shown in **Table 3.2**. It should be mentioned that the molecular weights of the studied compounds are probably much lower than the real compounds in bitumen.
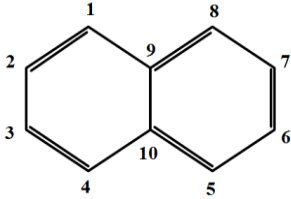
Table 3.1. Properties of the selected model compounds used for low temperature ozonation study

Name	CASRN[a]	Molecular formula	Boiling point [°C]	Purity by supplier[b][wt%]	Supplier
Naphthalene	91-20-3	$C_{10}H_8$	218	99	Aldrich
Tetralin	119-64-2	$C_{10}H_{12}$	207	99	Sigma-Aldrich
Indane	496-11-7	C_9H_{10}	176	95	Aldrich
Indene	95-13-6	C_9H_8	181	90	ACROS
Decalin – cis/trans	91-17-8	$C_{10}H_{18}$	189 – 191	≥99	Sigma-Aldrich
p-Cymene	99-87-6	$C_{10}H_{14}$	176 – 178	99	Aldrich
n-Decane	124-18-5	$C_{10}H_{22}$	174	≥99	Aldrich
Thianaphthene	95-15-8	C_8H_6S	221 – 222	98	Aldrich
Indoline	496-15-1	C_8H_9N	220 – 221	99	Aldrich
Indole	120-72-9	C_8H_7N	253 – 254	≥99	Aldrich
Quinoline	91-22-5	C_9H_7N	113 – 114	98	Aldrich
2,3-Dihydrobenzofuran	496-16-2	C_9H_7N	188 – 189	99	Aldrich
2,3-Benzofuran	271-89-6	C_8H_6O	173 – 175	99	Aldrich

[a] CASRN is Chemical Abstracts Service Registry Number.

[b] This is the purity of the chemical substrates from their material safety data sheets (MSDS) provided by the supplier.

Table 3.2. Structural formula of the selected model compounds used for low temperature ozonation study

Name	Structural formula
Naphthalene	

19

Tetralin
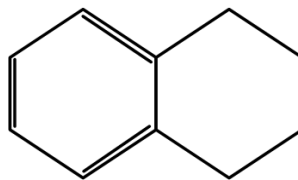
Indane
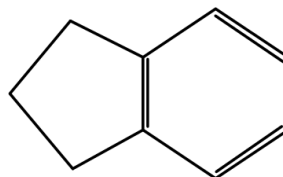
Indene
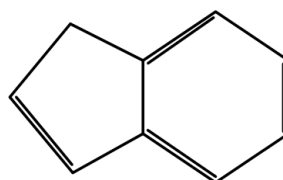
Decalin – cis/trans
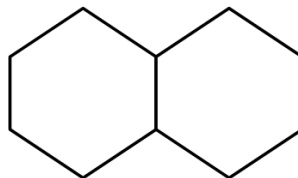
p-Cymene
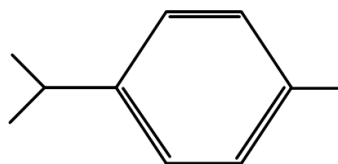
n-Decane

Thianaphthene
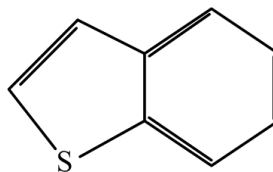
Indoline
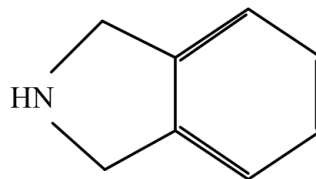
Indole
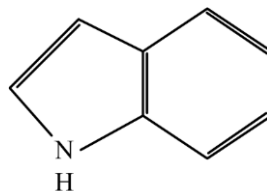
Quinoline
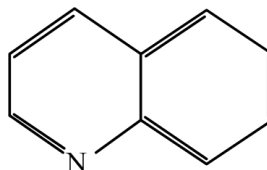
2,3-Dihydrobenzofuran
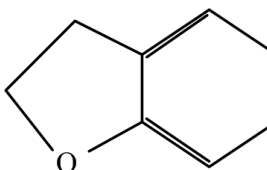
2,3-Benzofuran
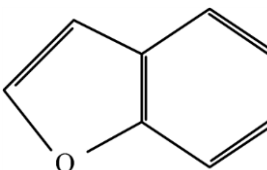
3.2.2 Apparatus and experimental procedure

Experiments were performed by transferring 50 g of model compounds into a 250 ml round-bottom three-neck flask which was used as a reactor. Then the model compound was heated using a heat-on-block (Heidolph MR Hei-Standard) to 130 °C before releasing the ozone-enriched air flow into the flask. The flask was fitted with a 300 mm reflux condenser which was cooled with a chilled water supply at 10 °C. Extra-dry air as feed gas from the cylinder was passed through the ozone-generator (OZO 2VTTL O_3 generator, Ozomax Ltd. Canada) in order to generate ozone. Ozone-enriched air from the ozone generator was used as the main oxidizing agent. In all the experiments, the ozone-enriched air flow rate was maintained at 120 ml min^{-1}. Ozone-enriched air flow rate was controlled by a certified Riteflow rotameter installed on the inlet line. A magnetic stirring bar with the stirring speed of 250 rpm was used for mixing. All the reactions were carried out at 130 °C for 6 hours. Compressed extra-dry air (O_2 19.5 − 23.5 %, H_2O <10 ppm, the quality specification is provided by the supplier) was supplied by Praxair Co., Canada.

In each experiment, the model compound was pre-heated and only after the model compound temperature was reached to the reaction temperature (130 °C), the ozone-enriched air injection to the flask was commenced. In this way the possibility of ozonation was limited during the pre-heating process.

In the experiments performed in this work, ozone has been generated using an ozone-generator equipped with a corona lamp in order to generate ozone from oxygen using electrical discharge produced between two electrodes separated by a dielectric. Voltage is provided by high voltage power supply (between 5000 to 20,000 volts).

In order to monitor the progress of the reactions and ozonation products, small samples (~1 g) were collected at fixed time intervals during experiments. Ozonation was stopped by turning off the ozone generator and disconnecting the extra-dry air supply. Products of ozonation were stored in clear glass vials (Fisherbrand Class B threaded vial, Fisher Scientific Company, Canada) with lid in ambient temperature and light for further analyses. The samples were stored for less than 24 hours before analysis. The experimental setup used for model compounds ozonation study is schematized in **Figure 3.1**.
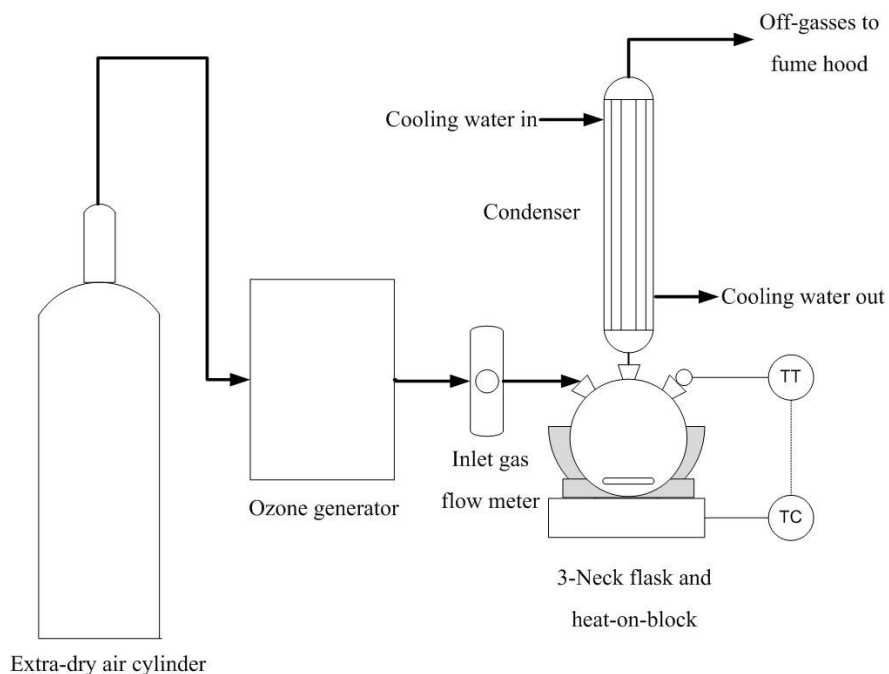
Figure 3.1. Schematic of the experimental setup used for low temperature ozonation study of the selected model compounds

22

3.2.3 Analyses and calculations

The ozonation products were analyzed and the progress of the reactions was monitored using different techniques and instruments.

3.2.3.1 Gas chromatography with flame ionization detector (GC-FID)

The gas chromatograph (GC) employed for quantitative analysis was an Agilent 7890A gas chromatograph (Agilent Technologies Inc., Canada) equipped with a flame ionization detector (FID). The condition used for the analysis of the parent model compounds and ozonized model compounds using GC-FID is presented in **Table 3.3**. Hexachlorobenzene was added to the samples as an internal standard for quantification purposes.

Table 3.3. GC-FID condition used for analysis of the parent model compounds and ozonized model compounds

Injection condition	Split mode, 250 °C, split ratio: 10:1, split flow: 20 ml min^{-1}
Sample injection volume	1 μl
Carrier gas	Helium, with flow rate of 2 ml min^{-1}
Column	DB-5 MS column, stationary phase composition: phenyl arylene polymer virtually equivalent to 5%-Phenyl-methylpolysiloxane (30 m length, 0.25 mm I.D., 0.25 μm film thickness)
Solvent delay	2 min
Oven temperatures and times	Initial: 75 °C for 0.5 min Ramp: 20 °C min^{-1} to 325 °C Final: 325 °C for 5 min
Preparation solvent	Chloroform (HPLC grade, Sigma-Aldrich, Canada)
Internal standard	Hexachlorobenzene (HCB)(analytical standard, Supelco, Canada)

3.2.3.2 Gas chromatography - mass spectroscopy (GC-MS)

GC–MS analysis was carried out using a gas chromatograph (GC) (Agilent 7890A gas chromatograph, Agilent Technologies Inc., Canada) equipped with a mass spectrometer (MS) (5977E MSD, Agilent Technologies Inc., Canada). The temperatures of transfer line and ion source were 325 and 280 °C respectively. Ions were generated by electron ionization mode. The HP-5 MS column (stationary phase composition: 5%-Phenyl-methylpolysiloxane, 30 m length,

0.25 mm I.D., 0.25 μm film thickness) which was used for GC-MS had similar phases and similar separation characteristics as DB-5 MS column used in GC-FID, so the same temperature program as GC-FID was used for these analyses. Solvent delay was 2 min. The specific identity of ozonation products was determined by interpretation of the electron ionization mass spectra with the help of the electron ionization mass spectra library of National Institute of Standards and Technology (NIST).

GC-MS and GC-FID analyses were conducted to identify the ozonation products, as well as calculating the conversion of the parent compounds and selectivity of the ozonation process. Quantitative analysis using GC-FID relies on the calculation of correction factors and using them for all the compounds. The amount of the correction is a function of the response of a given compound to the detecting device, which is called response factor. This response factor is 1 for heptane, which means the peak area obtained from GC for heptane and concentration of heptane have a 1 to1 relation.

The GC peak area and the concentration [wt %] of each component in the sample are used to calculate the response factor for that compound, as shown in **Equation 3.1**.

$$RF_i = {A_i}/{W_i}$$
<div align="right">**Equation 3.1**</div>

Where,
RF_i is the response factor of compound i with respect to heptane,
A_i is the peak area of compound i,
W_i is the concentration of compound i in the sample, in terms of wt %.

The calculated response factor for each component in the sample can be used to calculate the relative response factor (RRF) between two components, as shown in **Equation 3.2**.

$$RRF_{i,HCB} = {RF_i}/{RF_{HCB}}$$
<div align="right">**Equation 3.2**</div>

Where,
$RRF_{i,HCB}$ is the relative response factor of compound i with respect to HCB,

RF_{HCB} is the response factor of HCB with respect to heptane; experimentally measured as 0.36 ± 0.01.

Then as shown in **Equation 3.3**, $RRF_{i,HCB}$ can be used to calculate the unknown concentration [wt %] of compound i in the presence of known concentration of HCB as an internal standard in a sample.

$$W_i = \frac{A_i * W_{HCB}}{A_{HCB} * RRF_{i,HCB}}$$
                                                                    Equation 3.3

Where,

W_{HCB} is the concentration of HCB in terms of wt % in the sample,

A_{HCB} is the peak area of HCB.

If a mixture of aliphatic hydrocarbons were to be quantified, the mass fraction of any hydrocarbon i in the mixture can be determined using HCB as an internal standard, because the FID response factors for aliphatic hydrocarbons are approximately 1 (RF_i = 1) and the relationship is simply:

$$W_i = \frac{A_i * W_{HCB}}{A_{HCB}} * 0.36$$
                                                                    Equation 3.4

As the different organic compound classes have different response factors and there is a lack of suitable internal standard for each organic compound class, the results given in the following sections cannot be proven to be quantitative. Thus, the data should be viewed only as semi-quantitative. Considering this fact, the percentage of conversion in terms of wt % was calculated using **Equation 3.4** for all the parent model compounds and their ozonation products.

3.2.3.3 Differential scanning calorimetry (DSC)

Thermal analysis of the parent model compounds and ozonized model compounds was performed using differential scanning calorimeter (DSC 1 STAR^e system, Mettler Toledo Inc., Canada) equipped with FRS5 detector. The crucibles used for this thermal analysis were standard aluminum with 40 µL capacity which was sealed with a pierced lid to prevent pressure build up and possible deformation of the cup during the test. Nitrogen with the flow rate of 100 ml min^{-1} was used as an inert purge gas. The amount of sample loaded in the open crucibles for each

analysis was approximately 5 mg. The temperature program that was used for DSC of the model compound feed and ozonized model compounds is described in **Table 3.4**.

The instrument was calibrated utilizing high purity indium standard, which is a metallic standard with sharp melting peak and well-known enthalpy of fusion. Then, the integrity of the data gathered from the calibration check and the data found in literature was compared to check the instrument calibration.

Table 3.4. Temperature program applied for TGA and DSC of the parent and ozonized model compounds

Time	Description
0 – 37.5 min	Temperature was increased from 25 °C to 400 °C with the heating rate of 10 °C min^{-1}.
37.5 – 47.5 min	Temperature was remained at 400 °C for 10 min.

3.2.3.4 Thermogravimetric analysis (TGA)

Variations in the weights of the parent model compounds and ozonized model compounds were studied using a thermogravimetric analyzer (TA Q500, TGA/DSC 1 STAR^e system, Mettler Toledo Inc., Canada). Nitrogen was used as an inert purge gas with the flow rate of 100 ml min^{-1}. The crucibles used for the products and reference were alumina (Al_2O_3, white) crucibles with a capacity of 70 µL. For TGA of the parent and ozonized model compounds, the same temperature program as DSC was used, which is presented in **Table 3.4**.

3.2.3.5 Fourier transform infrared (FTIR) spectroscopy

The qualitative analysis was performed using Fourier transform infrared spectrometer (ABB MIRacleTM, MB 3000, ABB Inc, Canada) in order to confirm the presence of oxygenate functional groups in the ozonized model compounds. IR spectra of the small amount of samples embedded in potassium bromide (KBr) pellets were measured with the condition presented in **Table 3.5**.

Table 3.5. Condition applied for infrared spectroscopy of the parent and ozonized model compounds

Resolution [cm^{-1}]	2
Number of scans per sample	120
Wavenumber range [cm^{-1}]	4000 - 500
Detector gain	243
Acquisition mode	Absorbance

3.2.3.6 Refractometer (Refractive index meter)

Refractive indices of the studied model compounds were determined before and after ozonation experiments using Anton Paar Abbemat HP refractometer at two different temperatures of 20 and 60 °C. The refractometer is designed to be used with samples with lower refractive indices than the prism. To measure the refractive index of a liquid sample, it was placed on the measuring (refractive) prism and covered with a lid. Equilibrium time is usually required for the sample to attain the prism temperature and to give a constant reading. The liquid sample in contact with the prism is illuminated by an LED and the critical angle of the total reflection at 589.3 nm sodium D wavelength is measured with a high-resolution sensor array. The refractive index (n_D) is calculated from this value.

3.2.3.7 Density meter

Density of liquid studied model compounds before and after 6 h ozonation were measured using an Anton Paar density meter (DMA 4500M) at 20 °C.

3.3   Results and discussions

In this section, first, the measurement of ozone concentration in the ozone-enriched air utilizing a mass spectrometer has been discussed. Then, ozonation conversion and selectivity of the studied model compounds to reaction products are calculated based on the chromatograms obtained from GC-FID and GC-MS. Then, the results of thermal analyses of the model compounds and their ozonation products using TGA and DSC are discussed. After that, characterization of model compounds and ozonation products using their optical properties based on the results from FTIR spectroscopy and refractometer is discussed, and finally, changes in physical characteristics of the studied model compounds including physical appearance and density are discussed.

3.3.1 Ozone concentration measurement

The ozone-enriched gas stream from the ozone generator was introduced to a UV measuring cell (100 mm path length, StellarNet Inc., Florida, US), in which the absorption of UV radiation was measured at the 254 nm emission line of a deuterium + halogen light source for UV-VIS (SL5-DH, StellarNet Inc., Florida, US). A photodetector (BLK-C-SR, StellarNet Inc., Florida, US) connected to the other end of the cell measured the UV absorption in the range of 240 to 290 nm caused by the presence of ozone in the sample cell. The strong absorption by ozone at the wavelength of 254 nm produced a detectable absorption measurement when ozone was present in the cell.

The most important principle in absorption analysis is the Beer–Lambert law. The absorption was measured in the presence of ozone in the extra-dry air. The measured UV absorption in the presence of ozone, A, is related to the ozone concentration in the cell by the following expression:

$$A = \alpha C L \qquad\qquad \textbf{Equation 3.5}$$

Where,

α is the absorption cross-section of ozone at 254 nm [cm^2],

C is the concentration of ozone in the cell [molecules cm^{-3}],

L is the length of the cell [cm].

By utilizing the Beer–Lambert law, it is possible to determine the concentration of ozone in the cell, provided that the length of the cell and the absorption cross-section for ozone are known. From the literature, the absorption cross-section of ozone at 254 nm is on average 1.134465E-17 cm^2 at room temperature. [110] The calculated ozone concentration in the ozone-enriched air was 1.97E-4 $cm^3 O_3$ per cm^3 ozone-enriched air.

The UV-VIS spectroscopy could identify traces of other gases like NO_2, NO and SO_2 in the ozone-enriched air which are probably formed along with the ozone in the ozone generator. This small amount of formed gases may affect the reaction procedure but it has not been investigated in this study.

3.3.2 Conversion and selectivity

In this section, the results of ozonation conversion and selectivity of the studied model compounds to reaction products are discussed.

The progress of the reactions was monitored by measuring the principal reaction products formed during 6 h ozonation. To confirm the extent of the ozonation, quantitative analysis of the selected model compounds before and after 6 h ozonation at 130 °C was done using GC-FID and GC-MS. Since a non-polar column was used for chromatographic purposes, heavier compounds with higher boiling points and higher molecular weights tended to stick to the stationary phase and elute at longer retention times. The nature and proportions of the products formed in the ozonation process depend not only on the model compound nature but also on the condition under which the ozonation takes place. [111][112] During 6 h ozonation of the model compounds, identification of four types of ozonation products was possible: primary, secondary, ring-cleavage reaction and addition reaction products.

1. Primary ozonation products — Alcohols and ketones of the parent model compound, or in general the stable products after ozonation of a substrate which have not yet reacted further with ozone. [113]

2. Secondary ozonation products — Primary products can react further to give so-called secondary ozonation products, if ozone is still present in the system. [111][113] These products are mainly combinations of alcohols and ketones, and have more than one oxygenate functional group.

3. Addition reaction products — High molecular weight products formed due to free radical addition reaction of two parent molecule by ozonation. The structure of this group of products can provide information on the nature of the addition reactions happening due to ozonation.

4. Ring-cleavage reaction products — The last group of products is the one formed by ring-cleavage of cyclic hydrocarbons due to ozonation. In this study, only small traces of this group was observed in the ozonation products of the studied model compounds. Thus, this group of products is considered together with the primary and secondary ozonation products in calculations of the ozonation selectivity, since all of these products are

monomeric oxidation products. The structure of this group of products can provide information on the nature of the ring opening reactions happening due to ozonation.

As it can be seen in **Table 3.6**, the ozonation conversion of the studied model compounds was determined in term of disappearance of the parent component and it does not reflect the extent of ozonation. The selectivity to primary, secondary and ring-cleavage reaction products, as well as free radical addition reaction products was also calculated and presented in **Table 3.7**.

Table 3.6. Conversion of parent model compounds to ozonation products during 6 h ozonation at 130 °C with ozone-enriched air flow rate of 120 ml min^{-1} (equivalent to 144 ml h^{-1} per gram of feed)

Compound name	Conversion[a] [wt %]				
	30 min	60 min	120 min	240 min	360 min
Naphthalene	0	0.74	0.86	1.33	2.44
Tetralin	0	0	0	2.63	4.21
Indane	0.99	5.12	10.23	16.72	19.20
Indene	1.91	3.66	10.62	43.55	84.68
Decalin	0.68	2.15	5.91	16.11	36.84
p-Cymene	2.58	6.84	18.07	37.64	78.24
n-Decane	0	0	0	2.98	6.52
Thianaphthene	0	0.46	0.96	3.45	9.43
Indoline	0.05	0.17	0.34	1.17	3.60
Indole	0	0.45	1.62	3.84	6.67
Quinoline	0	0	0	0.19	0.52
2,3-Dihydrobenzofuran	0	0.55	0.96	2.95	4.73
2,3-Benzofuran	0	0.31	3.91	15.62	32.59

[a] Conversion of parent compounds to ozonation products were calculated by using GC-FID relative response factor of feed with respect to hexachlorobenzene as an internal standard.

Table 3.7. Selectivity of parent model compounds to different ozonation products during 6 h ozonation at 130 °C with ozone-enriched air flow rate of 120 ml min^{-1} (equivalent to 144 ml h^{-1} per gram of feed)

Compound class	Compound name	GC-MS retention time	Type of ozonation products	Selectivity of ozonation products[a] [wt %]				
				0.5 h	1 h	2 h	4 h	6 h
Aromatic	Naphthalene	4.9–7.6	Primary, secondary & ring-cleavage	0	0	0	100	100
		–[b]	Addition	0	0	0	0	0
Naphthenic-aromatic	Tetralin	5.0–8.0	Primary, secondary & ring-cleavage	100	100	99.0	98.8	96.9
		10.0–11.0	Addition	0	0	1.0	1.2	3.1
	Indane	4.0–7.0	Primary, secondary & ring-cleavage	0	0	0	41.6	38.8
		9.0–11.0	Addition	0	0	0	58.4	61.2
	Indene	3.5–7.0	Primary, secondary & ring-cleavage	100	100	83.4	61.1	45.4
		8.0–12.0	Addition	0	0	16.6	38.9	54.6

Naphthenic	Decalin	4.0–6.8	Primary, secondary & ring-cleavage	100	100	100	100	99.4
		7.0–12.0	Addition	0	0	0	0	0.6
Alkyl aromatic	*p*-Cymene	3.2–7.2	Primary, secondary & ring-cleavage	100	100	100	99.7	99.4
		7.5–10.7	Addition	0	0	0	0.3	0.6
Acyclic paraffinic	*n*-Decane	4.0–6.0	Primary, secondary & ring-cleavage	0	0	0	100	100
		– [b]	Addition	0	0	0	0	0
Heterocyclic sulphur-containing	Thianaphthene	4.6–7.2	Primary, secondary & ring-cleavage	0	50	42.6	27	24.6
		11.7–13.3	Addition	0	50	57.4	73	75.4
Heterocyclic nitrogen-containing	Indoline	4.8–7.2	Primary, secondary & ring-cleavage	100	100	48.0	46.7	36.9
		12.0–13.5	Addition	0	0	52.0	53.3	63.1
	Indole	6.4–7.2	Primary, secondary & ring-cleavage	0	100	100	35.4	22.5

Group	Compound	Retention time	Product					
		11.6–14.5	Addition	0	0	0	64.6	77.5
	Quinoline	4.2–7.2	Primary, secondary & ring-cleavage	0	0	0	28.2	20.4
		12.0–13.0	Addition	0	0	0	71.8	79.6
Heterocyclic oxygen-containing	2,3-Dihydrobenzofuran	4.5–5.5	Primary, secondary & ring-cleavage	0	100	69.8	45.9	0
		11.0–12.8	Addition	0	0	30.2	54.1	100
	2,3-Benzofuran	3.0–6.4	Primary, secondary & ring-cleavage	0	100	22.0	18.4	14.0
		8.7–14.6	Addition	0	0	78.0	81.6	86.0

[a] Selectivity of the ozonation products were calculated based on the GC-FID peak area of the products.

[b] GC-MS retention times were not reported in the table, as addition products were not observed.

Indene has the highest calculated ozonation conversion among other studied model compounds, as it can be seen in **Table 3.6**. This result is consistent with the results obtained by GC-MS for indene and ozonized indene. From the chromatogram of ozonized indene obtained by GC-MS presented in **Figure 3.2**, it can be observed that peaks before retention time of 4.0 min (elution time of the indene feed) in the chromatogram of ozonized indene is small in area. This is an indication of considerable conversion of indene feed to the ozonation products due to 6 h ozonation at 130 °C.

Due to free radical addition reactions, higher molecular weight compounds were formed during ozonation which can be observed at higher retention times in the chromatogram obtained by GC. The electron ionization mass spectra of one of a primary ozonation products of indene found at

retention time of 4.897 min, a secondary ozonation product found at retention time of 5.899 min, and a ring-cleavage reaction product found at retention time of 6.963 min are shown in **Figure 3.3**, **Figure 3.4** and **Figure 3.5**, respectively. One major addition reaction product of indene due to ozonation is found at retention time of 8.346 min and its electron ionization mass spectrum is shown in **Figure 3.6**. It is important to note that the nature of the addition product shown (**Figure 3.6**) is different to that produced by autoxidation.
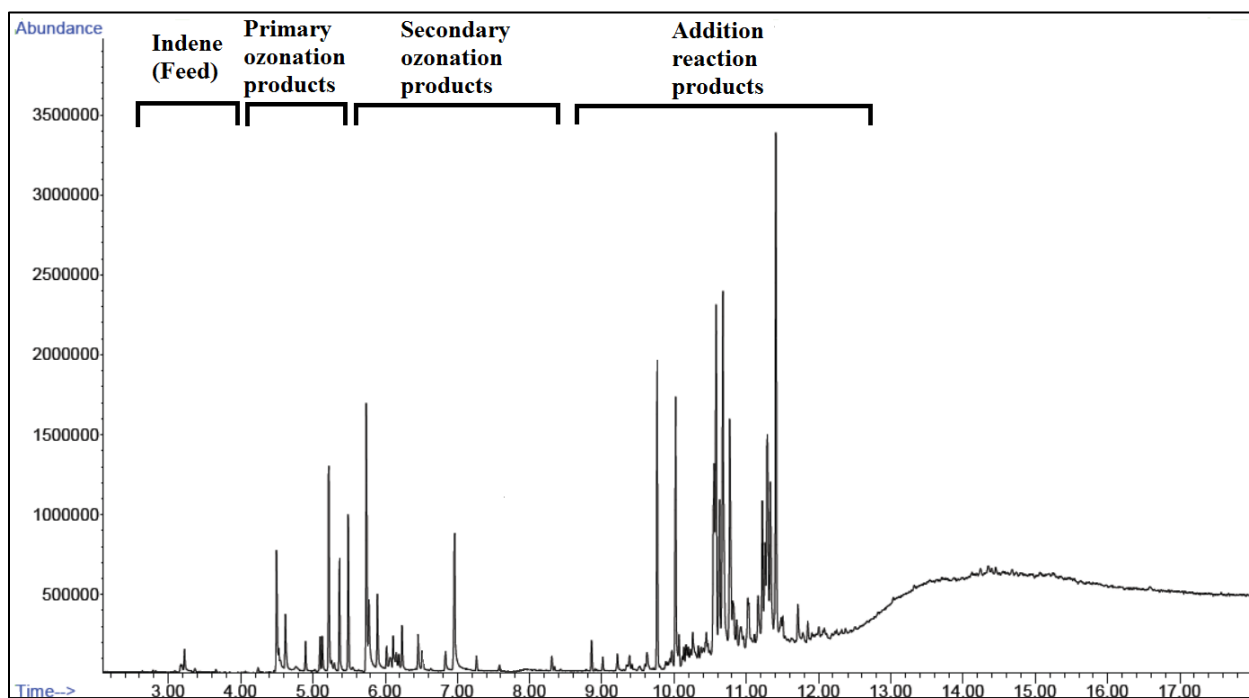
Figure 3.2. Total ion chromatogram of ozonized indene after 6 h ozonation at 130 °C; obtained by gas chromatograph of GC-MS
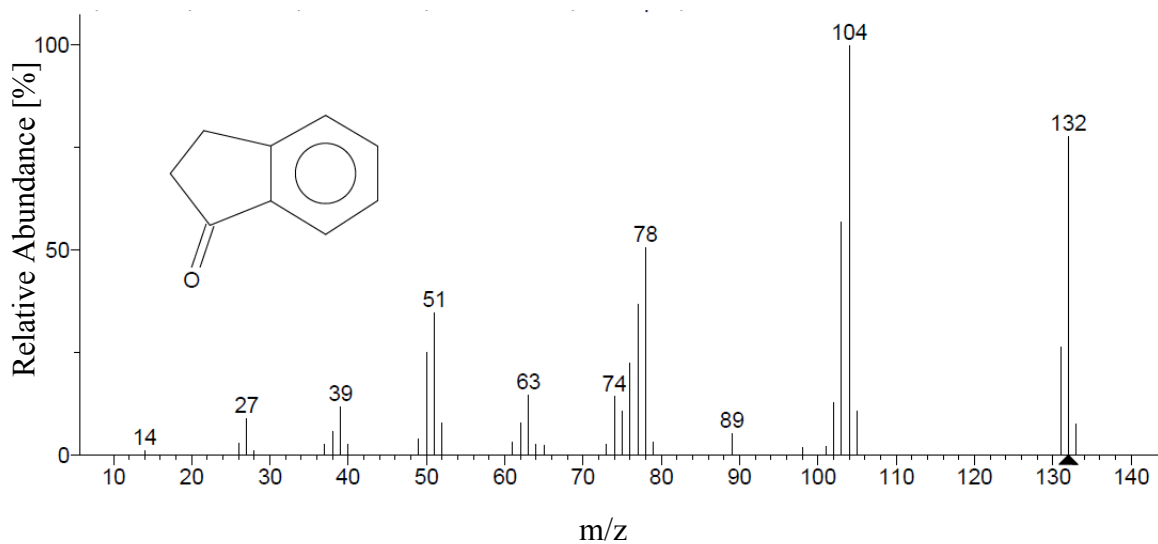
Figure 3.3. MS fragmentation pattern of a compound (retention time of 4.897) formed as a primary ozonation product of indene due to 6 h ozonation at 130 °C; obtained from NIST library
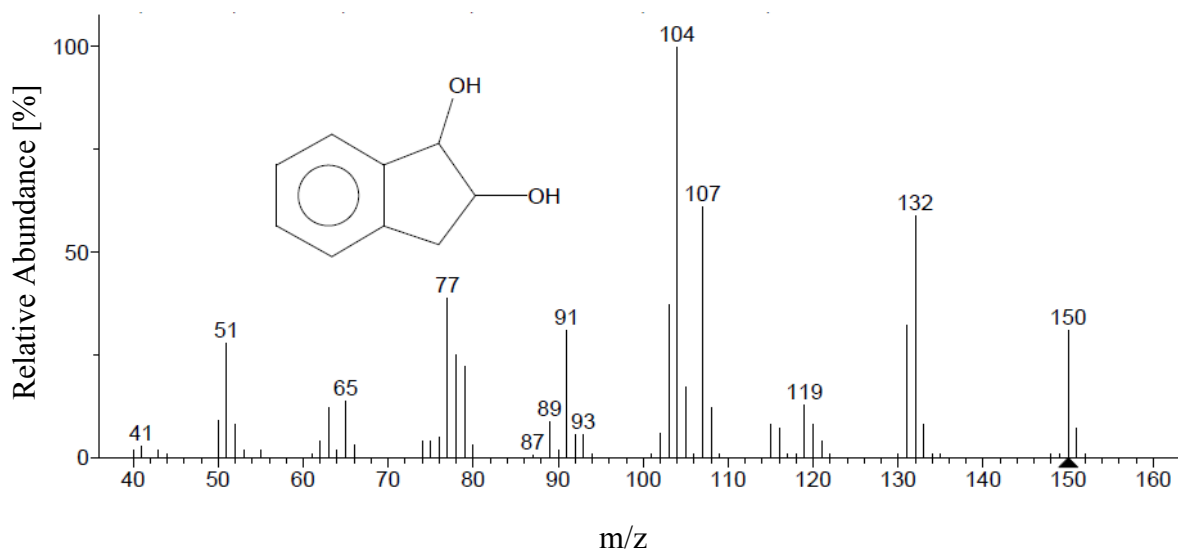
Figure 3.4. MS fragmentation pattern of a compound (retention time of 5.899) formed as a secondary ozonation product of indene due to 6 h ozonation at 130 °C; obtained from NIST library
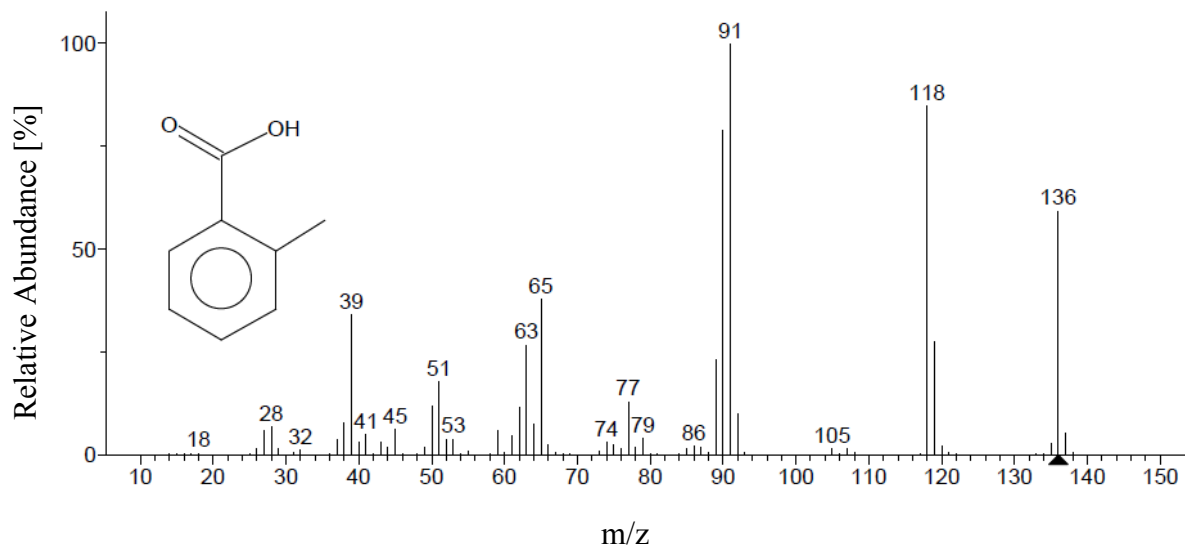
Figure 3.5. MS fragmentation pattern of a compound (retention time of 6.963) formed as a ring-cleavage reaction product of indene due to 6 h ozonation at 130 °C; obtained from NIST library
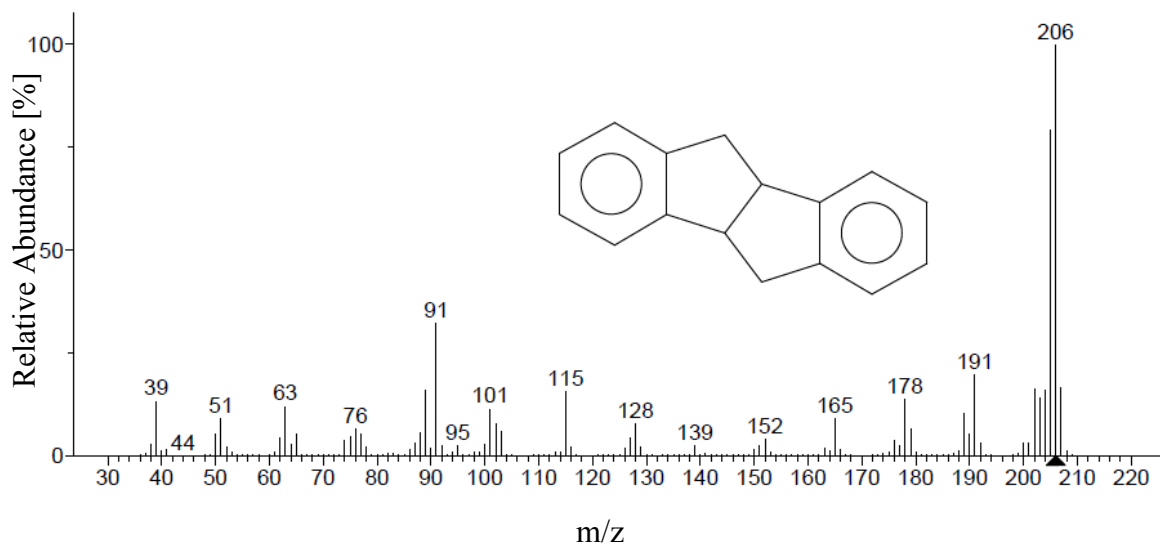
Figure 3.6. MS fragmentation pattern of a compound (retention time of 8.346) formed as an addition reaction product of indene due to 6 h ozonation at 130 °C; obtained from NIST library

3.3.3 Thermal analysis

In GC-MS and GC-FID, the sample is introduced into the top of the GC column. Sometimes there is a possibility that heavy components with very high molecular weights stick within the particle-removing filters at inlet of the analytical column which are provided to prevent contamination of the system. So these components might never make their way to the column for

detection purposes. Thermal analysis was performed in order to confirm the non-existence of these compounds in the ozonation products.

The peaks obtained by DSC and TGA for indene, *p*-cymene, 2,3-dihydrobenzofuran and decalin , which have the highest ozonation conversion among the others, before and after 6 h ozonation at 130 °C are presented in **Figure 3.7** to **Figure 3.14**. In DSC curves, although the integrated peak area and the peak height for ozonized model compounds are smaller compared to their corresponding parent component, the peak onsets or thermal events happened at approximately the same temperature. In TGA curves, for both parent and ozonized model compound, only one region of weight loss can be observed which is corresponding to the boiling point of the parent compounds. In DSC curves of the ozonized compounds, the non-existence of peaks at temperatures higher than the boiling point of its parent compound could indicate that no products with higher molecular weight is formed due to 6 h ozonation at 130 °C.

For decalin, 2,3-dihydrobenzofuran and their ozonation product, the peaks obtained by DSC are endothermic. For indene and *p*-cymene, thermodynamic nature of the peaks has changed. Since indene, *p*-cymene, 2,3-dihydrobenzofuran, decalin and their ozonation products are all in liquid phase, the only peak observed in DSC curve is the boiling point of the component. Due to formation of different compounds as a result of ozonation and co-existence of these complex products in the samples, it can be fairly concluded that for indene, *p*-cymene, 2,3-dihydrobenzofuran and decalin which have the higher conversion rate among the other studied model compounds, peak heights and even the nature of the peaks have changed considerably. The second order transitions seen in the DSC curves can be translated to a fundamental change in the sample chemistry due to ozonation.
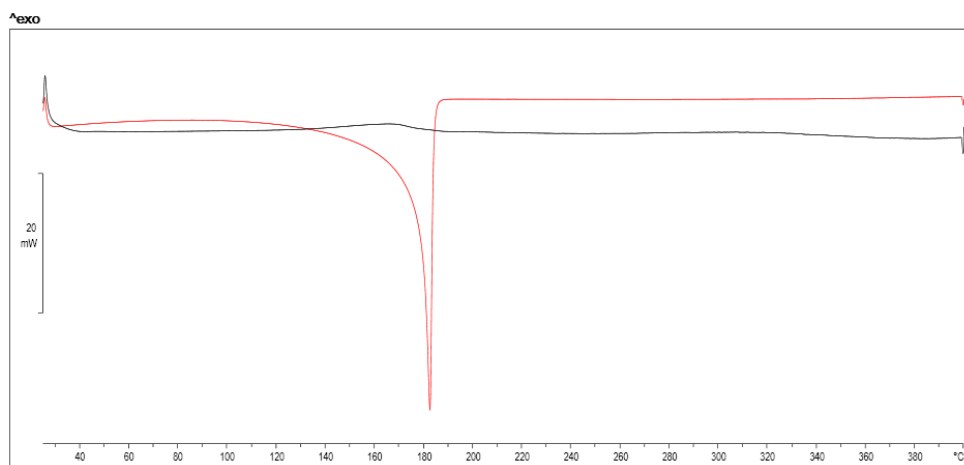
Figure 3.7. DSC curves of indene (red) and ozonized indene after 6 h ozonation at 130 °C (black)
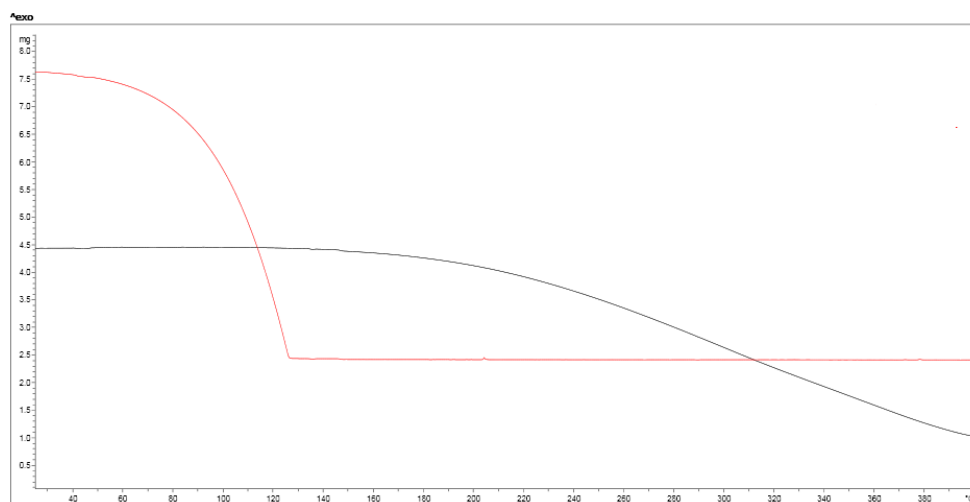
Figure 3.8. TGA curves of indene (red) and ozonized indene after 6 h ozonation at 130 °C (black)
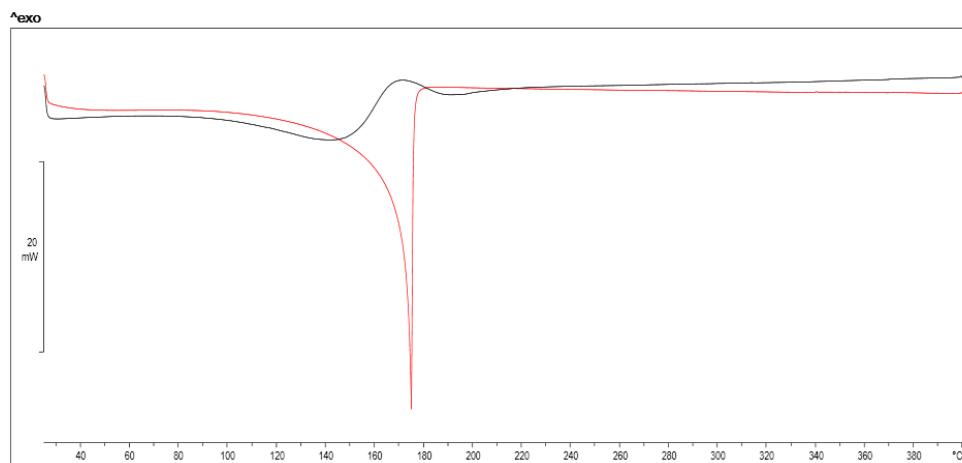
Figure 3.9. DSC curves of *p*-cymene (red) and ozonized *p*-cymene after 6 h ozonation at 130 °C (black)
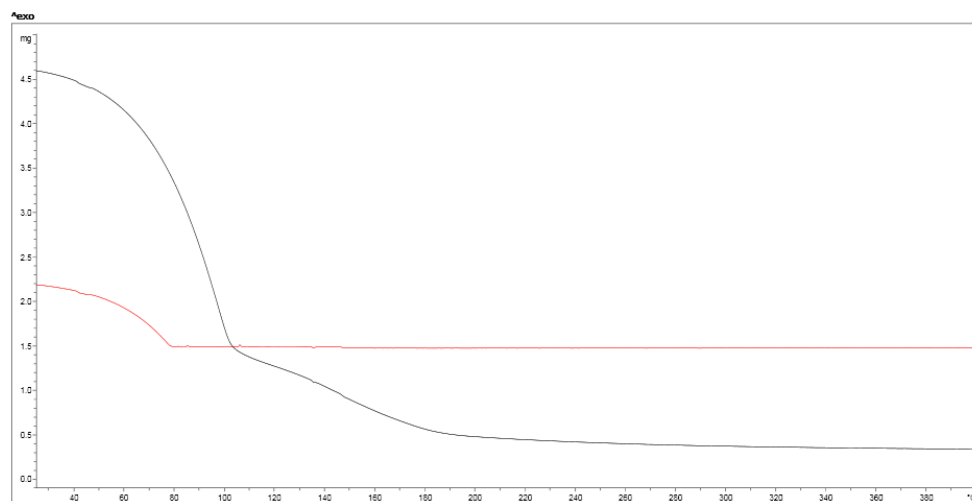
Figure 3.10. TGA curves of *p*-cymene (red) and ozonized *p*-cymene after 6 h ozonation at 130 °C (black)
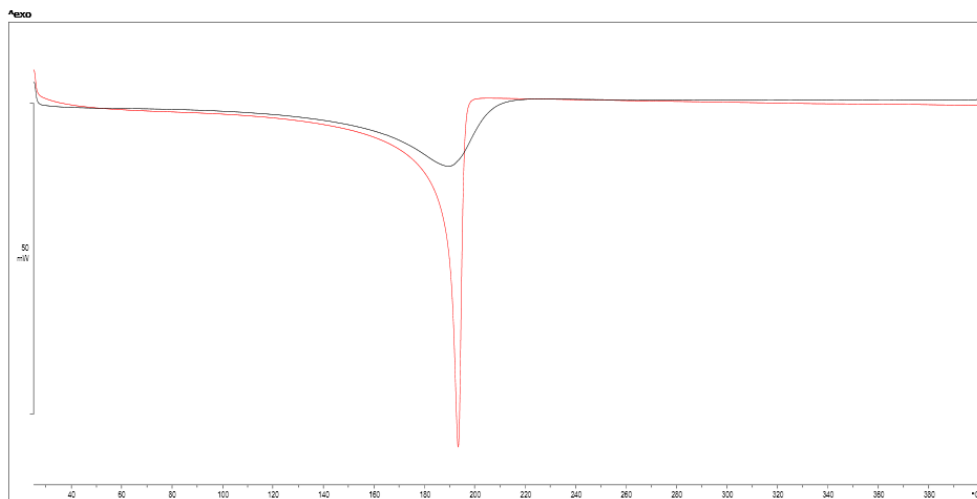
Figure 3.11. DSC curves of 2,3-dihydrobenzofuran (red) and ozonized 2,3-dihydrobenzofuran after 6 h ozonation at 130 °C (black)
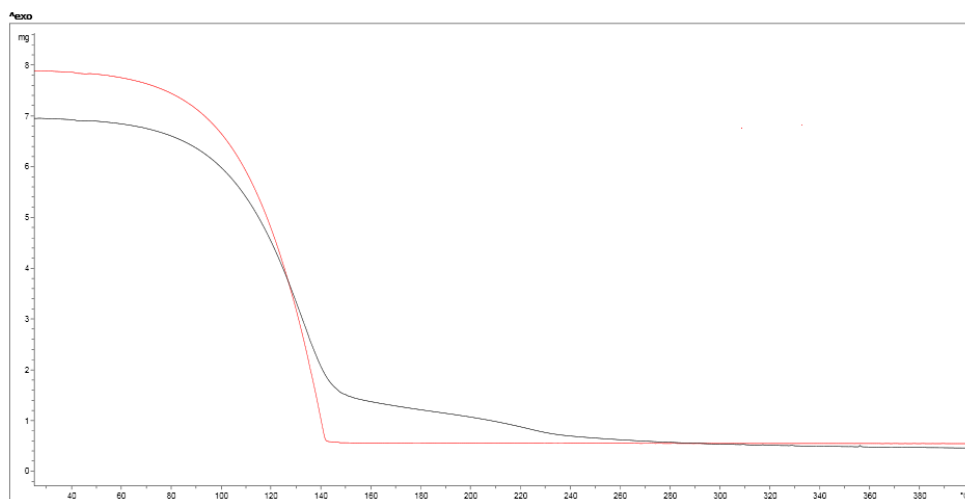
Figure 3.12. TGA curves of 2,3-dihydrobenzofuran (red) and ozonized 2,3-dihydrobenzofuran after 6 h ozonation at 130 °C (black)
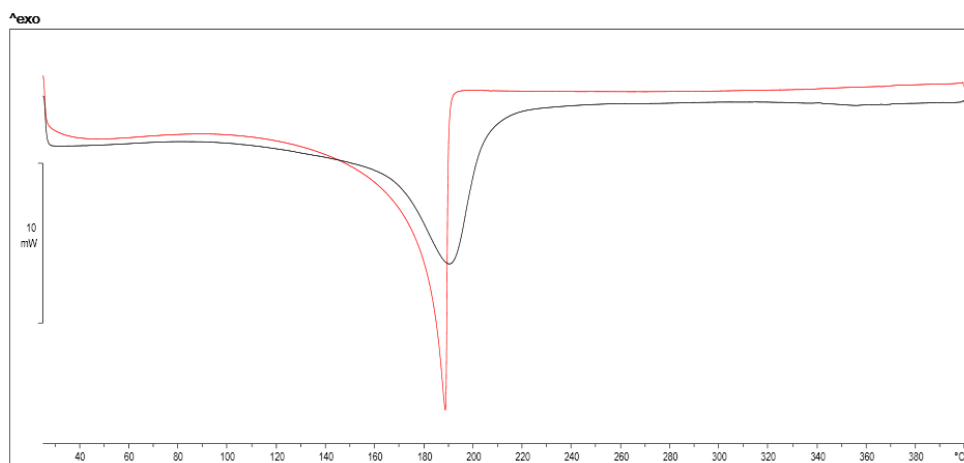
Figure 3.13. DSC curves of decalin (red) and ozonized decalin after 6 h ozonation at 130 °C (black)
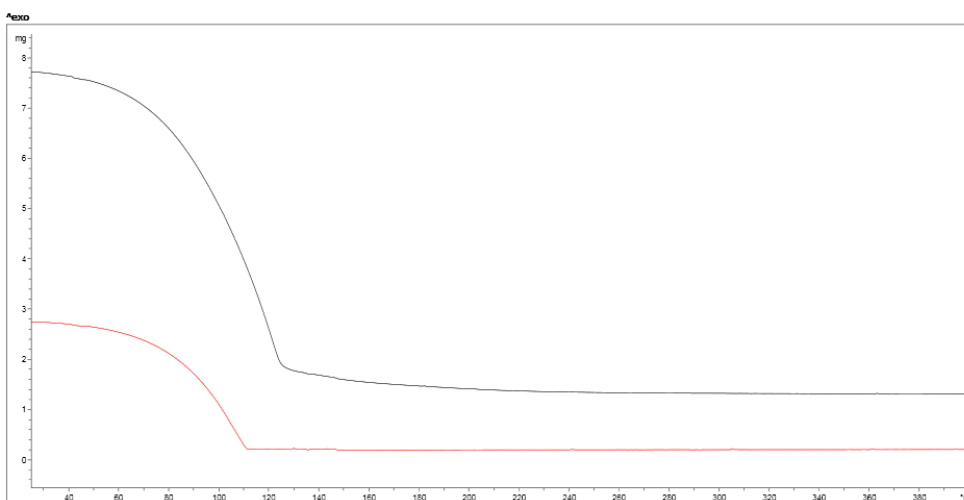
Figure 3.14. TGA curves of decalin (red) and ozonized decalin after 6 h ozonation at 130 °C (black)

3.3.4 Characterization of model compounds and ozonation products using their optical properties: Fourier transform infrared and refractive index

Infrared spectroscopy was performed to determine the nature of the functional groups formed during the ozonation. The wavenumbers of the observed peaks corresponding to specific oxygenate functional groups are given in **Table 3.8**. The identified oxygenate functional groups as well as sulphur functional group (S−O and S=O) for ozonized thianaphthene, and nitrogen functional group (N−O and N=O) for ozonized indoline, indole and quinoline identified by infrared spectroscopy are presented in **Table 3.9** and **Table 3.10**, respectively. The assignment

41

of wavenumbers to specific functional groups was based on literature. [114][115] The results obtained by infrared spectroscopy supported the identification of the ozonation products which were previously identified by mass spectroscopy.

Table 3.8. Oxygenate functional groups identified by infrared spectroscopy for ozonized model compounds

Name	Oxygenate functional group wavenumber [cm^{-1}]		
	C = O	O - H	C - O
Ozonized naphthalene	1796-1647	Not observed	1201-1181
Ozonized tetralin	1746-1649	Not observed	1165-1142; 1087-1051; 1031-1020; 1015-993
Ozonized indane	1753-1662	Not observed	1285-1270; 1213-1195; 1050-1027
Ozonized indene	1795-1649; 1620-1562; 1502-1444	3608-3236; 3116-2800	1305-1234; 1223-1186; 1172-961
Ozonized decalin	1749-1683	Not observed	Not observed
Ozonized *p*-cymene	1787-1640	3013-2993	1296-1250; 1223-1135; 1126-1106
Ozonized *n*-decane	Not observed	Not observed	Not observed
Ozonized 2,3-dihydrobenzofuran	1782-1699	Not observed	Not observed
Ozonized 2,3-benzofuran	1782-1568; 1516-1433	3156-3016; 2990-2813	1312-1220; 1186-1046

Table 3.9. Functional groups identified by infrared spectroscopy for ozonized heterocyclic S-containing model compound

Name	Oxygenate functional group wavenumber [cm^{-1}]				
	C = O	O - H	C - O	S=O	S-O
Ozonized thianaphthene	1766-1667	Not observed	Not observed	Not observed	Not observed

Table 3.10. Functional groups identified by infrared spectroscopy for ozonized heterocyclic N-containing model compounds

Name	Oxygenate functional group wavenumber [cm^{-1}]				
	C = O	O - H	C - O	N=O	N-O
Ozonized indoline	1801-1692	3090-2920	1236-1141	Not observed	Not observed
Ozonized indole	1726-1561	3113-3010	Not observed	Not observed	Not observed
Ozonized quinolone	Not observed	Not observed	1239-1222	Not observed	Not observed

As it can be observed in **Table 3.8**, **Table 3.9** and **Table 3.10**, the sensitivity of FTIR method is relatively poor and whenever the abundance of a functional group is relatively low, the IR absorption is too weak to be detected. Therefore, this method cannot detect the presence of the functional groups at very low concentrations.

As it can be seen in **Figure 3.15**, comparing the IR spectra of indene and ozonized indene revealed that the abundance of C-O, C=O and O-H bonds is significantly increased due to ozonation.
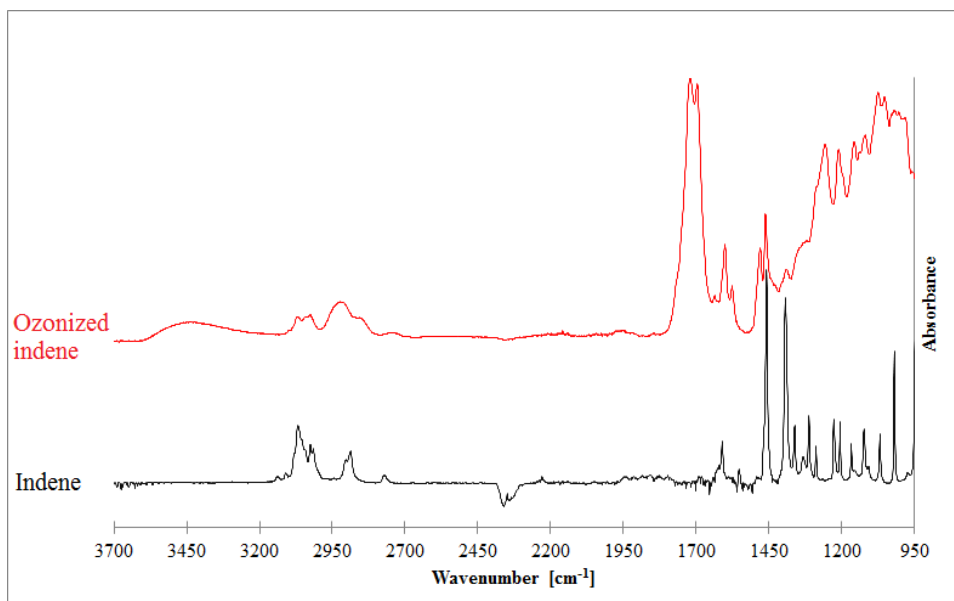
Figure 3.15. Infrared spectra of indene and ozonized indene in the spectral region of 3700 to 950 cm^{-1}

Refractive indices of the studied model compounds were determined before and after ozonation experiments at two different temperatures of 20 and 60 °C and the results are presented in **Table 3.11**.

Table 3.11. Refractive indices of the parent model compounds and ozonized model compounds, measured at 20 and 60 °C

Name	Refractive Index [n_D]		Reported RI
	20 °C	60 °C	(at 20 °C)[a]
Naphthalene	Not measured [b]	Not measured [b]	1.5821
Ozonized naphthalene	Not measured [b]	1.6098	-
Tetralin	1.5413	1.5224	1.5413
Ozonized tetralin	1.5462	1.5278	-
Indane	1.5361	1.5158	1.5370
Ozonized indane	1.5413	1.5219	-
Indene	1.5747	1.5530	1.5750
Ozonized indene	Not measured [b]	1.6071	-
Decalin	1.4755	1.4640	1.4810
Ozonized decalin	1.4797	1.5302	-
p-Cymene	1.4909	1.4715	1.4900
Ozonized p-cymene	1.5016	1.4834	-
n-Decane	1.4121	1.3937	1.4113
Ozonized n-decane	1.4130	1.3955	-
Thianaphthene	Not measured [b]	1.6191	1.6240
Ozonized thianaphthene	1.6805	1.6427	-
Indoline	1.5933	1.5739	1.5920
Ozonized indoline	1.6110	1.5927	-
Indole	Not measured [b]	1.6094	-
Ozonized indole	Not measured [b]	1.6366	-
Quinoline	1.6264	1.6070	1.6250
Ozonized quinolone	1.6283	1.6096	-
2,3-Dihydrobenzofuran	1.5536	1.5348	1.5490
Ozonized 2,3-dihydrobenzofuran	1.5549	1.5364	-
2,3-Benzofuran	1.5675	1.5472	1.5690
Ozonized 2,3-benzofuran	1.5741	1.5549	-

The effect of temperature on refractive index of the parent model compounds and ozonized model compounds was determined from the measurements at 20 and 60 °C. As it can be observed in **Table 3.11**, a decrease in refractive index with an increase in measuring temperature is established for all of the model compounds and ozonized model compounds, except for ozonized decalin. For ozonized decalin, the refractive index increased with increasing the measuring temperature from 20 to 60 °C. The decrease in the refractive index with an increase in the temperature is caused by the density of the liquid that usually decreases with temperature; accordingly the speed of light in a liquid normally increases as the temperature increases, according to **Equation 3.6** for calculating the refractive index of a compound: [116][117]

$$RI_i = {^C}\!/_{v_i} \qquad\qquad\qquad \textbf{Equation 3.6}$$

Where,

RI_i is the refractive index of compound i,

C is the speed of light in vacuum; c = 299792458 m s^{-1},

v_i is the speed of light in compound i [m s^{-1}].

Studying the refractive indices might be of assistance in interpreting spectroscopic data. Refractive index does not provide detailed information about molecular structure. However, one structural factor that influences the refractive index of a sample is its polarizability. [116] Substances containing more polarizable groups will normally have higher refractive indices than substances containing less polarizable groups. [116][118] Although aromatics have lower polarizability compared to paraffins, they have higher refractive indices compared to paraffins due to their higher density. Comparison of the refractive indices of the parent model compounds and ozonized model compounds measured at the same temperature revealed an increase in refractive index and polarizability due to 6 h ozonation at 130 °C, as it can be seen in **Table 3.11**. This could be an indication of an increase in the amount of oxygenate functional groups as

well as increase in the density of the studied model compounds due to ozonation, which leads to higher density and polarizability for ozonized compounds compared to their parent compounds which accordingly leads to an increase in their refractive index.

To test the hypothesis that the parent model compounds and ozonized model compounds are associated with statistically different mean refractive indices, an independent samples t-test at a 5% significance level was performed and the results are presented in Appendix B. Based on the results, it can be concluded that for all the studied model compounds the mean refractive index of the parent compound and the ozonized compound are statistically different in all the cases at both measurement temperatures of 20 and 60 °C.

3.3.5 Physical characteristics of model compounds: density and appearance

Introduction of oxygenate functional groups into model compounds caused significant changes in their physical properties, as claimed by Moschopedis (1978). The physical properties of the ozonized model compounds were significantly different from those of the parent compounds. [119]

Density of liquid studied model compounds before and after 6 h ozonation measured at 20 °C is presented in **Table 3.12**. Changes in the density of the parent model compounds indicate formation of different compounds due to 6 h ozonation at 130 °C, and it also correlates with the increase in the bitumen density due to formation of oxygenate functional groups. [120]

Table 3.12. Density of the liquid parent compounds and ozonized model compounds, measured at 20 °C

Name	Density at 20°C [kg.m^{-3}]
Naphthalene	Not measured [a]
Ozonized naphthalene after 6 h ozonation at 130 °C	Not measured [a]
Tetralin	968.8
Ozonized tetralin after 6 h ozonation at 130°C	1007.8
Indane	958.9
Ozonized indane after 6 h ozonation at 130°C	998.1
Indene	996.1
Ozonized indene after 6 h ozonation at 130 °C	Not measured [a]
Decalin	883.8
Ozonized decalin after 6 h ozonation at 130°C	915.2
p-Cymene	856.9
Ozonized p-cymene after 6 h ozonation at 130°C	924.1
n-Decane	730.1
Ozonized n-decane after 6 h ozonation at 130°C	-[b]
Thianaphthene	Not measured [a]
Ozonized thianaphthene after 6 h ozonation at 130°C	1212.6
Indoline	1063.7
Ozonized indoline after 6 h ozonation at 130°C	1180.3
Indole	Not measured [a]
Ozonized indole after 6 h ozonation at 130°C	Not measured [a]
Quinoline	1092.9
Ozonized quinolone after 6 h ozonation at 130°C	1108.0
2,3-Dihydrobenzofuran	1065.7
Ozonized 2,3-dihydrobenzofuran after 6 h ozonation at 130°C	1123.5
2,3-Benzofuran	1072.6
Ozonized 2,3-benzofuran after 6 h ozonation at 130°C	1094.8

[a] The density of powdered materials could not be measured with the employed density meter.

[b] There was not enough sample left for density measurement.

The physical appearance of the studied model compounds before ozonation experiments is presented in **Table 3.13**. The colour and in some cases the physical state of the parent model compound is changed over 6 h ozonation at 130 °C, as it can be observed in **Figure 3.16**. This could be an indication of formation of different compounds with different functional groups compared to the parent component due to reaction with ozone.

Table 3.13. Physical appearance of the selected model compounds used for ozonation study

Compound name	Appearance
Naphthalene	White flakes
Tetralin	Colourless clear liquid
Indane	Light yellow clear liquid
Indene	Yellow clear liquid
Decalin – cis/trans	Colourless clear liquid
p-Cymene	Light yellow clear liquid
n-Decane	Colourless clear liquid
Thianaphthene	Beige solidified mass or fragments
Indoline	Dark brown clear liquid
Indole	Light brown flakes
Quinoline	Light yellow clear liquid
2,3-Dihydrobenzofuran	Light yellow clear liquid
2,3-Benzofuran	Yellow clear liquid

Indane

30 min 60 min 120 min 240 min 360 min

Indene

30 min 60 min 120 min 240 min 360 min

Decalin

30 min 60 min 120 min 240 min 360 min

p-cymene

30 min 60 min 120 min 240 min 360 min

n-decane

30 min 60 min 120 min 240 min 360 min

Thianaphthene

30 min 60 min 120 min 240 min 360 min
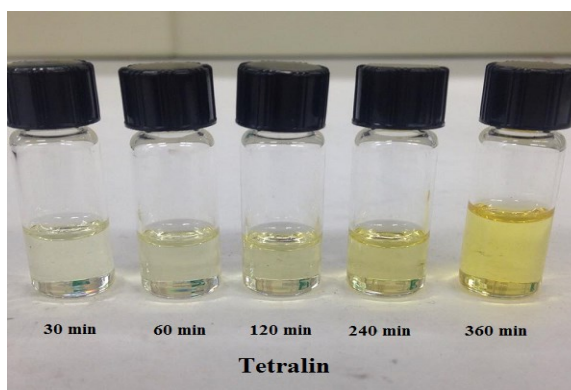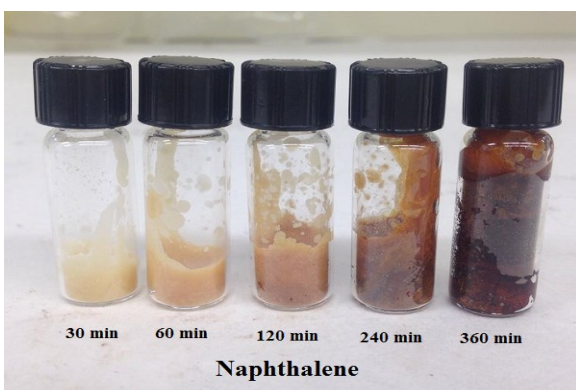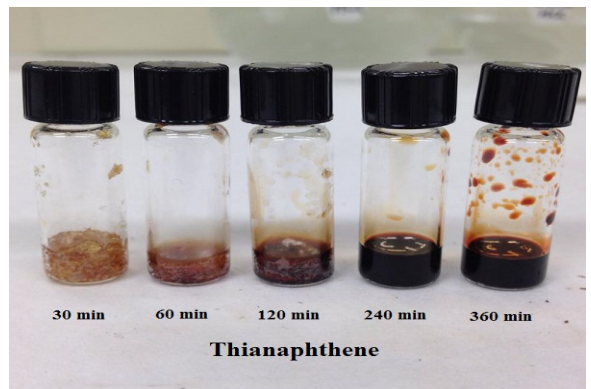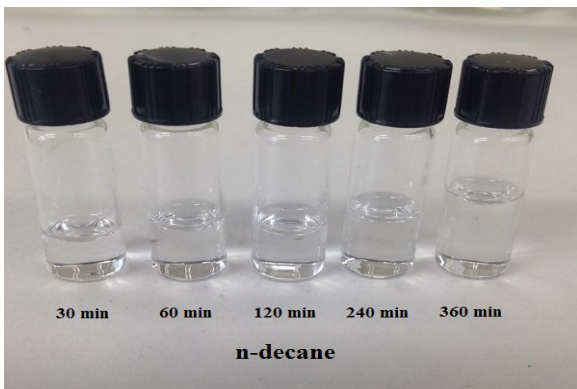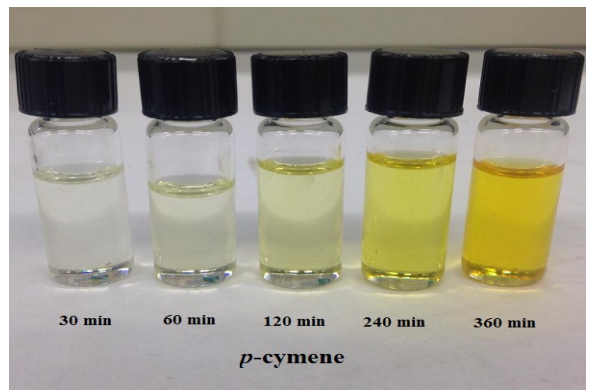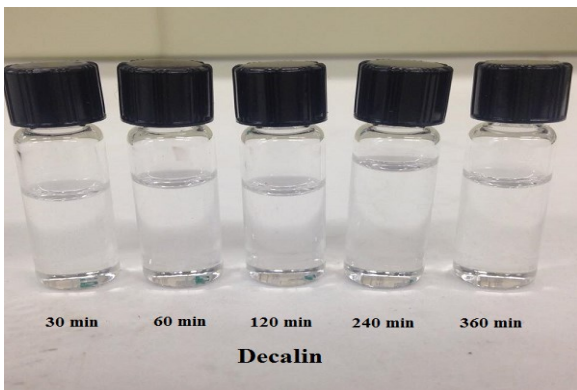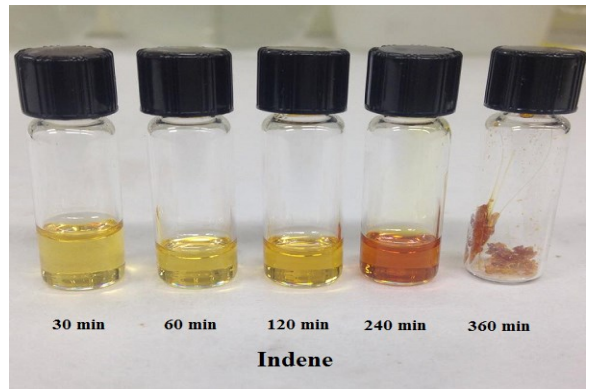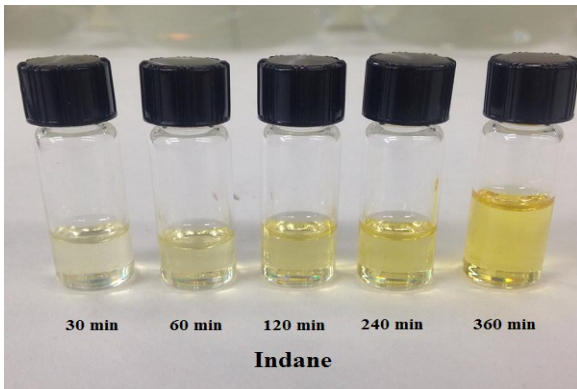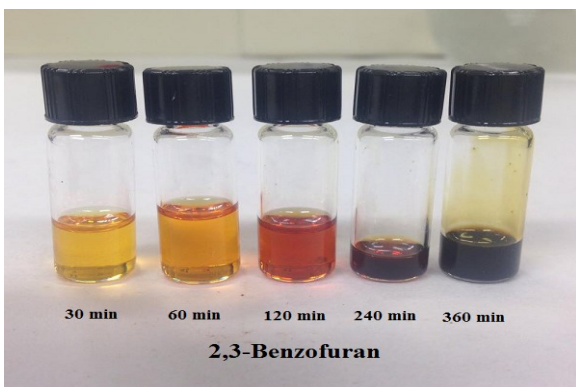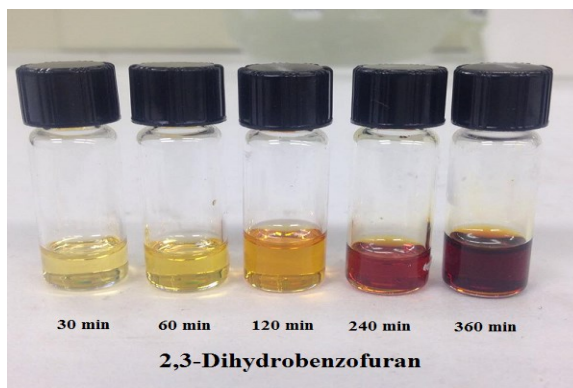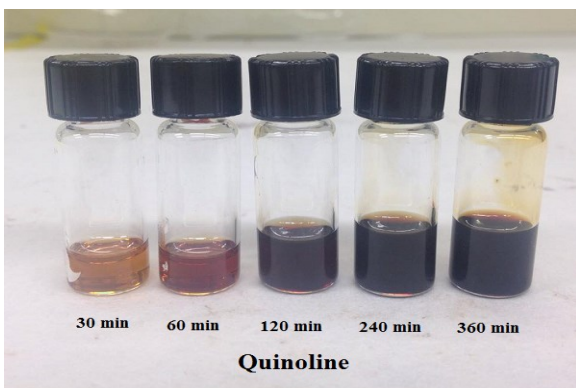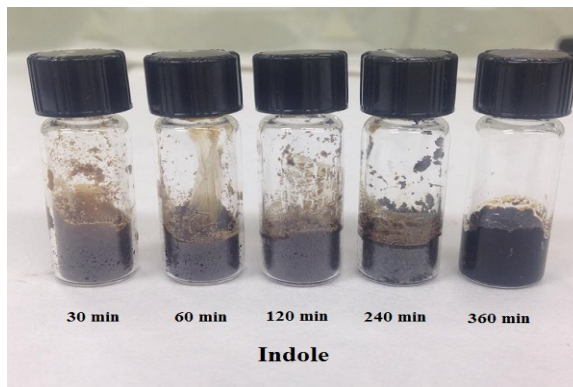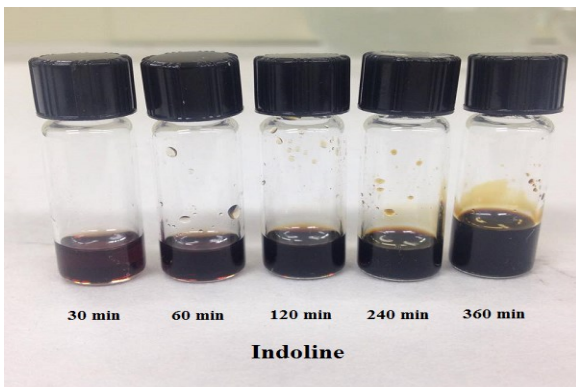
Figure 3.16. Samples collected during ozonation of model compounds at 30, 60, 120, 240 and 360 min from left to right

3.4 Ozonation of aromatic and alkylaromatic compounds

Recently there has been considerable interest in the mechanism of the reactions of C-H bonds in different hydrocarbon compound classes by ozone. [121][122][123][124][125][126][127][128][129] The conversion of naphthalene, as an aromatic compound, and *p*-cymene, as an alkylaromatic

compound found in bitumen over 6 h ozonation at 130 °C is studied and the profile of ozonation conversion versus time for naphthalene and *p*-cymene is presented in **Figure 3.17**. The ozone-enriched air flow rate of 120 ml min^{-1}, which is equivalent to 144 ml h^{-1} ozone-enriched air per gram of model compound feed, was used as the oxidant in the ozonation experiments.

Naphthalene was subjected to ozonation at 130 °C with a very low conversion rate over 6 h ozonation, whereas, *p*-cymene was more rapidly converted to ozonation products under the same reaction condition. As it can be seen in **Figure 3.17**, ozonation conversion of *p*-cymene increased with time and ozonation products formed early on during ozonation. For naphthalene, ring-cleavage reaction products as well as primary and secondary products were formed over the ozonation time. However, no addition products were formed in naphthalene ozonation. For *p*-cymene, primary, secondary and addition products were formed during ozonation. However, no ring-cleavage reaction products were formed in *p*-cymene ozonation. The maximum ozonation conversion for naphthalene was 2.44 wt % and for *p*-cymene was 78.24 wt %. Despite high ozonation conversion of *p*-cymene, the reaction was selective toward primary and secondary products. Addition reaction products appeared only when the ozonation conversion was more than 18.07 wt %.

Previous studies on ozonation of alkylaromatic compounds revealed that for this group of compound class, ozone attack on the benzylic carbon can be the major reaction, and some attack on the benzene ring could also occur. [130][131][132] In *p*-cymene the presence of two benzylic carbons located in α-position relative to the aromatic ring resulted in a high ozonation conversion rate compared to naphthalene. In *p*-cymene, the benzylic carbon in the isopropyl group is a tertiary carbon, and the other benzylic carbon in the methyl group is a primary carbon. Several studies have shown that in the ozonation of *p*-cymene, the tertiary benzylic carbon is attacked in preference to the primary benzylic carbons. [133] Thus, in ozonation of *p*-cymene the tertiary C–H bond in an α-position to the aromatic ring is particularly capable of ozonation and it has been reported that its ozonation reaction rate is approximately 18 times more than the primary C–H bonds. [134]

The alkyl side chain of aromatic ring in *p*-cymene can undergo ozonation by several mechanisms. Among which, the most common and dominant one is the attack of ozone molecule

at benzylic carbon and formation of *p*-cymene hydroperoxide at α-position relative to the aromatic ring as the reaction intermediate. [135][136] Then, the formation of addition reaction products could take place due to formation of C−C bond either by addition of two *p*-cymene free radicals, or addition reaction of a *p*-cymene free radical at a double bond formed by oxidative dehydrogenation due to scission of C−H bond on the primary carbon. [112] Some addition products were observed after 2 h of ozonation (**Figure 3.18**). In alkylaromatic compounds, depending on the reaction time, reaction temperature and quantity of ozone, the aromatic ring could participate in the ozonation reaction. [130][131][132] The ozone attack to the benzylic carbon of alkylaromatic compounds is free radical chain reaction mechanism, and the ozone attack to the aromatic ring of alkylaromatic compounds is an electrophilic reaction mechanism which might lead to cleavage of the aromatic ring. [121]

Figure 3.17. Ozonation conversion versus time for *p*-cymene and naphthalene over 6 h ozonation at 130 °C; with an ozone-enriched air flow rate of 120 ml min^{-1} which is equivalent to 144 ml h^{-1} per gram of model compound feed
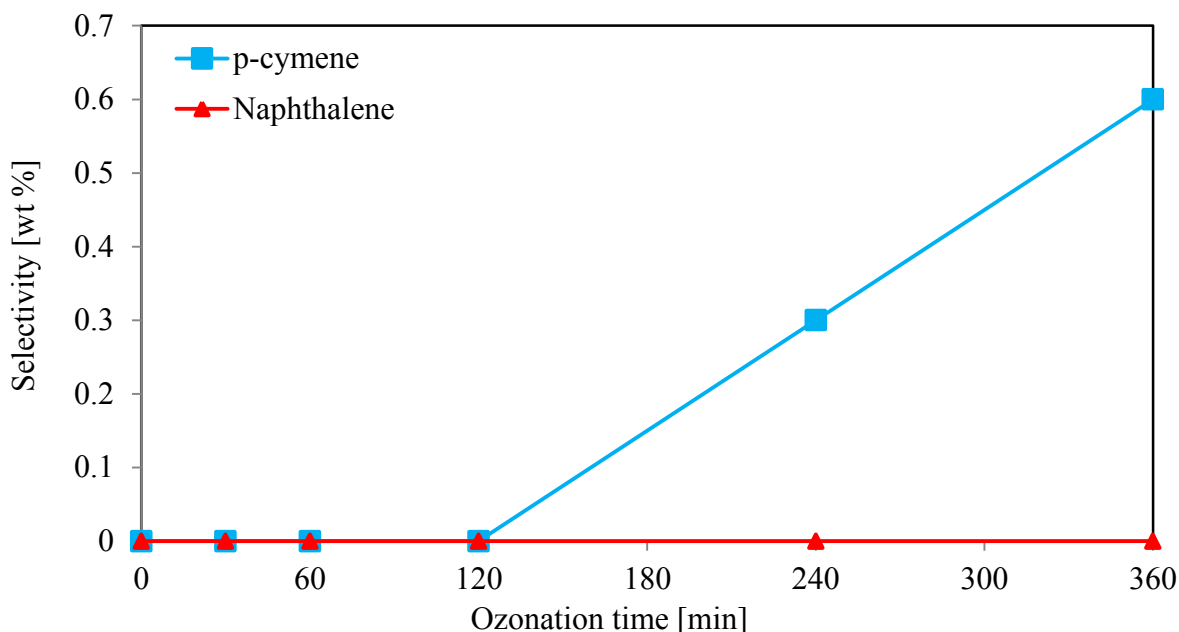
Figure 3.18. Selectivity to addition reaction products versus time for *p*-cymene and naphthalene over 6 h ozonation at 130 °C; with an ozone-enriched air flow rate of 120 ml min^{-1} which is equivalent to 144 ml h^{-1} per gram of model compound feed

In naphthalene, the most reactive atom with the lowest atom-localization energy (atom 1, as shown in **Table 3.2**) is included in the most reactive bond with the lowest bond-localization energy (1,2-bond), and the ozone attack presumably occurs at this bond first and leads to formation of mono-ozonide which has an olefinic 3,4-bond which is then rapidly attacked by ozone and leads to formation of highly reactive naphthalene diozonide, followed by rearrangements of the diozonide and formation of the ozonation reaction products. [121][137][138][139] It has been reported in aromatic compounds, ring-cleavage reaction might occur due to ozonation. [140][141] Few ring-cleavage reaction products, e.g. 1,2-benzenedicarboxylic acid, 1,2-benzenedicarboxaldehyde and 2-hydroxybenzaldehyde (shown in **Figure 3.19**), formed over 6 h naphthalene ozonation at 130 °C as the result of ozone attack on 1,2-bond of naphthalene.

| 2-hydroxybenzaldehyde | 1,2-benzenedicarboxylic acid | 1,2-benzenedicarboxaldehyde |
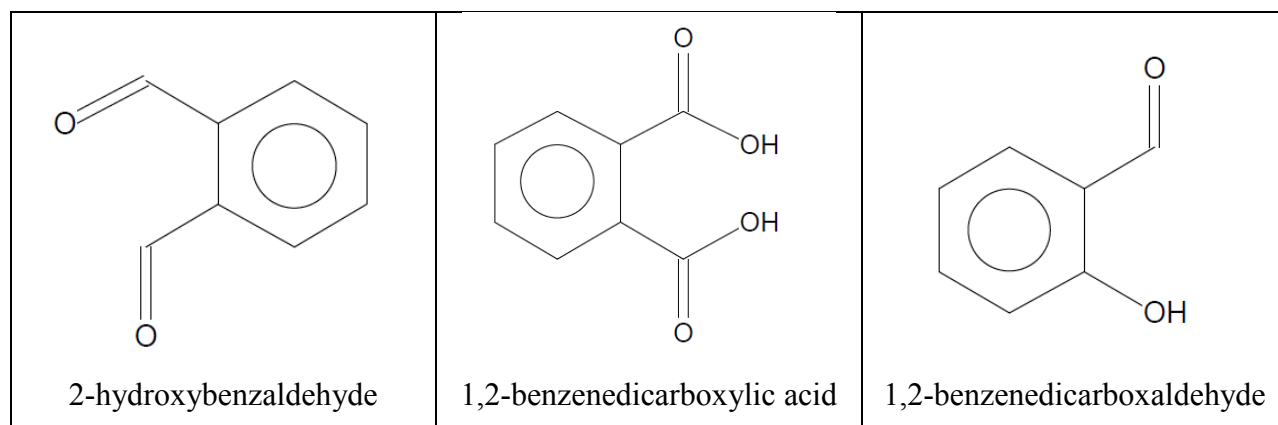
Figure 3.19. Structural formula of some of the ring-cleavage reaction products formed as a result of ozone attack on 1,2-bond of naphthalene after 6 h ozonation at 130 °C; obtained from NIST library

A Comparison between the results obtained for the ozonation and autoxidation conversion rate of *p*-cymene and naphthalene under the same reaction condition was performed. This comparison shows that naphthalene was not converted to the reaction products at all due to oxidation with air, but it had a slight conversion to the products due to ozonation. For *p*-cymene, in both ozonation and oxidation the conversion rate is approximately the same in the first 2 h of the reaction, but after that, ozonation conversion exceeds autoxidation conversion. This could be due to strong oxidation ability of ozone compared to oxygen in air. [112]

3.5 Ozonation of naphthenic-aromatic compounds

In order to understand the ozonation behaviour of naphthenic-aromatic compounds in bitumen, tetralin, indane and indene were ozonized at 130 °C for 6 h with an ozone-enriched air flow rate of 120 ml min^{-1} (equivalent to 144 ml h^{-1} ozone-enriched air per gram of model compound feed).

The ozonation conversion of tetralin, indane and indene versus time was determined and illustrated in **Figure 3.20**. As it can be seen, tetralin and indane had slow and moderate conversion rate respectively. However, indene had considerably higher conversion rate compared to the former. The ozonation conversion of all three molecules increased with time. During ozonation of tetralin, indane and indene, primary, secondary, ring-cleavage reaction products and also addition products were formed, however for tetralin the tendency to form addition products was very low compared to indane and indene, as presented in **Figure 3.21**. The maximum

55

calculated ozonation conversion of indene was approximately 84.68 wt %, which was the highest conversion among all the studied compound classes. For Indene, its silectivity to formation of addition reaction products increased with time after an induction period of 60 min.

The higher conversion of indene can be explained by the presence of unconjugated double bond in the naphthenic ring of indene. In ozonation of naphthenic-aromatic compounds, ozone preferentially attacks the C−H bond located at the α-position to the aromatic ring. [142][143] In hydrocarbons containing unconjugated double bonds ozone attacks the C−H bond located in α-position relative to the unconjugated double bond. [112][144][145] So in indene ozonation, ozone attack can take place at both the C−H bond located in α-position relative to the aromatic ring and the C−H bond located in α-position relative to the double bond. The indirect ozone attack at the unconjugated double bond in the five-membered ring of indene leads to formation of free radical addition reaction products. However, direct ozone attack at the unconjugated double bond of indene lead to scission of the double bond and formation of a single compound containing two carbonyl groups. [121]

In tetralin and indane, as the result of scission of C−H bond due to ozone attack, corresponding hydroperoxides with −OOH group formed at the carbon atom at α-position relative to the aromatic ring are produced as primary ozonation products. [142][143] Tetralin did not form addition reaction products during first stages of ozonation, and after 60 min induction period, its selectivity to formation of addition reaction products increased with a very slow rate. The selectivity to addition reaction products for indane ozonation had also an induction period of 60 min, but after that period it increased with a relatively higher rate compared to tetralin. The relatively higher conversion rate of indane compared to tetralin was likely due to the fact that the six-membered naphthenic ring of tetralin experiences less angle strain compared to the five-membered naphthenic ring of indane, and the former has a higher stability toward reaction with ozone than the latter. [146][147]

Figure 3.20. Ozonation conversion versus time for tetralin, indane and indene over 6 h ozonation at 130 °C; with an ozone-enriched air flow rate of 120 ml min^{-1} which is equivalent to 144 ml h^{-1} per gram of model compound feed

Figure 3.21. Selectivity to addition reaction products versus time for tetralin, indane and indene over 6 h ozonation at 130 °C; with an ozone-enriched air flow rate of 120 ml min^{-1} which is equivalent to 144 ml h^{-1} per gram of model compound feed

3.6 Ozonation of heterocyclic O-containing compounds

The ozonation conversion versus time for 2,3-dihydrobenzofuran and 2,3-benzofuran employed as heterocyclic O-containing compounds found in bitumen, due to 6 h ozonation at 130 °C is presented in **Figure 3.22**. The ozonation conversion of 2,3-dihydrobenzofuran had a polynomial increase with degree of 2 with respect to time, whereas, the conversion of 2,3-benzofuran had a slow and linear increase over time after 30 min induction period. Primary, secondary and ring-cleavage and addition product were formed during ozonation of 2,3-benzofuran and 2,3-dihydrobenzofuran. Tendency of both compounds to the formation of addition reaction products increased with time after 60 min induction period.

As it can be seen in **Figure 3.23**, for 2,3-benzofuran the rate of increase in its selectivity to addition products has markedly increased from 60 to 120 min, and afterwards it increased with a very slow rate over time. For 2,3-dihydrobenzofuran, at the end of the ozonation experiment, the only identified products were addition products. Higher conversion of 2,3-dihydrobenzofuran compared to 2,3-benzofuran can be explained by the presence of a non-aromatic five-membered

ring attached to a benzene ring in 2,3-dihydrobenzofuran which is highly unstable and highly reactive, and wants to aromatize and produce 2,3-benzofuran. In ozonation of furans, ozone preferentially attacks at the C–H bond located at the α-position to the aromatic ring. This is similar to the ozonation of naphthenic-aromatic compounds in which ozonation readily takes place at the C–H bond located at the α-position to the aromatic ring. The ozone attack can also take place at the C–H bond located at the α-position to the oxygen atom. [112][148] The radical intermediates formed by scission of either the C–H bond located at α-position to the benzene ring or the C–H bond located at α-position to the oxygen atom can lead to free radical addition reactions. In ozonation of 2,3-benzofuran, ozone can directly attack the double bond of the furan ring to form molozonide as the reaction intermediate, which will rearrange to form ozonation products.
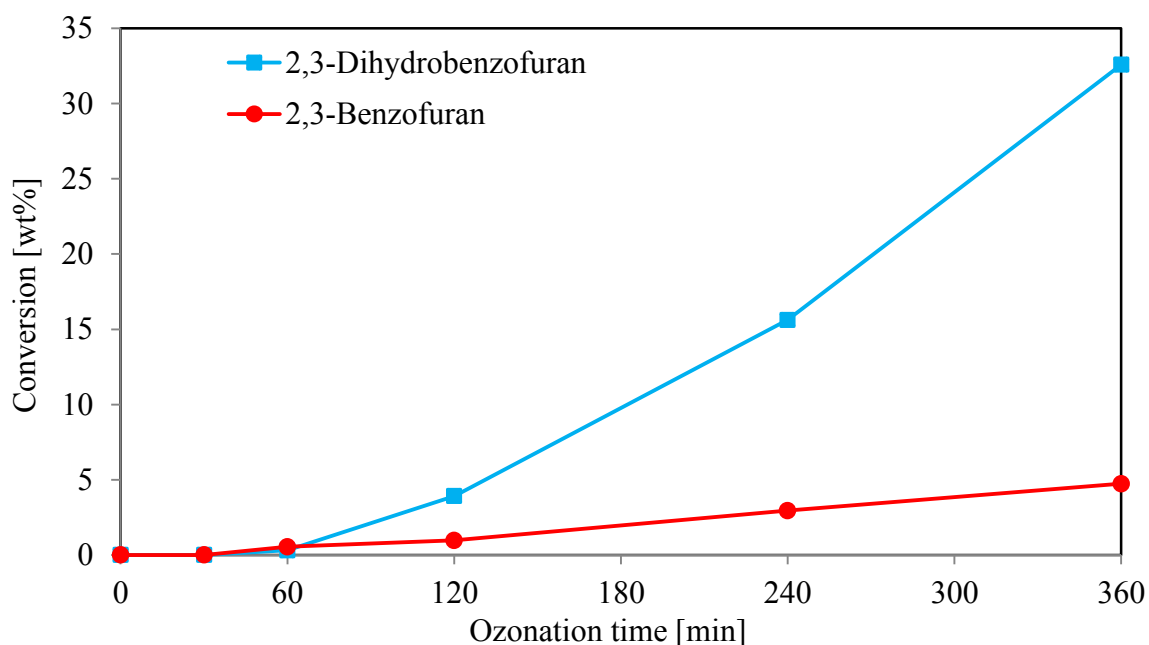
Figure 3.22. Ozonation conversion versus time for 2,3-dihydrobenzofuran and 2,3-benzofuran over 6 h ozonation at 130 °C; with an ozone-enriched air flow rate of 120 ml min^{-1} which is equivalent to 144 ml h^{-1} per gram of model compound feed
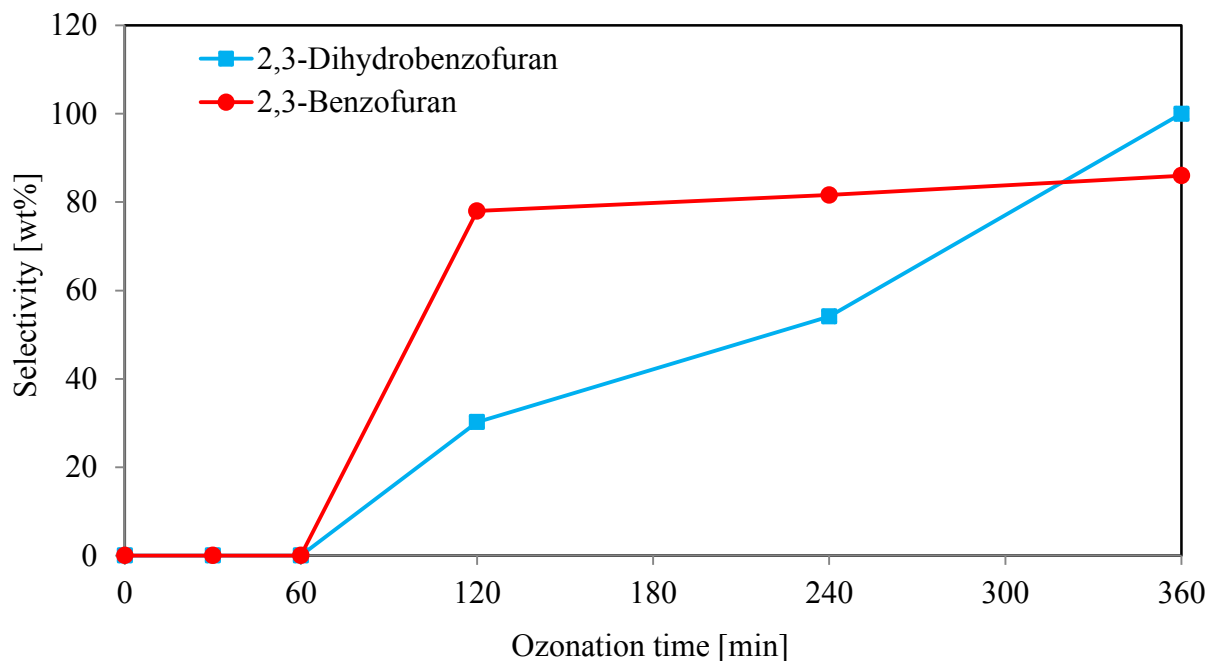
Figure 3.23. Selectivity to addition reaction products versus time for 2,3-dihydrobenzofuran and 2,3-benzofuran over 6 h ozonation at 130 °C; with an ozone-enriched air flow rate of 120 ml min^{-1} which is equivalent to 144 ml h^{-1} per gram of model compound feed

3.7 Ozonation of heterocyclic N-containing compounds

In order to understand the ozonation behaviour of heterocyclic N-containing compounds in bitumen, quinoline, indole and indoline were ozonized at 130 °C for 6 h with an ozone-enriched air flow rate of 120 ml min^{-1} (equivalent to 144 ml h^{-1} ozone-enriched air per gram of model compound feed). The ozonation conversion versus time for these model compounds is presented in **Figure 3.24**. Transformation of indole and quinoline under the action of ozone started after an induction period of 30 and 120 min respectively. The maximum ozonation conversion of quinoline was approximately 0.52 wt %, which was the lowest conversion observed among all the studied compound classes. Primary, secondary, ring-cleavage and addition products were formed during ozonation of indole, indoline and quinoline. Despite the relatively low conversion rate of quinolone, indole and indoline, they had a high tendency to form addition reaction products over the other types of reaction products, as it can be observed in **Figure 3.25**, and their tendency to form addition reaction products increased with time.

60

The higher ozonation conversion of indoline can be explained by the presence of non-aromatic five-membered ring attached to a benzene ring. In ozonation of indoline like 2,3-dihydrobenzofuran, ozone preferentially attacks at the C−H bond located at the α-position to the aromatic ring. [149][150][151][152] Ozone can also attack at the C−H bond located at the α-position to the nitrogen atom. [112][117] The radical intermediates formed by scission of either the C−H bond located at α-position to the benzene ring or the C−H bond located at α-position to the nitrogen atom can lead to free radical addition reactions. Indoline was aromatized by ozonation. For this group of compounds, addition reaction products could be formed through C−C, C−N and N−N linkage of the free radicals. [153][154][155]

The relatively higher ozonation conversion of indole compared to quinoline can be explained as the six-membered N-containing ring in quinoline experiences lower angle strains than the five-membered N-containing ring in indole, which makes quinoline more stable toward reaction with ozone compared to indole. [146][147][150]
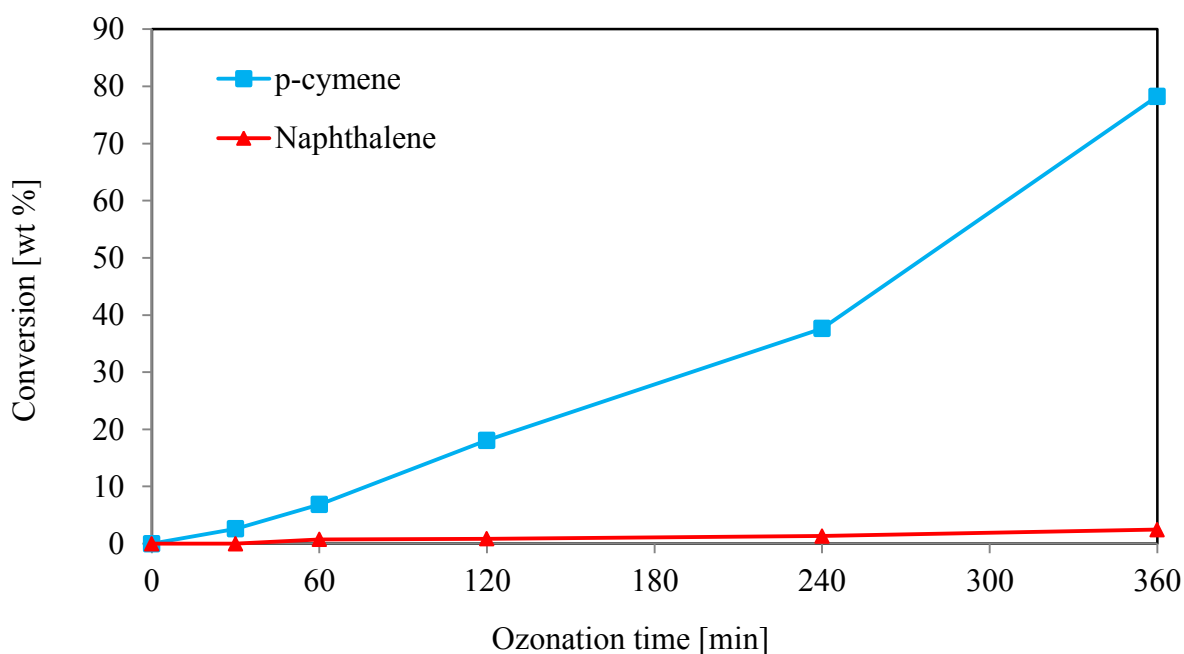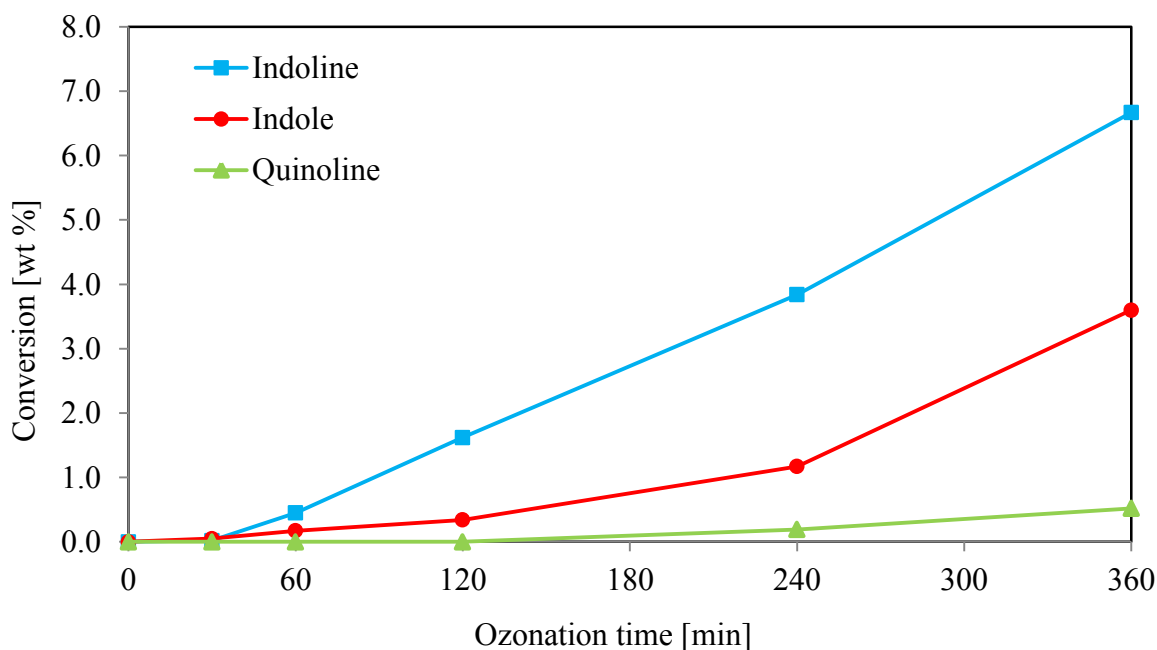

Figure 3.24. Ozonation conversion versus time for indole, indoline and quinoline over 6 h ozonation at 130 °C; with an ozone-enriched air flow rate of 120 ml min^{-1} which is equivalent to 144 ml h^{-1} per gram of model compound feed

3.8   Ozonation of heterocyclic S-containing compounds

Thianaphthene was ozonized at 130 °C for 6 h with an ozone-enriched air flow rate of 120 ml min^{-1} (equivalent to 144 ml h^{-1} ozone-enriched air per gram of model compound feed) in order to understand the ozonation behaviour of heterocyclic S-containing compounds found in bitumen. Ozonation conversion versus time for thianaphthene is shown in **Figure 3.26**. For thianaphthene, the increase in conversion rate was polynomial with order of 2 with respect to time. Primary, secondary, ring-cleavage and addition products were formed during ozonation of thianaphthene. The tendency of thianaphthene to form addition reaction products increased with time after an induction period of 30 min, and it stayed fairly constant from 240 to 360 min, 73 to 75.4 wt %. The ozonation mechanism of thiophene in thianaphthene is very similar to that of furan, such as 2,3-benzofuran. In ozonation of thianaphthene, ozone attacks at the C–H bond in α-position relative to the sulphur atom. [116]
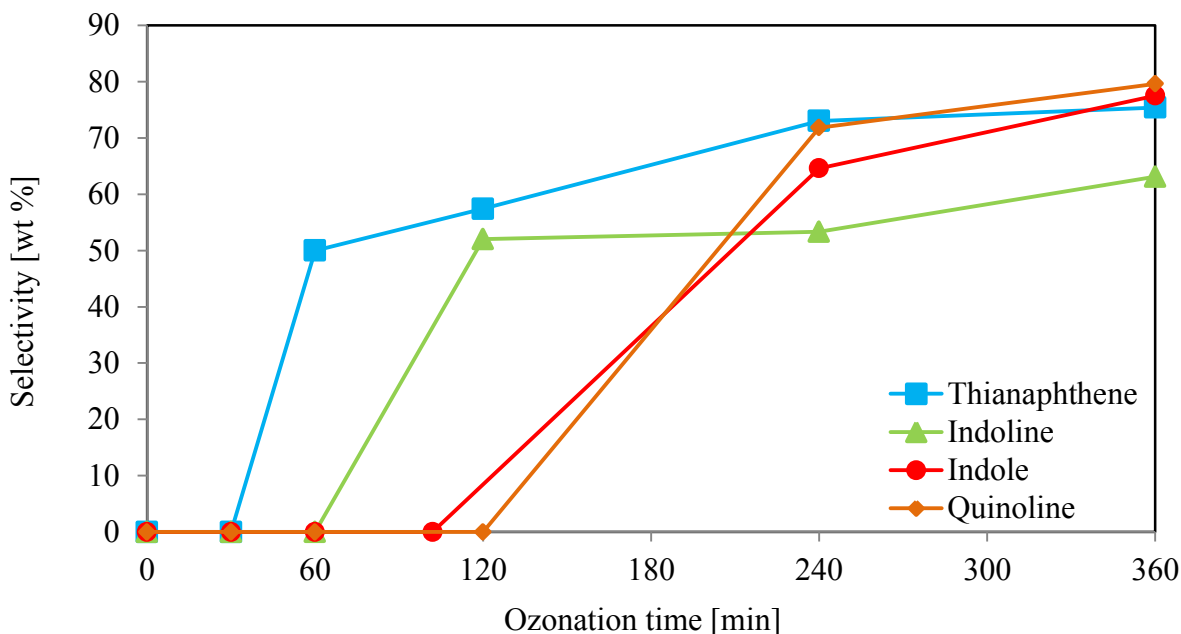
Figure 3.25. Selectivity to addition reaction products versus time for thianaphthene, indole, indoline, quinoline over 6 h ozonation at 130 °C; with an ozone-enriched air flow rate of 120 ml min^{-1} which is equivalent to 144 ml h^{-1} per gram of model compound feed
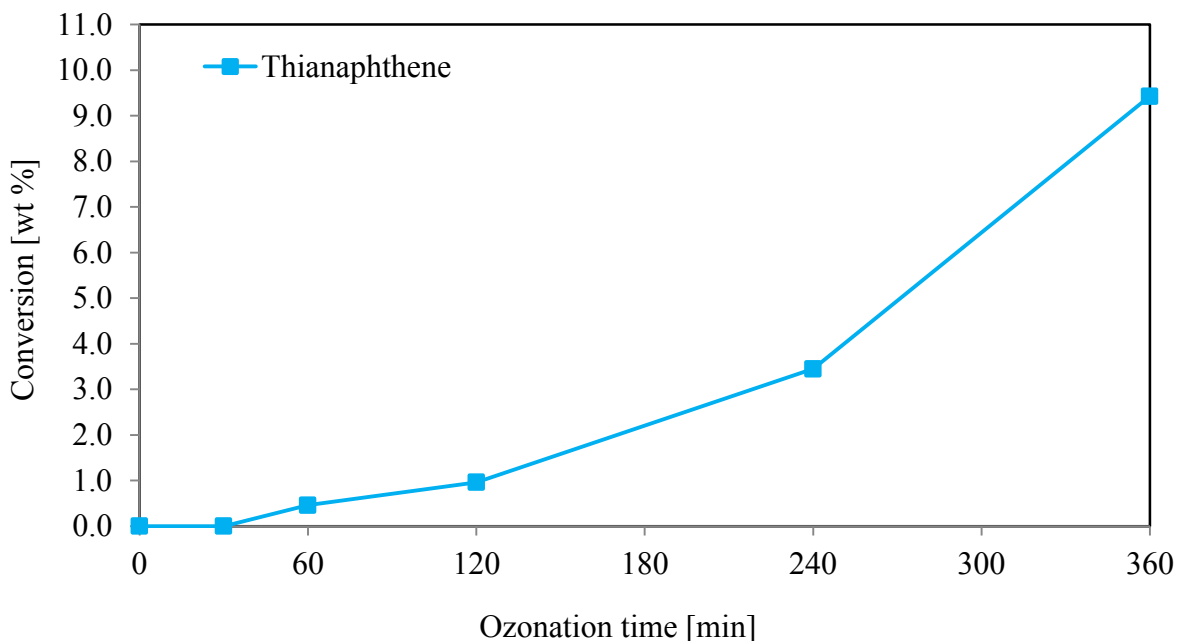
Figure 3.26. Ozonation conversion versus time for thianaphthene over 6 h ozonation at 130 °C; with an ozone-enriched air flow rate of 120 ml min⁻¹ which is equivalent to 144 ml h⁻¹ per gram of model compound feed

Like hydrocarbon compound classes, addition reaction of heterocyclic compound classes took place through C–C bond formation. In alkylaromatic compounds, naphthenic-aromatic and heterocyclic compounds, depending on the reaction time, temperature and the quantity of ozone, the benzene ring can participate in ozonation reaction as well. [121]

3.9   Ozonation of naphthenic and acyclic paraffinic compounds

The ozonation conversion versus time for decalin, as a naphthenic compound, and *n*-decane, as an acyclic paraffinic compound found in bitumen due to 6 h ozonation at 130 °C is shown in **Figure 3.27**. The ozonation conversion rate of naphthenic decalin was higher than acyclic paraffinic *n*-decane. The conversion rate from *n*-decane ozonation was significantly different from the conversion rate of decalin ozonation. As it can be observed in **Figure 3.28**, decalin produced primary and secondary ozonation products in the first 240 min of ozonation. The formation of addition products only can be observed after that period. Yet, the tendency of decalin to form addition products was significantly lower than naphthenic-aromatic and heterocyclic compounds. *n*-Decane only produced primary and secondary products over 6 h

63

ozonation at 130 °C, with significantly lower conversion rate compared to decalin. Although, both decalin and *n*-decane have eight methylene groups having C–H bonds on secondary carbons, decalin had a shorter induction period and higher conversion rate. This was because decalin also has two tertiary carbons and two C–H bonds located on the tertiary carbons, which resulted in a more stable tertiary carbon-centered free radical after C–H bond scission. Upon ozonation of decalin, the tertiary C–H bonds are attacked leading to the formation of corresponding tertiary alcohols. [156] Previous works done on decalin ozonation revealed that the major products of the reaction were the corresponding cyclic-alcohols, cyclic-ketones and cycloalkyl hydroperoxides and peroxides. Afterwards, secondary products were formed from further reactions of these compounds to provide ring-cleavage products. [157][158][159][160]

Several works reported on ozonation of paraffinic compounds, specifically decane. [140][160][161] For *n*-decane, the ozonation conversion had a prolonged induction period of more than 2 h, followed by slow ozonation. In *n*-decane, the C–H bonds on primary and secondary carbons are more difficult to be ozonized, because of the low stability of primary and secondary carbon centered free radicals that are formed. In general, tertiary C–H bonds are the most reactive, and primary C–H bonds are the least. [124][129] Here, the secondary C–H bonds were being the bond of lowest bond energy, which were the reaction center of *n*-decane molecule and were attacked by ozone. [156] Products obtained from ozonation of *n*-decane due to cleavage of secondary C–H bond by ozonation reaction were alcohols, ketones, carboxylic acid, esters and peroxides. [140][156][160] Only primary and secondary ozonation products were observed during the ozonation of *n*-decane.
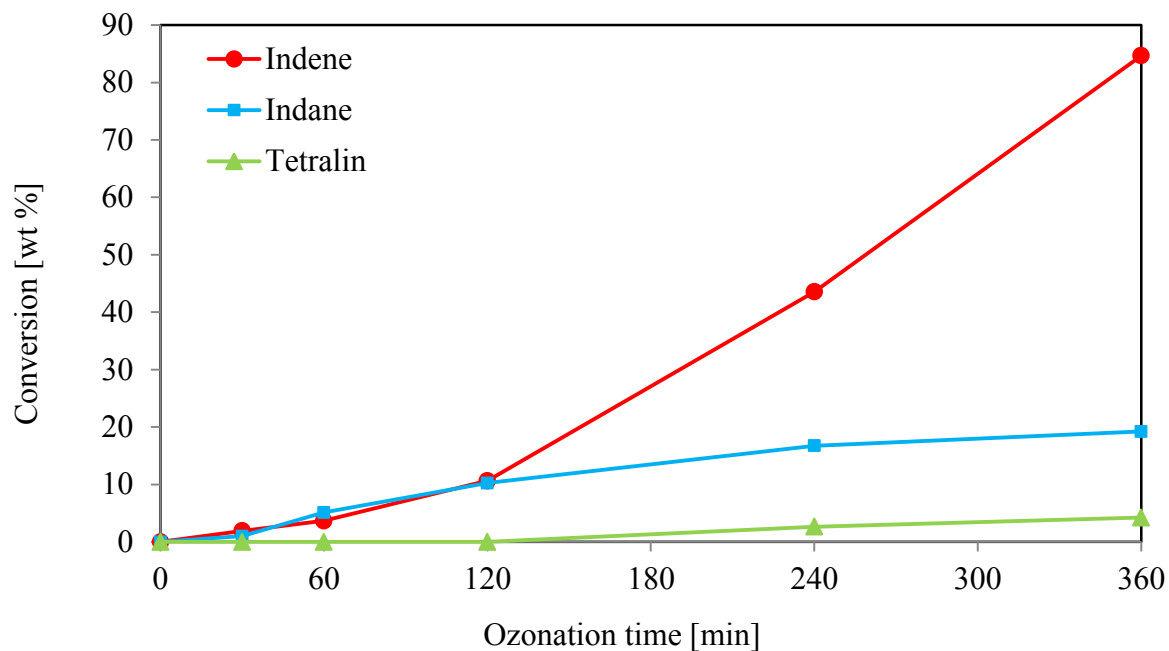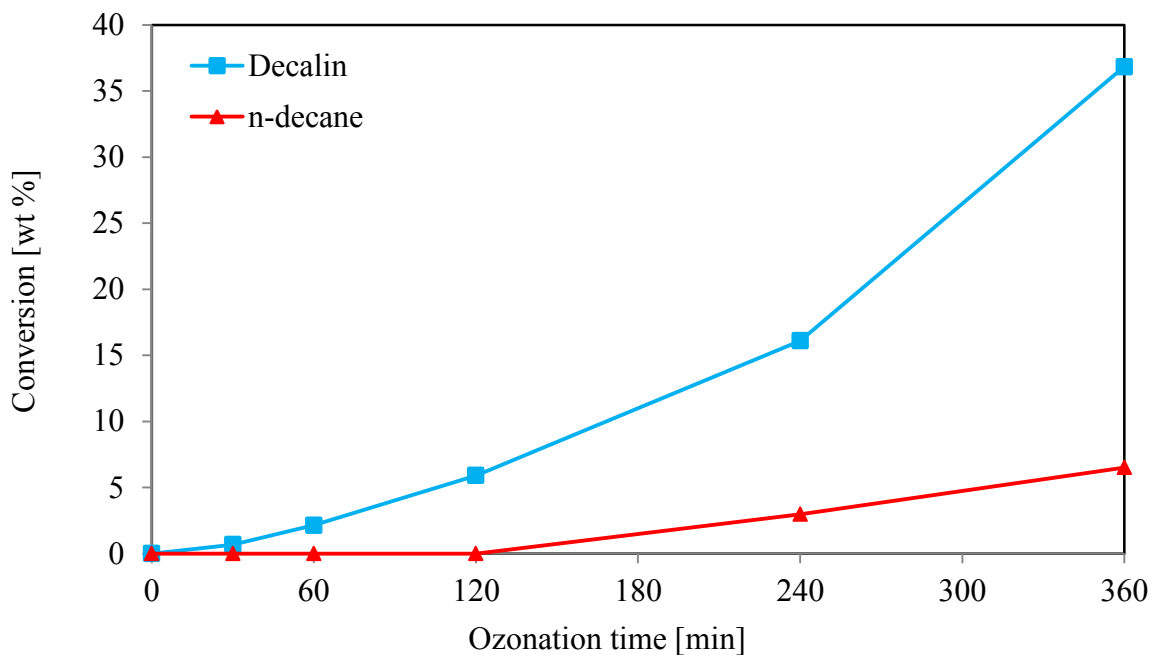
Figure 3.27. Ozonation conversion versus time for decalin and *n*-decane over 6 h ozonation at 130 °C; with an ozone-enriched air flow rate of 120 ml min^{-1} which is equivalent to 144 ml h^{-1} per gram of model compound feed
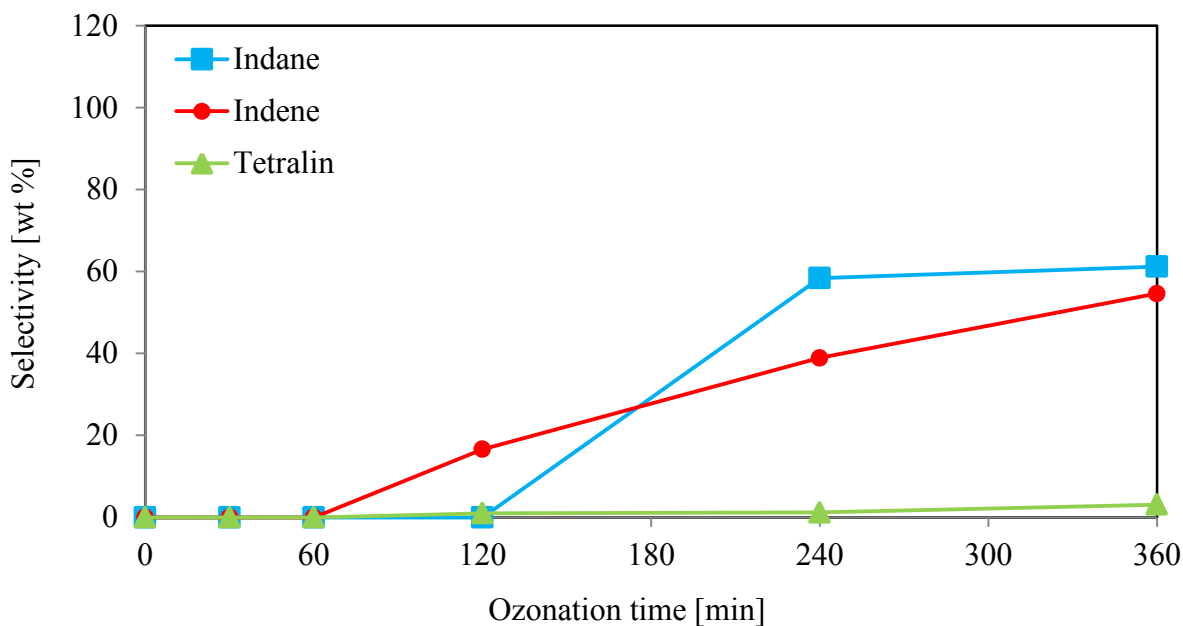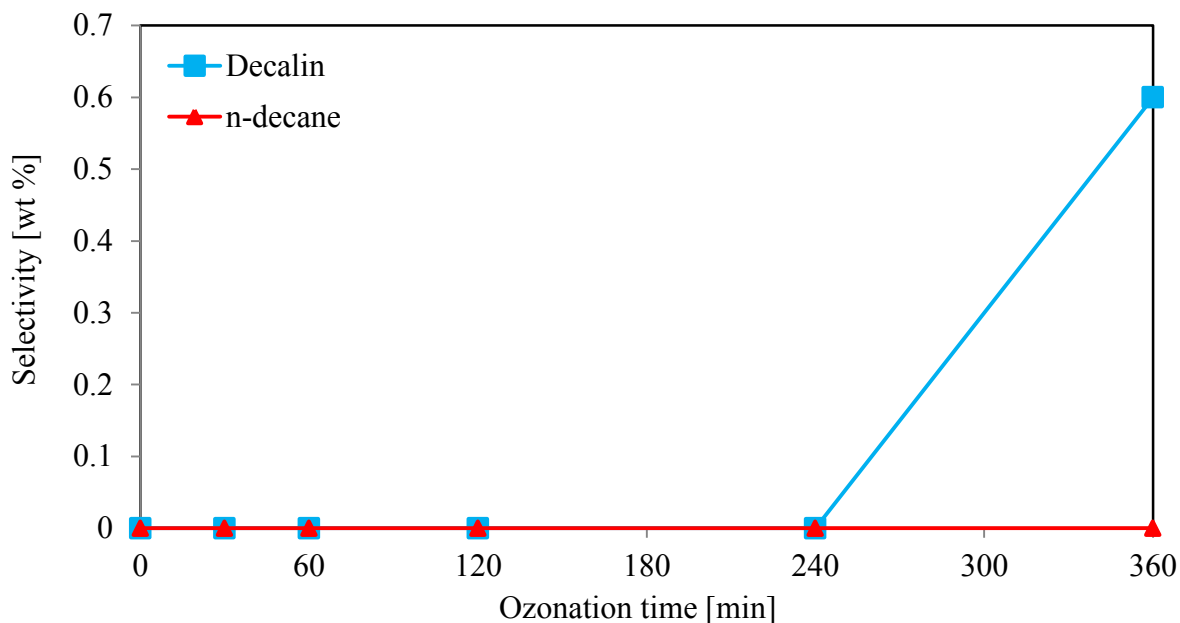
Figure 3.28. Selectivity to addition reaction products versus time for decalin and *n*-decane over 6 h ozonation at 130 °C; with an ozone-enriched air flow rate of 120 ml min^{-1} which is equivalent to 144 ml h^{-1} per gram of model compound feed

3.10 Conclusions

Ozonation of selected model compounds as representatives of different hydrocarbon compound classes found in oil sands bitumen at 130 °C resulted in chemical and physical changes and provided ozonation reaction products selectivity and ozonation conversion data for aromatic, alkylaromatic, naphthenic-aromatic, acyclic paraffinic, naphthenic and heterocyclic compound classes. The obtained results can be used to identify the nature of the free radical addition reaction and ring-cleavage reaction mechanisms of the studied compound classes happening during low temperature ozonation of bitumen.

The main observations and conclusions from this study are as follows:

1. Low temperature ozonation of the studied model compounds resulted in changes in their physical properties. For all the studied compounds, density increased due to ozonation, which correlates with the increase in the bitumen density due to ozonation.

2. For all the studied model compounds the colour and physical state changed due to low temperature ozonation, except for decalin and *n*-decane which were colourless clear

liquids both before and after the ozonation. This could be an indication of the formation of different compounds compared to the parent compound as a result of the ozonation reaction which was confirmed by thermal analyses using TGA and DSC.

3. There was an increase in the amount of oxygenate functional groups, i.e. C–O, C=O and O–H bonds in the ozonized model compounds which was confirmed by infrared spectroscopy.

4. Comparison of the refractive indices of the parent model compounds and ozonized model compounds measured at the same temperature revealed an increase in refractive index and polarizability due to 6 h ozonation at 130 °C. This could be an indication of an increase in the amount of oxygenate functional groups in the studied model compounds due to ozonation, which leads to higher density and polarizability for ozonized compounds compared to their parent compounds which accordingly leads to an increase in their refractive index.

5. The results indicate that different compound classes exhibit different reaction activity under the low temperature ozonation condition. The hydrocarbon classes present in oil sands bitumen which are primarily responsible for free radical addition reactions during ozonation are naphthenic-aromatic and heterocyclic compounds. In general, they were particularly more open to form addition reaction products. No addition reaction products were formed during aromatic and acyclic paraffinic ozonation. Naphthenic and alkylaromatic compounds had very low tendency to form of addition reaction products.

6. The formation of addition reaction products in the ozonation experiments was likely because of the low ozone generation yield of the employed ozone generator which converted only a small portion of the oxygen in the extra-dry air feed gas to ozone. The high concentration of oxygen left unconverted in the ozone-enriched gas led to the formation of addition reaction products in the model compounds.

7. Ozonation of the studied model compounds led to scission of C=C bonds and formation of the ring-cleavage reaction products due to the direct reaction mechanism of ozone with hydrocarbons. Ozone attack to a C–H bond of the model compounds (indirect mechanism) happens more frequently compared to direct attack of ozone to a C=C bond which leads to scission of a double bond in a ring. Oxidation of the same compounds

only led to destruction of C–H bonds and linkage of oxygen to the carbon and oxidative polymerization. [148][162]

8. In ozonation, both direct and indirect reactions of ozone proceed simultaneously, whereas the reaction of oxygen with hydrocarbon compounds only takes place via free-radical reaction mechanism, similar to the indirect reaction mechanism of ozone. Free radicals have a natural tendency to participate in radical chain reactions which leads to formation of addition reaction products. The negligible formation of ring-cleavage reaction products due to low temperature ozonation of the studied model compounds might be due to low concentration of ozone in the ozone-enriched air. Also, the direct reaction mechanism of ozone with hydrocarbons is slower and more selective compared to its indirect reaction mechanism. Still this little amount of ring cleavage reaction products is distinctive between ozonation and oxidation. With increasing ozone concentration, we can expect more ring cleavage reaction to occur.

4.   LOW TEMPERATURE OZONATION OF ATHABASCA BITUMEN AT LOW GAS FLOW RATE

4.1 Introduction

As mentioned earlier in Chapter 1, an alternative to current heavy oil and bitumen upgrading methods is to convert bitumen into methane in a two-step process. The first step is converting heavy oil or bitumen components into smaller fragments using an oxidizing agent and the second step is bioconverting the oxidized fragments into methane using microbial digestion.

As mentioned in Chapter 2, one of the major obstacles in converting large molecules of bitumen feed into high-value smaller fragments is bitumen hardening phenomenon due to oxidative addition reactions and introducing oxygenate functional groups into bitumen. This phenomenon is accompanied by a significant increase in viscosity and hardness as well as a significant decrease in penetration of the bitumen feed. It has been reported that if the oxidizing agent is inserted into the bitumen feed and it does not break the large bitumen molecules, the number of hydrogen bonds will increase due to formation of oxygenate functional groups. Hydrogen bonds are partly responsible for aggregation of bitumen molecules via polymerization ability. An increase in the number of hydrogen bonds can cause an increase in bitumen viscosity if the oxidizing agent is not selected carefully. [163][164][165][166][167]

In previous work performed in our research group, it was concluded that air is not a suitable oxidizing agent for bitumen oxidation in the absence of any additional reagent, such as catalysts,

solvents, etc. It has been concluded that oxygen and air accelerates the hardening process of bitumen under mild oxidation reaction condition. [168][169]

Previous studies on different bitumen samples have shown that a major part of bitumen components has cyclic structure based on their carbon to hydrogen ratio, and that paraffinic compounds are in the minority. [170] Ozone can react with ring containing compounds leading to ring opening. [171][172]

In Chapter 3, in order to test the hypothesis of ring-cleavage reaction of cyclic hydrocarbons, e.g., aromatic compounds, naphthenic compounds, etc. which are dominant in bitumen, the low temperature ozonation of the selected model compounds was studied and it was observed that ring-opening and addition reaction products were formed as the products of ozonation reaction. However, the ozonation of a mixture of the selected model compounds was not investigated, and it remained an open-ended question whether ring-opening or addition reactions would dominate in a mixture of the model compounds. The Ph.D. study of Cha (2009) seemed promising, but the work-up procedure that was implied was onerous. It was therefore not clear whether a simplified approach would work as well as the approach of Cha. [165] In this chapter, experiments have been done on Athabasca bitumen at relatively mild temperature condition and low ozone-enriched air flow rate as the oxidizing agent. Due to high viscosity of bitumen, low temperatures (below 50 °C) are not desirable for conducting experiments, while several studies on bitumen oxidation have reported that over the temperature range of 150 to 300 °C the oxygen uptake rates are significant. [165][173][174][175][176][177] It has been reported that there is a change in the oxidation kinetics around 150 °C. Thus, three different temperatures of 140, 150 and 160 °C were selected for this study, which covers the transition from below 150 to above 150 °C.

This chapter aims at experimentally investigating the feasibility of converting heavy hydrocarbons in Athabasca bitumen to lighter useful products, and treating bitumen through ozonation. In this chapter, ozonation, oxidation using air and oxidation using pure oxygen as oxidizing agents were conducted on Athabasca bitumen at three different temperatures of 140, 150 and 160 °C with the inlet oxidizing gas flow rate of 120 ml min^{-1} in each experiment. Another set of experiments were performed by conditioning Athabasca bitumen under a flow of

nitrogen as an inert atmosphere at three different temperatures of 140, 150 and 160 °C for 6 hours.

4.2   Experiments

4.2.1   Materials

Canadian Athabasca bitumen provided by Centre for Oil Sands Innovation (COSI), University of Alberta (Edmonton, AB, Canada) was used as bitumen feed for ozonation and oxidation experiments. **Table 4.1** summarizes the properties of the bitumen feed used for this study.

Table 4.1. Properties and composition of Athabasca bitumen

Property	Athabasca bitumen
Viscosity at 60 °C [Pa s]	2.67 ± 0.01
Density at 20 °C [Kg m^{-3}]	1025.1 ± 0.1
Refractive index at 60 °C	1.567 ± 0.001
Penetration at 25 °C [mm]	2.7 ± 0.1
Elemental composition [wt %] [a]	
C	81.7 ± 0.6
H	10.2 ± 0.1
S	5.1 ± 0.1
N	0.5 ± 0.1
O	0.7 ± 0.1
SARA fractions [wt %] [b]	
Saturates	19
Aromatics	47
Resins	17
Asphaltenes	17

[a] Elemental analysis for CHNS and O of Athabasca bitumen was performed using a Carlo Erba EA1108 Elemental Analyzer (Triad Scientific Inc., Manasquan, NJ, USA).

[b] Average class composition of Athabasca bitumen from literature. [178][179][180]

Compressed air, pure oxygen and pure nitrogen all in extra dry grade supplied by Praxair Canada Inc. (Edmonton, AB, Canada) were used in the experiments.

4.2.2 Apparatus and experimental procedure

4.2.2.1 Ozonation of Athabasca bitumen

The experimental setup used for bitumen ozonation reaction was identical to the setup described and used for the ozonation of model compounds, as illustrated in **Figure 3.1**. In each experiment, approximately 100 g of Athabasca bitumen was pre-heated to 100 °C and then transferred to a 250 ml round bottom three-neck flask. A magnetic stirring bar with the stirring speed of 500 rpm was used to obtain a homogeneous oxidant concentration and temperature throughout the bitumen samples. The experiments in this section were done with ozone-enriched air flow rate of 120 ml min^{-1} (equivalent to 72 ml h^{-1} ozone-enriched air per gram of bitumen feed) for 6 hours at three different temperatures of 140, 150 and 160 °C.

In each experiment, only after the bitumen temperature was reached to the reaction temperature the ozone-enriched air supply was released to the flask. In this way, the possibility of ozonation was limited during the pre-heating process.

At the end of each experiment, the ozone-enriched air flow was stopped and the ozonized bitumen was allowed to cool down to the ambient temperature. Afterwards, the products were weighed and collected in clear glass vials (Fisherbrand Class B Clear Glass Threaded Vials with Closures, Fisher Scientific Company, Canada) with lid in ambient temperature and light for further analyses. The samples were stored for less than 24 hours before analysis and characterization. All the experiments were triplicated in order to gain confidence about the accuracy of the results.

4.2.2.2 Oxidation study of Athabasca bitumen using extra-dry grade air as oxidizing agent

Similar to bitumen ozonation experiments, approximately 100 grams of Athabasca bitumen was pre-heated to 100 °C and transferred to 250 ml three-neck flask. Only after the bitumen temperature was reached to the reaction temperature, the air injection into the flask was commenced. The air flow rate was maintained at 120 ml min^{-1}, which is equivalent to 72 ml h^{-1} air per gram of bitumen feed. The experiments were carried out at three different temperatures of 140, 150 and 160 °C for 6 hours.

At the end of each experiment, the air flow was stopped and the oxidized bitumen was allowed to cool down to the ambient temperature. Afterwards, the products were weighed and collected in vials for further analysis and characterization. Each experiment was triplicated in order to gain confidence about the accuracy of the results. The experimental setup employed for bitumen oxidation experiments was the same as the equipment illustrated in **Figure 3.1**, but without the ozone generator.

4.2.2.3 Oxidation study of Athabasca bitumen using extra-dry grade pure oxygen as oxidizing agent

The experimental setup and procedure for this set of experiments was similar to the bitumen oxidation using extra-dry air, except that in this part, extra-dry pure oxygen was employed as the oxidant. The pure oxygen flow rate was maintained at 120 ml min^{-1}, which is equivalent to 72 ml h^{-1} pure oxygen per gram of bitumen feed. The experiments were performed at three different temperatures of 140, 150 and 160 °C for 6 hours. Each experiment was triplicated in order to gain confidence about the accuracy of the results.

4.2.2.4 Athabasca bitumen under a flow of nitrogen as an inert atmosphere

Another set of experiments were performed by conditioning Athabasca bitumen under a flow of nitrogen as an inert atmosphere at three different temperatures of 140, 150 and 160 °C for 6 hours. The purpose of this part of the study was to compare the viscosity of the heated reaction products in the absence of oxidizing agent with the viscosity of ozonized and oxidized bitumen products under the same reaction condition. These blank runs were conducted in order to determine whether the increase in the viscosity of bitumen in low temperature ozonation/oxidation is actually due to oxidative addition reactions and addition of oxygenate functional groups to the bitumen only and not partly due to prolonged (6 h) heating up the bitumen feed.

The experimental setup used for this part of the study is shown in **Figure 3.1**. The only difference was that an extra-dry pure nitrogen cylinder was used as the gas supply.

4.2.3   Analyses and calculations

The reaction products were analyzed using different techniques and instruments.

4.2.3.1 Rheometer

Viscosity was measured by placing the samples in the cylindrical cup (model CC-17) of the rotational rheometer (RheolabQC, Anton Paar, US) using a cylindrical spindle (16.664 mm diameter and 24.970 mm length, model CC-17) with rotational speed of 7.75 min^{-1}, and shear rate of 10 sec^{-1} at 60 °C.

4.2.3.2 Penetrometer

To measure the hardness of the bitumen samples, the penetration test was conducted, which measures the depth of penetration of a H-1280 bituminous penetration needle during 0.01 sec, expressed in tenths of millimetres in order to confirm the viscosity results obtained by rheometer for bitumen samples. Measurements were performed with an electric penetrometer, model H-1240 and an applied load of 100 g at 25 °C. The Penetration numbers obtained by means of the penetration test indicate the hardness of the bitumen samples.

4.2.3.3 Refractometer (Refractive index meter)

Refractive indices of the products of ozonation and oxidation experiments as well as the products of bitumen conditioning under nitrogen was measured using thermostatically controlled Abbe Anton Paar refractometer (Abbemat 500) at 60 °C as described in Chapter 3 (section 3.2.3.6).

4.2.3.4 Fourier transform infrared (FTIR) spectroscopy

The infrared analysis of ozonation and oxidation products, and also the products of conditioning of bitumen under nitrogen was performed using Fourier transform infrared spectrometer to confirm the presence of specific functional groups. IR spectra of the samples were measured as described in Chapter 3 (section 3.2.3.5) with the resolution of 4 cm^{-1} and detector gain of 81.

4.2.3.5 Hydrogen nuclear magnetic resonance (^{1}H-NMR) spectroscopy

The hydrogen nuclear magnetic resonance (^{1}H-NMR) spectra of the bitumen feed and ozonized bitumen samples were measured using a ^{1}H-NMR spectrometer (NMReady 60, Nanalysis Corp., Calgary, Canada) to estimate the aliphatic and aromatic hydrogen % of the bitumen samples. Samples were analyzed using standard 5 mm NMR tubes (NORELL, Landisville, USA). Characterization was performed by dissolving each sample in chloroform-d (CDCl$_3$, 99.96 % deuterium, Sigma). Experimental conditions were: spectral range = 14 ppm, number of scans = 256.

4.3   Results and discussions

In this section, first the viscosity results obtained by rheometer for the bitumen feed, ozonized bitumen, oxidized bitumen using air, oxidized bitumen using pure oxygen and bitumen conditioned under nitrogen atmosphere are presented. Then, the penetration results obtained by penetrometer are presented and compared for all the bitumen samples. After that, characterization of the bitumen feed and the experiment's products using their optical properties based on the results obtained by refractometer and FTIR spectroscopy are discussed. Afterwards, the results obtained by ^{1}H-NMR spectroscopy for the bitumen feed and the ozonized bitumen samples are presented.

4.3.1   Rheometer

Viscosity is the main parameter investigated in this study for evaluating the ozonation and oxidation process. It is a key physical property of the Athabasca bitumen and the ozonation products. The measured viscosities are shown in **Table 4.2**. As it can be seen in this table, the bitumen viscosity increased after ozonation, oxidation using air and oxidation using pure oxygen. This behaviour is consistent with the published results of Adegbesan (1986) and Campbell and Wright (1964) who reported that both oxygen and ozone accelerate the hardening process under mild reaction conditions and increase the bitumen viscosity. [168][181]

As it can be seen in **Table 4.2**, bitumen underwent a transformation from lower viscosity state to considerably more viscous state after oxidation using pure oxygen. In other words, severe bitumen hardening was observed due to oxidation using pure oxygen as the oxidizing agent. There is a slight difference between the viscosity of oxidized bitumen at 140 and 150 °C. However, the bitumen viscosity has significantly increased due to oxidation using pure oxygen at 160 °C. One possible explanation for this could be that oxidation reactions are exothermic and energy is being generated during oxidation reactions. At higher reaction temperatures, the oxygen uptake rates increase. At temperatures below 150 °C, there is not enough energy available to break oxygen bonds and produce a meaningful amount of oxygen free radicals. So that any free radical chain reactions could be over-shadowed by the thermal cracking reactions. However, above this critical temperature (150 °C) the system has enough energy to sustain a meaningful level of oxygen bond dissociation, and free radical chain reactions propagate without

much interference. [182][183] Raising the temperature of the reaction in ozonation experiments and oxidation experiments using air leads to a slight increase in the bitumen viscosity, which is consistent with the results published by Xu and co-workers (2001). [183] This conclusion is however based upon only three data points.

Table 4.2. Characterization of the bitumen conditioned under inert nitrogen atmosphere, ozonized bitumen, oxidized bitumen using air and oxidized bitumen using pure oxygen for 6 h at different temperatures, average of 3 runs

Description	Property	Reaction temperature [°C]		
		140	150	160
Bitumen conditioned under nitrogen	Viscosity at 60 °C [Pa s]	2.6 ± 0.1	2.7 ± 0.1	2.8 ± 0.1
	Penetration [mm]	2.5 ± 0.1	2.5 ± 0.1	2.4 ± 0.1
	Refractive Index [nD]	1.567 ± 0.001	1.568 ± 0.001	1.568 ± 0.001
Oxidized bitumen using air	Viscosity at 60 °C [Pa s]	5.7 ± 0.4	6.7 ± 0.7	8.0 ± 0.4
	Penetration [mm]	2.0 ± 0.1	1.8 ± 0.1	1.5 ± 0.1
	Refractive Index [nD]	1.570 ± 0.001	1.571 ± 0.001	1.572 ± 0.001
Oxidized bitumen using oxygen	Viscosity at 60 °C [Pa s]	18.3 ± 0.9	29.5 ± 3.4	81.6 ± 2.7
	Penetration [mm]	1.0 ± 0.1	1.0 ± 0.1	0.5 ± 0.1
	Refractive Index [nD]	1.572 ± 0.001	1.574 ± 0.001	1.577 ± 0.001
Ozonized bitumen	Viscosity at 60 °C [Pa s]	14.9 ± 1.6	16.5 ± 1.1	18.7 ± 1.4
	Penetration [mm]	1.0 ± 0.1	1.0 ± 0.1	0.9 ± 0.1
	Refractive Index [nD]	1.571 ± 0.001	1.572 ± 0.001	1.573 ± 0.001

The increase in the bitumen viscosity in the experiments using nitrogen as an inert atmosphere is negligible when compared to the bitumen feed (**Table 4.1** and **Table 4.2**). By comparing the viscosity of the products from experiments under nitrogen and the viscosity of the products from bitumen ozonation, oxidation using air and oxidation using pure oxygen, all performed under the same reaction condition, it can be concluded that the increase in the bitumen viscosity is due to oxygen uptake and free radical addition reactions, not due to prolonged heating up the bitumen feed. The effect of temperature on the viscosity of the ozonized and oxidized bitumen, also the viscosity of bitumen heated up under the inert nitrogen atmosphere is presented in **Figure 4.1**. It

can be concluded for all of the performed experiments the higher the reaction temperature, the more increase in the viscosity of bitumen products.

As it can be seen in **Figure 4.1**, the viscosity of ozonized bitumen lays between the viscosity of the oxidized bitumen using air and the viscosity of the oxidized bitumen using pure oxygen under the same reaction temperature. Even though, only a small portion of extra-dry air feed gas was converted to ozone using the ozone generator, this small amount of ozone made a big difference in the viscosity of the products. The higher viscosity of the ozonized bitumen products compared to oxidized bitumen samples using air could be due to strong oxidizing ability of ozone, which leads to a higher reaction rate and higher conversion of the bitumen feed to the reaction products under the same reaction condition as oxidation using air. [184] Indirect reaction of ozone with bitumen molecules will lead to free radical addition reaction, and direct reaction of ozone with bitumen will lead to condensation polymerization reactions (after ring-cleavage reaction and formation of aromatic carbonyls). In both cases, higher molecular weight compounds will form, which accordingly will lead to an increase in the bitumen viscosity.

As it can be seen in **Figure 4.1**, prolonged heating up the bitumen in the experiments using nitrogen leads to a negligible increase in the bitumen viscosity, as well as a negligible increase in bitumen hardness. This type of hardening which is probably due to loss of volatiles at elevated temperatures is physical hardening. But the hardening taking place in bitumen due to ozonation, oxidation using air and oxidation using pure oxygen is due to formation of more complex materials with higher molecular weight and addition of oxygenate functional groups to the bitumen molecules. This type of hardening is chemical hardening. [166][167][185]

Now it is required to give a brief explanation of two different types of bitumen hardening:

1) **Physical hardening:**

   The increase in the bitumen viscosity after heating it up in the absence of any oxidizing agent might be due to the loss of small amounts of volatile materials at elevated temperatures. This phenomenon is irreversible and will lead to bitumen hardening. [172][186]

   The mentioned phenomenon which is called steric hardening or physical hardening might have another possible root. Changes in the relative positions of the bitumen molecules

can also cause changes in mechanical properties of the bitumen sample and leads to stronger intermolecular associations, therefore more energy is required to deform bitumen, and bitumen will become harder. [187] Physical hardening caused by a change in structure and molecular rearrangements is a reversible phenomenon. [188][189] As it can be seen in **Figure 4.2**, the penetration results for the bitumen conditioned under nitrogen at 140, 150 and 160 °C for 6 h has a negligible decrease compared to the penetration of the Athabasca bitumen feed. It can be concluded that the increase in the viscosity and hardness of the reaction products in ozonation and oxidation experiments is not due to physical hardening and loss of volatile materials at elevated temperatures.

2) **Chemical Hardening:**

The polar oxygen containing functional groups formed by ozonation/oxidation of bitumen tend to associate to micelles with higher weight and thus the viscosity of bitumen will significantly increase which is an irreversible phenomenon and is called chemical hardening. [186] As it can be seen in **Figure 4.1** and **Figure 4.2**, addition of oxygenate functional groups into the bitumen feed due to ozonation, oxidation using pure oxygen and oxidation using air resulted in an increase in the viscosity of the ozonation and oxidation products and a decrease in their penetrability. However, prolonged heating up the bitumen under nitrogen has not significantly changed the viscosity and penetrability of the bitumen feed.

4.3.2 Penetrometer

The penetration value as shown in **Table 4.2**, the reaction products in ozonation and oxidation experiments reflect significant hardening compared to the Athabasca bitumen feed and bitumen conditioned under nitrogen atmosphere. The results obtained by penetrometer for the bitumen samples as shown in **Figure 4.2** are consistent with the results obtained by the rheometer. The higher the viscosity of the bitumen sample, the lower the penetrability and the harder the bitumen sample.

4.3.3 Refractometer (Refractive index meter)

Refractive indices of the bitumen feed, the products of bitumen ozonation and oxidation experiments as well as the products of bitumen conditioned under nitrogen were measured at 60

°C. As it can be seen in **Figure 4.3**, refractive index of bitumen increased due to 6 h ozonation, oxidation using air and oxidation using pure oxygen compared to the original Athabasca bitumen. It can also be seen that the higher the reaction temperature, the higher the measured refractive index and polarizability of the reaction products. Comparison of the refractive indices of the original Athabasca bitumen, ozonized and oxidized bitumen products measured at the same temperature indicates that the refractive indices of the products of oxidation using pure oxygen was more than ozonation, oxidation using air, conditioning under nitrogen and the bitumen feed respectively.

As mentioned in Chapter 3 (section 3.2.3.6), the refractive indices of the bitumen samples are useful as an indicator of their molecular structure and polarizability. [190][191] Addition of oxygen as hydroxyl, carbonyl or ozonation/oxidation of heteroatoms will bring a polarizability change in the bitumen samples. [192] The O–H hydrogen bonds have a considerable large polarizability. [193] As mentioned earlier in this chapter if the oxidizing agent is only added into the bitumen feed and it does not break the large bitumen molecules, the number of hydrogen bonds will increase. [165][166][167] Hydrogen bonds are partly responsible for aggregation of bitumen molecules and increase in bitumen viscosity. So the results obtained by refractometer are consistent with the results obtained by rheometer for the bitumen samples.

In bitumen ozonation, ozone may lead to cleavage of large cyclic bitumen molecules due to the direct reaction of ozone, as was explained in Chapter 2. In bitumen oxidation using pure oxygen, since oxygen is not as strong as ozone, it will not break the large cyclic molecules of bitumen. The insertion of pure oxygen in the bitumen feed will only lead to an increase in the number of hydrogen bonds, which will accordingly lead to an increase in the amount of free radical addition reactions.
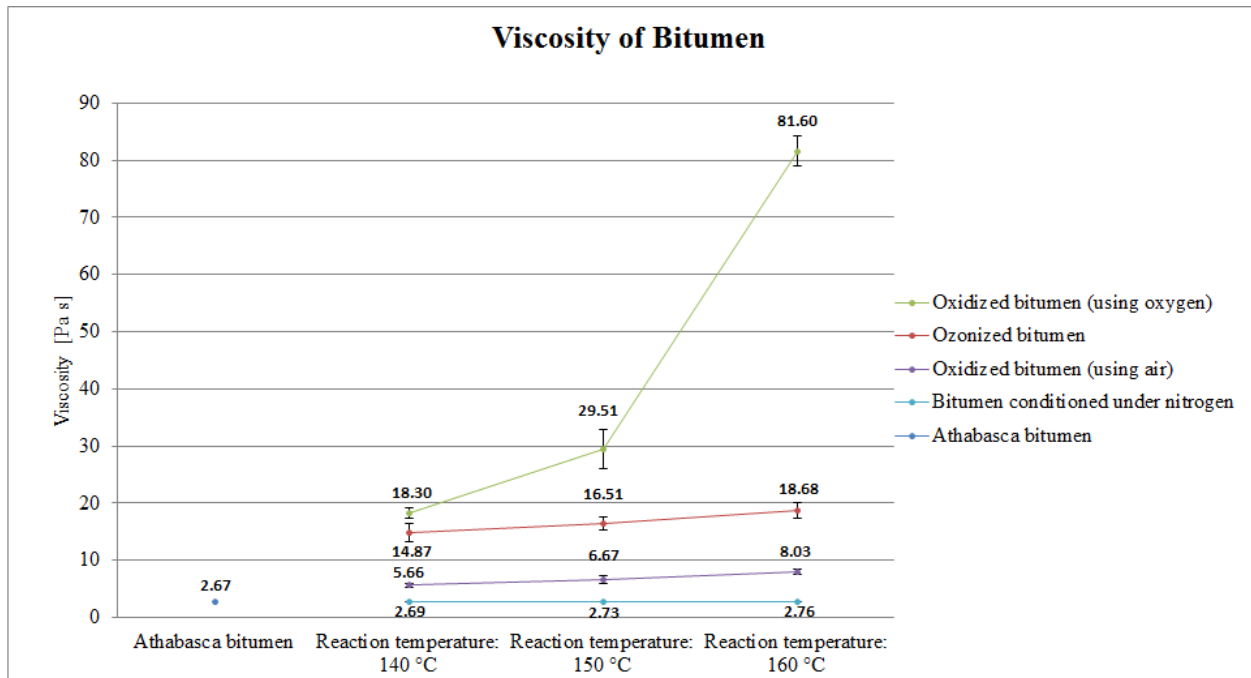
Figure 4.1. Viscosity of Athabasca bitumen, bitumen conditioned under nitrogen atmosphere, ozonized bitumen, oxidized bitumen using air and oxidized bitumen using pure oxygen after 6 h experiments at different temperatures; viscosity measured at 60 °C, average of 3 runs
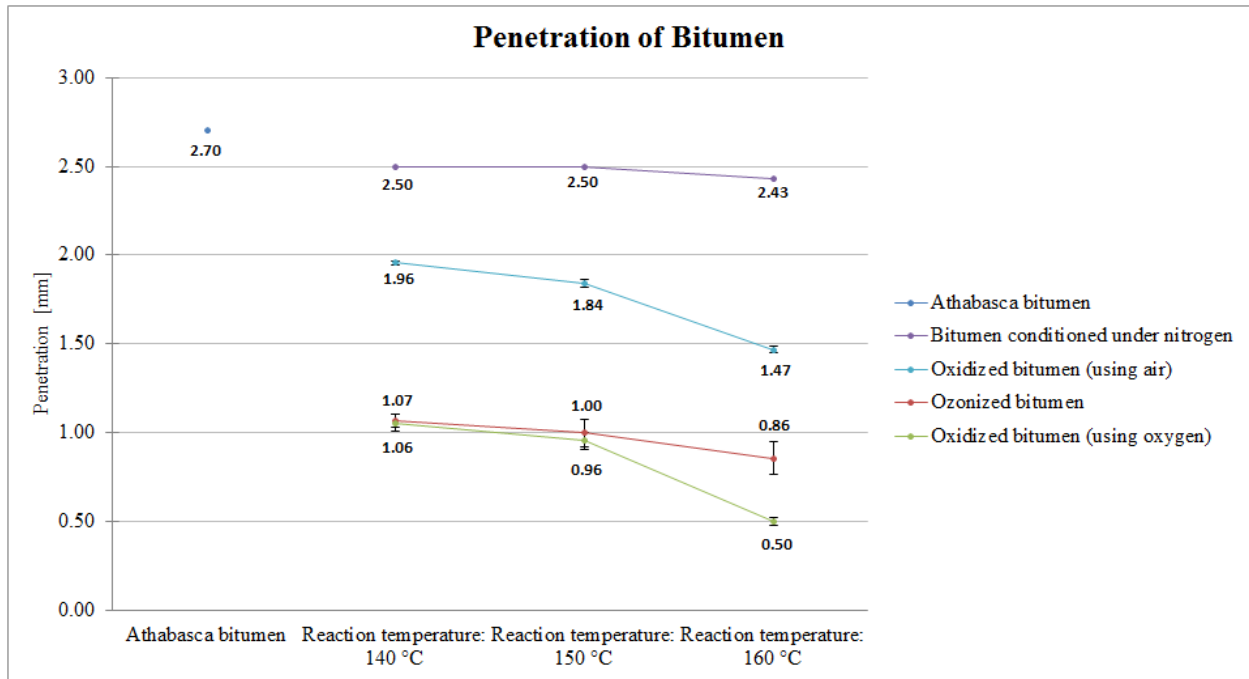
Figure 4.2. Penetration of Athabasca bitumen, bitumen conditioned under nitrogen atmosphere, ozonized bitumen, oxidized bitumen using air and oxidized bitumen using pure oxygen after 6 h experiments at different temperatures; penetration measured at room temperature measured, average of 3 runs
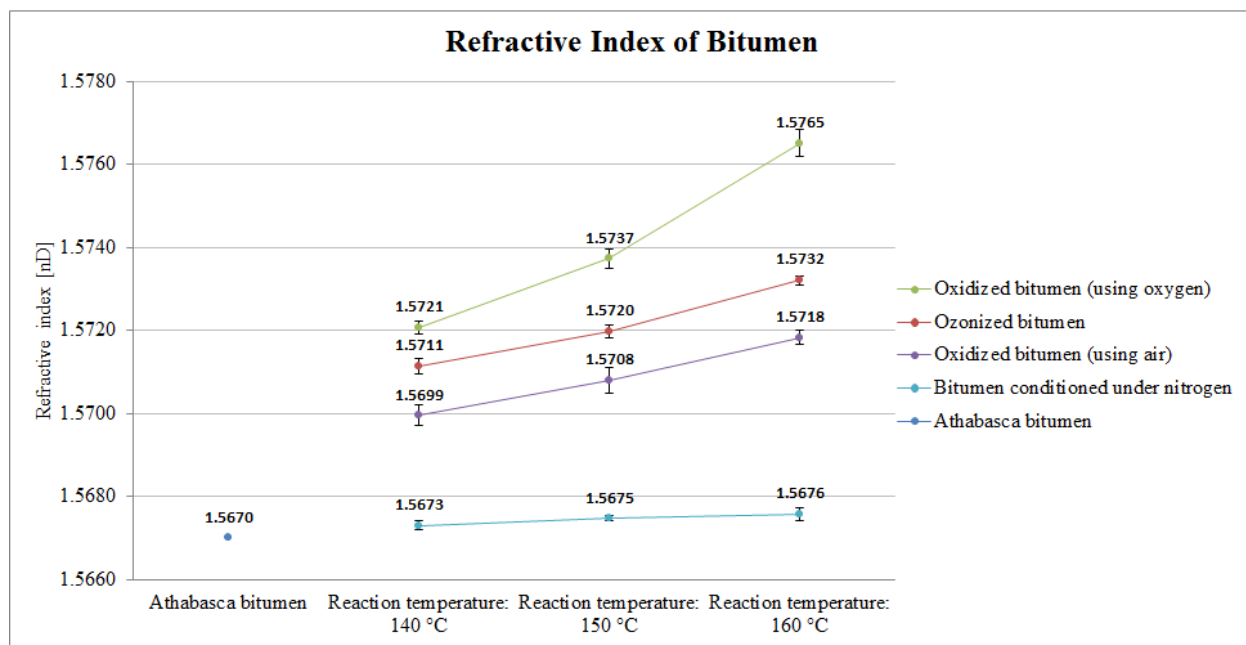
Figure 4.3. Refractive index of Athabasca bitumen, bitumen conditioned under nitrogen atmosphere, ozonized bitumen, oxidized bitumen using air and oxidized bitumen using pure oxygen after 6 h experiments at different temperatures; refractive index measured at 60 °C, average of 3 runs

An independent samples t-test at a 5% significance level was performed in order to test the hypothesis that the oxidized bitumen using pure oxygen, ozonized bitumen, oxidized bitumen using air and bitumen conditioned under nitrogen are associated with statistically different mean viscosity, penetrability and refractive index, and the results are presented and discussed in Appendix B.

4.3.4 FTIR

According to Beer-Lambert law, presented in **Equation 3.5** (Chapter 3, section 3.3.1), the intensity of the infrared absorption for a component is a function of its concentration. [194]

The path lengths of the obtained infrared spectra for different samples are not the same and must be normalized. In order to compensate for this, the absorbance of the samples' spectra are multiplied by a scaling factor based on the absorption of a reference peak, i.e. CH_3 group at ~1375 cm^{-1} in the Athabasca bitumen feed spectrum as a scaling spectrum, with the assumption

82

that the absorption of CH$_3$ at ~1375 cm^{-1} will not change too much due to the investigated reactions in this study. The normalized spectra are shown in **Figure 4.4**.

Because of the relatively short reaction time (6 h), formation of oxygenate functional groups in bitumen was negligible in the ozonation, oxidation using pure oxygen and oxidation using air even at the highest experimented reaction temperature (160 °C). At very low concentration of the functional groups, the IR absorption bands are simply too weak to be detected. [195] As it can be seen in **Figure 4.4**, in the case of ozonized bitumen, oxidized bitumen using pure oxygen and oxidized bitumen using air after 6 h reaction at 160 °C, the peaks observed in the region of 1072 – 983 and 1733 – 1677 cm^{-1} have slightly grown bigger which could be respectively indication of an increase in the number of sulfoxide (S=O) and carbonyl (C=O) functional groups in the bitumen feed due to ozonation/oxidation.
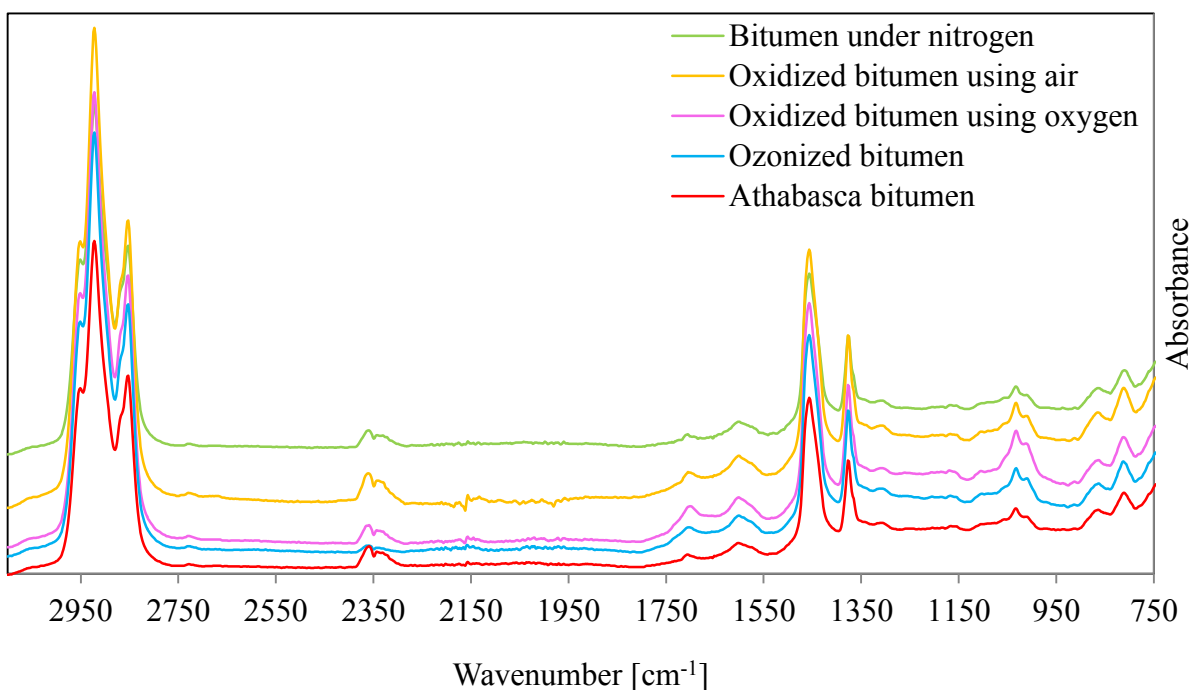
Figure 4.4. Normalized infrared spectra of the bitumen feed, ozonized bitumen after 6 h ozonation at 160 °C, oxidized bitumen after 6h oxidation using pure oxygen at 160 °C, oxidized bitumen after 6h oxidation using air at 160 °C and bitumen conditioned for 6 h under nitrogen at 160 °C in the spectral region of 1850 – 950 cm^{-1}

Table 4.3. Oxygenate functional groups identified by infrared spectroscopy of the bitumen feed, ozonized bitumen, oxidized bitumen using oxygen, oxidized bitumen using air and bitumen conditioned under nitrogen

Name	Oxygenate functional group absorption [cm^{-1}]				
	C = O	O - H	C - O	N=O	S=O
Athabasca bitumen	1691–1720	2798–2995	1108–1151	1550–1643	985–1049
Ozonized bitumen	1683–1736	2785–2981	1107–1159	1554–1635	983–1066
Oxidized bitumen using oxygen	1677–1749	2790–2993	1101–1159	1546–1637	981–1072
Oxidized bitumen using air	1677–1720	2783–3008	1101–1153	1552–1645	985–1066
Bitumen conditioned under nitrogen	1687–1718	2798–3002	1103–1153	1554–1643	991–1047

4.3.5   Hydrogen nuclear magnetic resonance (^{1}H-NMR) spectroscopy

Recently, ^{1}H-NMR spectroscopy has emerged as a very powerful and versatile tool for bitumen characterization. [196][197][198][199] In the obtained ^{1}H-NMR spectra the chemical shift values of 0.5 – 4.0 ppm was assigned to aliphatic protons and the chemical shift values of 6.0 to 9.0 ppm was assigned to aromatic protons. [198] The percentages of two different types of proton obtained from the NMR spectra are listed in **Table 4.3**.

Ozone attack to cyclic structures and occurrence of ring-cleavage reaction will lead to formation of an aromatic compound with two carbonyl groups (aromatic ketone, aromatic ester and aromatic carboxylic acids) which can afterwards be involved in condensation polymerization reactions to form high molecular weight compounds. Aromatic hydrogen loss could be due to the ring opening of the cyclic molecules of bitumen. [200][201] Ring-cleavage reaction usually occurs with the elimination of two aromatic hydrogens in the form of water. [202]

Aliphatic hydrogen could be lost due to either formation of carbonyl or formation of olefinic bonds, which each of them are accounted for the loss of two aliphatic hydrogens in the form of water. [169]

The NMR results presented in **Table 4.4** indicate that the ratio of aliphatic to aromatic hydrogen increased. The increase in the ratio of aliphatic to aromatic hydrogen indicated that the ratio of oxidative hydrogen loss from aromatic carbons due to ring-cleavage reactions by ozone under the applied reaction condition was higher than oxidative hydrogen loss from aliphatic carbons. Majority of the aliphatic and aromatic hydrogen loss during ozonation is loss as water due to carbonyl formation (or hydrogen elimination to produce double bonds in aliphatic compounds). Since the formation of alcohols is not associated with any hydrogen loss. This could be an indication of the higher selectivity of ozone to react with aromatic part of the bitumen over aliphatic part. [169][203][204][205] However, the NMR spectra of the bitumen and ozonized bitumen samples were too complex to confirm any of the above mentioned assumptions and make a strong conclusion.

Table 4.4. ^{1}H-NMR analyses of Athabasca bitumen and ozonized bitumen samples after 6 h ozonation at different temperatures

Property	Athabasca bitumen	Ozonized bitumen		
		140 °C	150 °C	160 °C
Aliphatic hydrogen [wt %]	93.77	94.51	94.55	95.25
Aromatic hydrogen [wt %]	6.23	5.49	5.45	4.75

4.3.6 Differential scanning calorimetry (DSC) of bitumen samples

Thermal analysis of Athabasca bitumen before and after 6 h ozonation at 140, 150 and 160 °C was conducted using differential scanning calorimeter as described in Chapter 3 (section 3.2.3.3). The total heat flow curves for Athabasca bitumen and ozonized bitumen samples after 6 h ozonation at 140, 150 and 160 °C were obtained by DSC and the analysis was triplicated for each sample. The obtained curves by DSC are presented and discussed in Appendix A.

4.4 Conclusions

Ozonation, oxidation using pure oxygen and oxidation using air were conducted on Athabasca bitumen feed for 6 hours at low temperatures in the range of 140 to 160 °C, which resulted in physical and chemical changes in bitumen.

The main observations and conclusions from this study are as follows:

1. Low temperature ozonation of Athabasca bitumen (below 250 °C) resulted in undesirable changes in its physical properties, such as viscosity and hardness which both increased due to ozonation. But the increase in the bitumen viscosity and hardness was relatively lower than oxidation using pure oxygen under the same reaction condition. This difference is not due to the chemistry per se, but due to the higher partial pressure of the oxidant leading to an increased rate of oxidation.

2. Insertion of ozone into the bitumen feed was accompanied by a decrease in the aromatic protons of the bitumen and an increase in its aliphatic proton content due to the ring opening ability of ozone. It was concluded that ozone has higher selectivity to react with aromatic part of the bitumen compared to its aliphatic part and this was partially confirmed by ^{1}H-NMR.

3. Ozonation, oxidation using pure oxygen and oxidation using air changed the amount of oxygenate functional groups (C=O, C–O, O–H, S=O, S–O, N=O, N–O and etc.) in the bitumen feed. As discussed in Chapter 3 (Section 3.3.3.1), the sensitivity of FTIR method is relatively poor and whenever the abundance of a functional group is relatively low, the IR absorption is too weak to be detected. Therefore, this method cannot detect the presence of the mentioned functional groups at very low concentrations in bitumen.

4. The ozonation reaction rate of bitumen depends slightly on the reaction temperature. The higher the reaction temperature, the higher the ozonation rate and the bigger the increase in the viscosity and hardness and the decrease in the penetrability.

5. It was proposed that free radical addition reactions of hydrocarbons in bitumen are responsible for hardening phenomenon. In Chapter 3, it was concluded that ozone has the ability of opening the rings in cyclic hydrocarbons. But in this chapter, it was shown that the increase in the bitumen viscosity due to ozonation is more than oxidation using air. It can be concluded that although ring-cleavage in bitumen occurs due to ozonation, this

phenomenon does not necessarily lead to less hardening. In other words, based on the results, ring-cleavage of the cyclic compounds in bitumen does not prevent hardening. Ozone may cleave the rings in cyclic hydrocarbons in bitumen, but still these ring-cleavage reaction products might participate in condensation polymerization reactions and form larger molecules with higher molecular weights.

6. Even though, only a small portion of extra-dry air feed was converted to ozone using the ozone generator, this small amount of ozone made a big difference in the viscosity and hardness of the ozonation and oxidation products using air. Strong oxidizing ability of ozone compared to the extra-dry air which was used as the ozone generator's feed gas leads to a higher reaction rate and accordingly higher conversion of the bitumen feed to the reaction products under the same reaction condition as oxidation using air.

5. CONCLUSIONS

In the first part of the study, the possibility of ring-cleavage reactions in ring-containing hydrocarbons, e.g., aromatic and naphthenic class compounds, which are dominant in bitumen, by treatment using ozone enriched air as the oxidizing agent at relatively mild temperature (130 °C) and low gas flow rate (120 ml min^{-1} which is equivalent to 144 ml h^{-1} per gram of model compound feed) was investigated. It was concluded that ozone can react directly and indirectly with hydrocarbon molecules due to its resonance hybrid structure. In ozonation, both direct and indirect reactions of ozone proceed simultaneously. Ozonation of the studied model compounds led to scission of C=C bonds and ring-cleavage of the aromatics, naphthenic-aromatics and heterocyclic class compounds due to the direct reaction mechanism of ozone. Also, free radical addition reactions observed due to the indirect reaction mechanism of ozone. Free radicals have a natural tendency to participate in radical chain reactions which leads to the formation of addition reaction products. The negligible formation of ring-cleavage reaction products due to the ozonation of the studied model compounds might be due to the low concentration of ozone in the ozone-enriched air. It might also be due to the fact that direct reaction mechanism of ozone which leads to ring-opening of cyclic hydrocarbons is much slower compared to the indirect mechanism. Still, this little amount of ring-cleavage reaction products was distinctive between ozonation and oxidation and with increasing ozone concentration, we can expect more ring cleavage reactions to occur. It was also concluded that the hydrocarbon classes present in oil sands bitumen which are primarily responsible for free radical addition reactions during ozonation are naphthenic-aromatic and heterocyclic compounds.

In the second part of the study, low temperature ozonation and oxidation of Athabasca bitumen (140, 150 and 160 °C) at low oxidizing gas flow rate (120 ml min^{-1} which is equivalent to 72 ml

h^{-1} per gram of bitumen feed) was investigated. In all the experiments, undesirable changes in the chemical and physical properties of the bitumen were observed, such as an increased viscosity and hardness due to ozonation and oxidation. However the increase in the bitumen viscosity and hardness in ozonation was relatively lower than oxidation using pure oxygen under the same reaction condition. This was due to the higher partial pressure of the oxidant leading to an increased rate of oxidation in the experiments using pure oxygen. However, it was shown that the increase in the bitumen viscosity and hardness due to ozonation was more than oxidation using air. This is because although ozone has the ability of ring-opening of cyclic hydrocarbons in bitumen, this phenomenon does not necessarily lead to less hardening. The ring-cleavage products formed due to ozonation of cyclic hydrocarbons might participate in condensation polymerization reactions and form larger molecules with higher molecular weights which lead to an increase in the bitumen viscosity and hardness. Based on the results, ring cleavage of the cyclic hydrocarbon compounds in bitumen does not prevent hardening but hardening due to ozonation is much less compared to the oxidation using pure oxygen under the same reaction condition. In ozonation experiments of the model compounds and the bitumen, the high concentration of oxygen left unconverted in the ozone-enriched air led to formation of addition reaction products, which accordingly led to an increase in the bitumen viscosity and hardness.

In order to increase the ring-cleavage reaction products due to the ability of ozone to react directly with cyclic hydrocarbons, we might add the compounds that terminate the chain reactions very quickly (scavengers) to the bitumen. This might reduce the rate of indirect reactions of ozone (free-radical chain reactions). Therefore, the direct reaction mechanism of ozone may exceed the indirect reactions, and we can expect more ring-opening reaction products. Also, we can use an ozone-generator with higher ozone generation yield to increase the ozone concentration in the ozone-enriched air, so the concentration of oxygen left unconverted in the ozone-enriched air will decrease which might lead to formation of more ring-opening products compared to the free-radical addition reaction products.

BIBLIOGRAPHY

1. Platomov, V. V.; Kudrya, A. N.; Proskuryakov, S. V. Ozonolysis of Asphaltene from Semicoking Tar of G17 Coal. *Russ. J. Appl. Chem.* **2003**, *76*, 148–152.

2. Rahimi, P.; Gentzis, T.; Taylor, E.; Carson, D.; Nowlan, V.; Cotte, E. The Impact of Cut Point on the Processability of Athabasca Bitumen. *Fuel* **2001**, *80*, 1147–1154.

3. Kapadia, P. R.; Wang, J.; Kallos, M. S.; Gates, I.D. Practical Process Design for In-Situ Gasification of Bitumen. *Applied Energy* **2013**, *107*, 281–296.

4. Pereira, A. S.; Shahinoor-Islam, M. D.; Gamal-El-Din, M.; Martin, W. J. Ozonation Degrades All Detectable Organic Compound Classes in Oil Sands Process-Affected Water: An Application of High Performance Liquid Chromatography/Obitrap Mass Spectroscopy. *Rapid Commun. Mass Spectrom.* **2013**, *27*, 2317–2326.

5. Hoiberg, A. J. *Bituminous Materials*: *Asphalts, Tars and Pitches*; Interscience Publisher: New York, 1964.

6. Hunt, J. M. *Petroleum Geochemistry and Geology. 2ⁿᵈ Edition*; W. H. Freeman & Company: San Francisco, USA, 1979.

7. Shah, A.; Fishwick, R.; Wood, J.; Leeke, G.; Rigby, S.; Greaves, M. A Review of Novel Techniques for Heavy Oil and Bitumen Extraction and Upgrading. *Energy & Environmental Science* **2010**, *3*, 700–714.

8. Martinez, A. R. Report of Working Group on Definitions. In: *The Future of Heavy Crude and Tar Sands*; Meyer, R. F.; Wynn, J. C.; Olson, J. C. Eds.; Second International Conference: McGraw-hill, New York, USA, pp. 1xvii-1xviii.

9. Meyer, R. F.; Attanasi, E. D.; Freeman, P. A. Heavy Oil and Natural Bitumen Resources in Geological Basins of the World. *USGS* **2007**.

10. Petersen, N. F.; Hickey, P. J. California Plio-Miocene Oils: Evidence of Early Generation. In: *Exploration for Heavy Crude Oil and Natural Bitumen*; Meyer, R. F. Eds.; Am. Assoc. Petrol. Geol.: USA, 1987, pp. 351–359.

11. Byran, J. L.; Kantzas, A.; Mai, A.; Hum, F. M. Applications of Low Field NMR Techniques in the Characterization of Oil Sand Mining, Extraction and Upgrading Processes. *The Canadian Journal of Chemical Engineering* **2005**, *83*, 145–150.

12. Speight, J. G.; Luque, R. *Gasification for Synthetic Fuel Production: Fundamentals, Processes and Applications: 1ˢᵗ Edition*; Woodhead Publishing: Cambridge, UK, 2014.

13. Wu, W.; Chen, J. Characteristics of Chinese Heavy Crudes. *J. Pet. Sci. Eng.* **1999**, *22*, 25–30.

14. Leon, V. Composition and Structure of Heavy Oils. *J. CODICID* **2000**, *2*, 34–43.

15. Yaghi, B. M.; Al-Bemani, A. Heavy Crude Oil Viscosity Reduction for Pipeline Transportation. *Energy Sources* **2002**, *24*, 93–102.

16. Foght, J. M. Anaerobic Biodegradation of Aromatic Hydrocarbons: Pathways and Prospects. *J. Mil. Microbial. Biotechnol.* **2008**, *15*, 93–120.

17. Galarraga, C. E.; Pereira-Almao, P. Hydrocracking of Athabasca Bitumen Using Submicronic Multimetallic Catalysts at Near In-Reservoir Conditions. *Energy Fuels* **2010**, *24*, 2383–2389.

18. Moschopedis, S. E.; Speight, J. G. Oxidation of a Bitumen. *Fuel* **1975**, *54*, 210–212.

19. Nassar, N. N.; Hassan, A.; Pereira-Almao, P. Application of Nanotechnology for Heavy Oil Upgrading: Catalytic Steam Gasification/Cracking of Asphaltenes. *Energy Fuels* **2011**, *25*, 1566–1570.

20. Nassar, N. N.; Hassan, A.; Pereira-Almao, P. Metal Oxide Nanoparticles for Asphaltene Adsorption and Oxidation. *Energy Fuels* **2011**, *25*, 1017–1023.

21. Pereira-Almao, P. R.; Larter, S.; Lines, L.; Maini, B.; Moore, G. M. An Alberta Ingenuity Fund Proposal for the Establishment of the Alberta Ingenuity Centre for In Situ Energy, Calgary, Alberta, Canada, 2004.

22. Hashemi, R.; Nassar, N. N.; Pereira-Almao, P. In Situ Upgrading of Athabasca Bitumen Using Multimetallic Ultradispersed Nanocatalysts in an Oil Sands Packed-Bed Column: Part 1. Produced Liquid Quality Enhancement. *Energy Fuels* **2014**, *28*, 1338−1350.

23. Moschopedis, S. E.; Speight, J. G. The Oxidation of a Bitumen in Relation to Its Recovery from Tar Sand Formations. *Fuel* **1974**, *53*, 21–25.

24. Leon, V. Biological Upgrading of Heavy Crude Oil. *Biotechnology and Bioprocess Engineering* **2005**, *10*, 471–481.

25. Bret-Rouzaut, N.; Favennec, J. P. *Oil and Gas Exploration and Production, Reserves, Costs and Production*; Institut Francais Du Petrole Publications: Paris, France, 2004.

26. Gray, M. R. Tutorial on Upgrading of Oil sands Bitumen. Department of Chemical and Materials Engineering, University of Alberta, Edmonton, Alberta, Canada, 2001.

27. Bernard, F. P.; Connan, J.; Magot, M. Indigenous Microorganism in Connate Water of Many Oil Fields: A New Tool in Exploration and Production Techniques. In: *Proceedings of the SPE Annual Technical Conference and Exhibition*, Washington, D. C., **1992**, 467–476.

28. Bryant, R. S.; Burchfield, T. E. Review of Microbial Technology for Improving Oil Recovery. In: *Proceedings Volume, Nat. Inst. Petrol. Energy Res. Microbial Enhanced Oil Recovery Short Course*; Bartlesville, Okla, 1989.

29. Hitzman, D. O.; Sperl, G. T. A New Microbial Technology for Enhanced Oil Recovery and Sulfide Prevention and Reduction. Proceedings of the SPE/DOE ninth Symposium of Improved Oil Recovery, Tulsa, Ok, USA, 1994, 171–179.

30. Fedorak, P. M.; Foght, J. M.; Gray, M. R. Conversion of Heavy Oil and Bitumen to Methane by Chemical Oxidation and Bioconversion, US Patent Application 2009/0130732.

31. Foght, J. M. Anaerobic Biodegradation of Aromatic Hydrocarbons: Pathways and Prospects. *J. Mil. Microbial. Biotechnol.* **2008**, *15*, 93–120.

32. Ahrens, C.D. *Meteorology Today*; West Publishing Co.: St. Paul, MN, 1994.

33. Siddiquee, M. N.; de Klerk, A. Hydrocarbon Addition Reactions during Low-Temperature Autoxidation of Oil sands Bitumen. *Energy Fuels* **2014**, *59*, 6848–6859.

34. Hollemann, F.; Wiberg, E.; Wiberg, N. *Lehrbuch der Anorganischen Chemie (Inorganic Chemistry)*; De Gruyter: Berlin, New York, 1995.

35. Bailey, P. S. *Ozonation in Organic Chemistry. Volume I: Olefinic Compounds*; Academic Press: New York, 1978.

36. Beltran, F. J. *Ozone Reaction Kinetics for Water and Wastewater Systems*; Lewis Publishers: Boca Raton, FL, 2004.

37. Cha, Z. *Ozonation of Canadian Athabasca Asphaltene*; UMI Microform: The University of Utah, Salt Lake City, Utah, 2009.

38. Sheu, E. Y.; Mullins, O. C. *Asphaltenes, Fundamentals and Applications*; Plenum Press: New York, 1995.

39. Gunten, U. V. Ozonation of Drinking Water: Part II. Disinfection and By-Product Formation in Presence of Bromide, Iodide or Chlorine. *Water Research* **2003**, *37*, 1469–1487.

40. Murugan, P.; Mani, T.; Mahinpey, N.; Asghari, K. The Low Temperature Oxidation of Fosterton Asphaltenes and Its Combustion Kinetics. *Fuel Processing Technology Journal* **2011**, *92*, 1056–1061.

41. Cao, X.; Lei, Y.; Wang, W. Study on Thermal Oxidation of Asphalt Fractions by In-Situ FTIR Analysis. *Advanced Materials Research* **2011**, *160–162*, 330–335.

42. Harries, C. D. The Effect of Ozone on Organic Compounds. *Berichte der deutschen chemischen Gesellschaft* **1915**, *410*, 1–21.

43. Strausz, O. P.; Lown, E. M.; Morales-Izquierdo, A.; Kazmi, N.; Mongomery, D. S.; Payzant,. J. D.; Murgich, J. Chemical Composition of Athabasca Bitumen: The Distillable Aromatic Fraction. *Energy Fuels* **2011**, *25*, 4552–4579.

44. Criegee, R.; Werner, G. The ozonation of 9,10-octalins. *Justus Liebigs Ann. Chem.* **1949**, *6*, 632–637.

45. Glozman, E. P.; Akhmetova, R. S. Chemical Composition of Bitumen Components. *Chemistry and Technology of Fuels and Oils* **1970**, *6*, 364–367.

46. Akbarzadeh, K.; Ayatollahi, S.; Moshfeghian, M.; Alboudwarej, H.; Yarranton, H. W. Estimation of SARA Fraction Properties with the SRK EOS. *Journal of Canadian Petroleum Technology* **2004**, *43*, 31–39.

47. Centi, G. *New Developments in Selective Oxidation*; Elsevier Science Pub.: Rimini, Italy, 1989.

48. Cha, Z. *Ozonation of Canadian Athabasca Asphaltene*; UMI microform: The University of Utah, Salt Lake City, Utah, 2009.

49. Schonbein, C. F. On the Odour Accompanying Electricity and on the Probability of its Dependence on the Presence of a New Substance. *Philosophical Magazine* **1840**, *17*, 293–294.

50. Speight, J. G.; Moschopedis, S. E. The Effect of Oxygen Functions on the Properties of Bitumen Fractions. *Journal of Canadian Petroleum Technology* 1978, *17*, 73–75.

51. Moschopedis, S. E.; Speight, J. G. The Effect of Air Blowing on the Properties and Constitution of a Natural Bitumen. *J. Mater. Sci.* **1977**, *12*, 990–998.

52. Selucky, M. L.; Chu, Y.; Ruo, T.; Strausz, O. P. Chemical Composition of Athabasca Bitumen. *Fuel* **1977**, *56*, 369–381.

53. Dore, M.; Langlais, B.; Legube, B. Mechanism of the Reaction of Ozone with Soluble Aromatic Pollutants. *Ozone: Science and Engineering* **1980**, *2*, 39–54.

54. Akhmetova, R. S.; Glozman, E. P.; Changes in Quality and Group Composition of Bitumens Obtained by Continuous and Batch Oxidation. *Chemistry and Technology of Fuels and Oils* **1969**, *5*, 414–417.

55. Zhang, H.; Ji, L.; Wu, F.; Tan, J. In Situ Ozonation of Anthracene in Unsaturated Porous Media. *Journal of Hazardous Materials* **2005**, *120*, 143–148.

56. Redford, D. A.; Cotsworth, P. F. Development of Communication Paths within a Tar Sand Bed. *American Chemical Society* **1976**, *19*, 112–120.

57. Becker, H. G. O.; Domschke, G.; Fanghanel, E. *Organikum : organisch-chemisches Grundpraktikum*; Berlin Dt. Verl. der Wiss.: Berlin, Germany, 1986.

58. Rudenskaya, I. M. Upgrading of Petroleum Bitumens. Conference Papers: Russian, GOSINTI ,1964.

59. Sixma, F. L. J. Kinetical Experiments on Ozonization Reactions. IV. Pyridine and Some of Its Derivatives. *Recueil des Travaux Chimiques des Pays-Bas* **1952**, *71*, 1124–1130.

60. Babu, D. R.; Cormack, D. E. Effect of Oxidation on the Viscosity of Athabasca Bitumen. *Can. J. Chem. Eng.* **1984**, *62*, 562–564.

61. Babu, D. R.; Cormack, D. E. Low Temperature Oxidation of Athabasca Bitumen. *Can. J. Chem. Eng.* **1983**, *61*, 575–580.

62. Hong, P. K.; Cha, Z. *Ozonation Conversion of Heavy Hydrocarbons for Resource Recovery*; the University of Utah: Salt Lake City, Utah, 2011.

63. Moschopedis, S. E.; Speight, J. G. The Oxidation of a Bitumen in Relation to Its Recovery from Tar Sand Formations. *Fuel* **1974**, *53*, 21–25.

64. Reid, R. C.; Prausnitz, J. M.; Poling, B. E. *The Properties of Gases and Liquids*; McGraw-Hill: New York, 1987.

65. Taylor, K. M. *The Chemical Oxidation of Polycyclic Aromatic Hydrocarbons at a Former ManufacturedGas Plant in Bay Shore;* M.Sc.Thesis, Stony Brook University, New York, 2012.

66. Ahrens C. D. *Meteorology Today*; West Publishing Co.: St. Paul, MN, 1994.

67. Bailey, P. S. *Ozanation in Organic Chemistry: Volume 1 – Olefinic Compounds*; Academic Press: New York, San Francisco, 1978.

68. Bailey, P. S. *Ozanation in Organic Chemistry: Volume II – Nonolefinic Compounds*; Academic Press: New York, San Francisco, 1982.

69. Siegrist, R. L.; Crimi, M.; Simpkin, T. J. *In Situ Chemical Oxidation for Groundwater Remediation*. Springer: New York, NY, USA, 2011.

70. Bufalini, J. J.; Altshuller, A. P. Kinetics of Vapour-Phase Hydrocarbon-Ozone Reactions. *Canadian Journal of Chemistry* **1964**, *43*, 2243–2249.

71. Nonhebel, D. C.; Walton, J. C. *Free Radical Chemistry: Structure and Mechanisms*; Cambridge University Press: London, 1974.

72. Santoro, R. J.; Glassman, I. A Review of Oxidation of Aromatic Compounds. *Combustion Science and Technology* **1979**, *19*, 161–164.

73. Hoiberg, A. J. *Bituminous Materials*: *Asphalts, Tars and Pitches*; Interscience Publisher: New York, 1964.

74. Rakovsky, S.; Zaikov, G. *Kinetics and Mechanism of Ozone Reactions with Organic and Polymeric Compounds in Liquid Phase*; Nove Scenice Publishers: New York, 1998.

75. Kampschmidt, L. W. F.; Wibaut, J. P. On the Ozonization and the Ozonolysis of Naphthalene, 2,3-Dimethylnaphthalene, and 1,4-Dimethylnaphthalene in Connection with the Reactivity of the Ring System. *Recueil des Travaux Chimiques des Pays-Bas* **1954**, *73*, 431–454.

76. Platonov, V. V.; Kudrya, A. N.; Proskuryakov, S. V. Ozonolysis of Asphaltenes from Semicoking Tar of G17 Coal. *Russian Journal of Applied Chemistry* **2003**, *76*, 148–152.

77. Beltran, F. J. *Ozone Reaction Kinetics for Water and Wastewater Systems*; Lewis Publishers: Boca Raton, FL, 2004.

78. Nobis, M.; Roberge, D. M. Mastering Ozonolysis: Production from Laboratory to Ton Scale in Continuous Flow. *Chimica oggi/Chemistry Today* **2011**, *29*, 56–58.

79. Chu, Y.; Selucky, M. L.; Strausz, O. P. Chemical Composition of Cold Lake Bitumen. *Fuel* **1978**, *57*, 9–16.

80. Claus, R. E.; Schreiber, S. L. Ozonolytic Cleavage of Cyclohexene to Terminally Differentiated Products: Methyl 6-Oxohexanoate, 6,6-Dimethoxyhexanal, Methyl 6,6-Dimethoxyhexanoate. In: *Org. Synth.*; John Wiley & Sons, Inc.: New York, 1990.

81. Criegee, R. The Course of Ozonation of Unsaturated Compounds. *Rec. Chem. Progr.* 1957, *18*, 111–120.

82. Cyr, N.; McIntyre, D. D.; Toth, G.; Strausz, O. P. Hydrocarbon Structural Group Analysis of Athabasca Asphaltene and Its GPC Fractions by ^{13}C NMR. *Fuel* **1987**, *66*, 1709–1714.

83. Vassiliev, N. Y.; Davison, R. R.; Williamson, S. A.; Glover, C. J. Air Blowing of Supercritical Asphalt Fractions. *Ind. Eng. Chem. Res.* **2001**, *40*, 1773–1780.

84. Braslavsky, S. E.; Rubinb, M. B. The History of Ozone: Part VIII. Photochemical Formation of Ozone. *Photochem. Photobiol. Sci.* **2011**, *10*, 1515–1520.

85. Hassan, A.; Carbognani, L.; Pereira-Almao, P. Oxidation of Oils and Bitumen at Various O_2 Concentrations. *Energy Fuels* **2010**, *24*, 5378–5386.

86. Harries, C. D.; de Osa, A. S. Ozonation of Unsaturated Hydrocarbons. *Berichte der deutschen chemischen Gesellschaft* **1904**, *37*, 842–845.

87. Harries, C. D. The Action of Ozone on Organic Compounds. *Liebigs Annalen der Chemie* **1912**, 390, 235.

88. Trambarulo, R.; Ghosh, S. N.; Burrus, Jr. C. A.; Gordy, W. The Molecular Structure, Dipole Moment, and g Factor of Ozone from Its Microwave Spectrum. *J. Chem. Phys.* **1953**, *21*, 851–855.

89. Turoski, V. *Chlorine and Chlorine Compounds in the Paper Industry*; Ann Arbor Press: Chelsea, Michigan, 1998.

90. Langlais, B.; Reckhow, D. A.; Brink, D. R. *Practical Application of Ozone: Principle and Case Study*. In *Ozone in Water Treatment*; Lewis Publishers: Chelsea, Michigan, 1991.

91. Razumovskii, S. D.; Zaikov, G. E. *Ozone and Its Reactions with Organic Compounds*; Elsevier Science Ltd.: Amsterdam, 1984.

92. Feuer, H.; Rubinstein, H.; Nielsen, A. T. Reaction of Alkyl Isocyanides with Ozone. A New Isocyanate Synthesis. *J. Org. Chem*. **1958**, *23*, 1107–1109.

93. Calvert, J. G.; Atkinson, R.; Becker, K. H.; Kamens, R. M.; Seinfeld, J. H.; Wallington, T. J.; Yarwood, G. *The Mechanism of Atmospheric Oxidation of Aromatic Hydrocarbons*; Oxford University Press, Inc.: New York, NY, USA, 2002.

94. Gottschalk, C.; Libra, J. A.; Saupe, A. *Ozonation of Water and WasteWater: A Practical Guide to Understanding Ozone and its Application, 2nd Edition*; Wiley-VCH: New York, 2009.

95. Mohr, P. J.; Taylor, B. N.; Newell, D. B. CODATA Recommended Values of the Fundamental Physical Constants. *Re. Mod. Phys.* **2008**, *80*, 633–730.

96. Elovitz, M. S.; von Gunten, U. U.; Kaiser, H. P. Hydroxyl Radical/Ozone Ratios during Ozonation Processes. II. The Effect of Temperature, pH, Alkalinity, and DOM Properties. *Ozone Sci. Tech.* **2000**, *22*, 123–150.

97. Elliot, A. J.; Simsons, A. S. Rate Constants for the Reactions of Hydroxyl Radicals as a Function of Temperature. *Radiat. Phys. Chem.* **1984**, *24*, 229–231.

98. Silaev, M. M. Simulation of the Initiated Addition of Hydrocarbon Free Radicals and Hydrogen Atoms to Oxygen via a Non-Branched Chain Mechanism. *Theoretical Foundations of Chemical Engineering* **2007**, *41*, 831–838.

99. Morrison, W. L. Photoimmunology. *Photochem. Photobiol.* **1984**, *40*, 781–787.

100. Mill, T.; Tse, D. S.; Loo, B.; Yao, C. C. D.; Canavesi, E. Oxidation Pathways for Asphalt. *Prepr. ACS Div. Fuel Chem.* **1992**, *37*, 1367–1375.

101. Oesper, R. E. Christian Friedrich Schonbein. *Journal of Chemical Education* **1929**, *6*, 432–440.

102. Phillips, C. R.; Hsieg, I. C. Oxidation Reaction Kinetics of Athabasca Bitumen. *Fuel* **1985**, *64*, 985–989.

103. Strausz, O. P. *The Chemistry of the Alberta Oil Sand Bitumen*; Alberta Energy Research Institute: Edmonton, Alberta, Canada, 1924.

104. Nassar, N. N.; Hassan, A. Comparative Study on Thermal Cracking of Athabasca Bitumen. *J. Therm. Anal. Calorim.* **2013**, *114*, 465–472.

105. Read, J.; Whiteoak, D. *The Shell Bitumen Handbook*; Thomas Telford Publishing: London, UK, 2003.

106. Goodrich, J. L.; Goodrich, J. E.; Kari, W. J. Asphalt Composition Tests: Their Application and Relation to Field Performance. *TRB Record* **1986**, *1096*, 146–167.

107. Gunten, U. V. Ozonation of Drinking Water: Part I. Oxidation Kinetics and Product Formation. *Water Research* **2003**, *37*, 1443–1467.

108.   Jia, N.; Moore, R. G.; Mehta, S. A.; Van Fraassen, K.; Ursenbach, M. G.; Zalewski, E. Compositional Changes for Athabasca Bitumen in the Presence of Oxygen under Low Temperature Conditions. *J. Can. Petrol. Technol.* **2005**, *44*, 51–56.

109.   Wibaut, J. P.; Sixma, F. L. J.; Kampschmidt, L. W. F.; Boer, H. The Mechanism of the Reaction between Ozone and Aromatic Compounds. (Preliminary Communication). *Recueil des Travaux Chimiques des Pays-Bas* **1950**, *69*, 1355–1363.

110.   Molina, L. T.; Molina, M. J. Absolute Absorption Cross Section of Ozone in the 185- to 350-nm Wavelength Range. *Journal of Geophysical Research* **1986**, *91*, 14501–14508.

111.   Guillen, M. D.; Goicoechea, E. Oxidation of Corn Oil at Room Temperature: Primary and Secondary Oxidation Products and Determination of Their Concentration in the Oil Liquid Matrix from ^{1}H Nuclear Magnetic Resonance Data. *Food Chemistry* **2009**, *116*, 183–192.

112.   Siddiquee, M. N.; de Klerk, A. Hydrocarbon Addition Reactions during Low-Temperature Autoxidation of Oil-sands Bitumen. *Energy Fuels* **2014**, *28*, 6848−6859.

113.   Ramseier, M. K.; von Gunten, U. Mechanisms of Phenol Ozonation – Kinetics of Formation of Primary and Secondary Reaction Products. *Ozone: Science & Engineering* **2009**, *31*, 201–215.

114.   Coates, J. *Interpretation of Infrared Spectra, a Practical Approach*; John Wiley & Sons Inc.: California, 2000.

115.   Silverstein, R. M.; Bassler, G. C.; Morrill, T. C. *Spectrometric Identification of Organic Compounds: 4th Ed*; John Wiley & Sons Inc.: California, 1981.

116.   Atkins, P.; de Paula, J. *Physical Chemistry: 8th edition*; W. H. Freeman and Company: New York, 2006.

117.   Jones, R. A.; Bean, G. P. *The Chemistry of Pyrroles*; Academic Press: London, 1977.

118.   Anslyn, E.; Dougherty, D. A. *Modern Physical Organic Chemistry*; University Science Books: Sausalito, CA, 2006.

119.   Moschopedis, S. E.; Speight, J. G. Introduction of Oxygen Functions into Asphaltenes and Resins. *Fuel* **1978**, *57,* 25–28.

120.   Siddiquee, M. N.; de Klerk, A. Continuous and Prolonged Oxidation of Bitumen for Upgrading by Microbial Digestion. *Prepr. Pap. Am. Chem. Soc., Div. Energy Fuels* **2013**, *58*, 649–651.

121.   Bailey, P. S. *Ozonation in Organic Chemistry, Volume II: Nonolefinic Compounds*; Academic Press, The University of Texas at Austin: Austin, Texas, 1982.

122.   Deslongchamps, P.; Moreau. C.; Frehel, D.; Atlanti, P. In the Oxidation of Acetals by Ozone. *Canad. J. Chem.* **1972**, *50*, 3651−3664.

123.   Erickson, R. E.; Hansen, R. T.; Harkins, J. Mechanism of Ozonation Reactions, III. Ethers. *J. Am. Chem. Soc.* **1968**, *90*, 6777-6783.

124.   Hamilton, G. A.; Ribner, B. S.; Hellman, T. M. The Mechanism of Alkane Oxidation by Ozone. *Advan. Chem. Ser.* **1968**, *77*, 15−25.

125.   Price, C. C.; Tumolo, A. L. The Course of Ozonation of Esters I. *Journal of the American Chemical Society* **1964**, *86*, 4691−4964.

126.   Syrov, A. A.; Tsyskovskii, Z. H. The Present State of the Theory of the Oxidation of Cyclo-olefins. *Org. Khim.* **1970**, *39*, 817−838.

127.   White, H. M.; Bailey, P. S. Ozonation of Aromatic Aldehydes1. *Journal of Organic Chemistry* **1965**, *30*, 3037−3041.

128.   Whiting, M. C.; Bolt, A. J. N.; Parrish, J. H. The Reaction between Ozone and Saturated Compounds. *Advan. Chem. Ser.* **1968**, *77*, 119.

129.   Williamson, D. G.; Cvetanovic, R. J. Rates of Ozone-Paraffin Reactions in Carbon Tetrachloride Solution. *J. Am. Chem. Soc.* **1970**, *92*, 2949–2952.

130. Cavill, G. W. K.; Robertson, A.; Whalley, W. B.; Badcock, G. G. The Chemistry of the "Insoluble Red" Woods. Part IV. Some Mixed Benzoins. *J. Chem. Soc.* **1950**, 1567, 2961-2965.

131. Emanuel, N. M.; Denisov, E. T.; Maizus, Z. K. *Liquid-Phase Oxidation of hydrocarbons*; Plenum Press: New York, 1967.

132. Rakovsky, S. K.; Cherneva, D.; Shopov, D.; Parfenov, V. Applying of Barbotage method to Investigation the Kinetic of Ozone Reactions with Organic Compounds., Izv. Khim. BAN, XI (4), **1978**, *11*, 153.

133. Serif, G. S.; Hunt, C. F.; Bourns, A. N. Liquid Phase Oxidation of *p*-Cymene: Nature of Intermediate Hydroperoxides and Relative Activity of the Alkyl Groups. *Can. J. Chem.* **1953**, *31*, 1229, 1229–1238.

134. Boardman, H. The Mechanism of Oxidation of *p*-Cymene. *J. Am. Chem. Soc.,* **1962**, *84*, 1376–1382.

135. Ciamician, G.; Silber, P. Photochemistry. *European Journal of Inorganic Chemistry* **1901**, *34*, 2040–2046.

136. Rao, T. S. S.; Awasthi, S. Oxidation of Alkylaromatics. *E-Journal of Chemistry* **2007**, *4*, 1–13.

137. Bufalini, J. J.; Altshuller, A. P. Kinetics of Vapour Phase Hydrocarbon-Ozone Reactions. *Can. J. Chem.* **1965**, *43*, 2243–2250.

138. Kampschmidt, L. W. F.; Wibaut, J. P. On the Ozonization and the Ozonolysis of Naphthalene, 2,3-Dimethylnaphthalene, and 1,4-Dimethylnaphthalene in Connection with the Reactivity of the Ring System. *Recueil des Travaux Chimiques des Pays-Bas* **1954**, *73*, 431–454.

139. Wibaut, J. P.; Kampschmidt, L. W. F.; Sixma, F. L. J.; Boer, H. The Mechanism of the Reaction between Ozone and Aromatic Compounds. (Preliminary Communication). *Recueil des Travaux Chimiques des Pays-Bas* **1950**, *69*, 1355–1363.

140.   Razumovskii, S. D.; Kefeli, A. A.; Trubnikov, G. R.; Zaikov, G. E. Determination of the Kinetic Parameters in the Ozone-Polyethylene and Ozone-Polystyrene Reactions with Allowance for Topochemical Features, *Polymer Science U.S.S.R.* **1972**, *14*, 2812–2820.

141.   Saito, T.; Niki, E.; Shiono, T.; Kamiya, Y. Oxidative Degradation of Polymers. V. Ozonization of Polypropylene and Polystyrene in Carbon Tetrachloride. *Bulletin of the Chemical Society of Japan* **1978**, *51*, 1153-1157.

142.   Hartmann, M.; Seiberth, M. About a Tetralin Peroxide. *Helvetica Chimica Acta* **1932**, *15*, 1390–1392.

143.   Hock, H.; Lang, S. Autoxydation von Kohlenwasserstoffen, V. Mitteil.: Über sekundäre Vorgänge bei der Peroxyd-Reduktion zu Alkoholen. *Berichte der deutschen chemischen Gesellschaft* **1942**, *75*, 313–316.

144.   Emanuel, N. M.; Denisov, E. T.; Maizus, Z. K. *Liquid Phase Oxidation of Hydrocarbons*; Plenum Press: New York, 1967.

145.   Waters, W. A. *Mechanism of Oxidation of Organic Compounds*; Methuen: London, 1964.

146.   McMurry, J. E. *Organic Chemistry. 8th Edition*; Cengage Learning Inc.: Boston, MA, 2012.

147.   Peter, K.; Vollhardt, C.; Schore, N. E. *Organic Chemistry: Structure and Function. 5th Edition*; W. H. Freeman & Company: New York, NY, 2005.

148.   Morrison, R. T.; Boyd, R. N. *Organic Chemistry, 5th Edition*; Allyn and Bacon Inc.: Boston, US, 1987.

149.   Jones, G.; Baty, D. J. *Quinoline N-Oxides. In Quinolins. Part II*; Jones, G. Ed.; John Wiley and Sons: Chichester, 1982, pp. 377–605.

150.   Katritzky, A. R.; Lagowski, J. M. *Chemistry of the Heterocyclic N-Oxides*; Academic Press: London, 1971.

151. Lindenstruth, A. F.; Vander Werf, C. A. The Preparation of Quinolinic and Cinchomeronic Acids by Ozone Oxidation. *J. Am. Chem. Soc.* **1949**, *71*, 3020–3021.

152. Schenck, L. M.; Bailey, J. R. Nitrogen Compounds in Petroleum Distillates. XVIII. Isolation, Ozonization and Synthesis of 2,4-Dimethyl-8-s-butylquinoline. *J. Am. Chem. Soc.* **1940**, *62*, 1967–1969.

153. Kovalev, I. S.; Kopchek, D. S.; Zaryanov, G. V.; Rusinov, V. L.; Chepakhin, O. N. Nucleophilic Dimerization of Indoline Under Oxidative Conditions. *Mendeleev Commun.* **2014**, *24*, 40–41.

154. Linhares, M.; Rebelo, S. L. H.; Simoes, M. M. Q.; Silva, A. M. S.; Neves, M. G. P. M. S.; Cavaleiro, J. A. S.; Freire, C. Biomimetic Oxidation of Indole by Mn(III) Porphyrins. *Appl. Catal. A Gen.* **2014**, *470*, 427–433.

155. Talbi, H.; Monard, G.; Loos, M.; Billuad, D. Theoretical Study of Indole Polymerization. *J. Mol. Struc. Theo. Chem.* **1998**, *434*, 129–134.

156. Rakovsky. S. K.; Zaikov, G. E. *Kinetics and Mechanism of Ozone Reaction with Organic and Polymeric Compounds in Liquid Phase*; Nova Science Publishers Inc.: Commack, New York, 1998.

157. Komissarov, V. D.; Galimova, L. G.; Komissarova, I. N.; Shereshovets, V. V.; Denisov, E. T. Kinetics, Products, and Mechanism of the Reaction of Ozone with Cumyl Hydroperoxide. *Bulletin of the Academy of Sciences of the USSR, Division of chemical science* **1978**, *27*, 2210–2214.

158. Syroezhko, A. M.; Korotkova, N. P.; Vikhorev, A. A.; Proskuryakov, V. A. Studies in the Field of Chemistry and Technology of Products of Fossil Fuel Processing. *Zh. Prikl. Khim.* **1975**, *48*, 39 –43.

159. Vikhorev, A. A.; Syroezhko, A. M.; Proskuryakov, V. A.; Yakovlev, A. S. Ozonation of Cyclohexane in the Presence of Homogeneous Catalysts. *Zh. Prikl. Khim.* **1983**, *26*, 121–122.

160.   Vikhorev, A. A.; Syroezhko, A. M.; Proskuryakov, V. A.; Yakovlev, A. S. Oxidation of *n*-Decane by Ozone–Air Mixtures. *J. Appl. Chem.* **1978**, *51*, 2448–2451.

161.   Rakovsky, S. K.; Razumovskii, S. D.; Zaikov, G. E.; Shopov, D. M.Ozone and Its Reactions with Organic Compounds. *Publishing House of the Bulgarian Academi of Science* **1983**, *1*, 278.

162.   Waters, W. A. *Mechanism of Oxidation of Organic Compounds*; Methuen: London, 1964.

163.   Babu, D. R.; Cormack, D. E. Low Temperature Oxidation of Athabasca Bitumen. *Can. J. Chem. Eng.* **1983**, *61*, 575–580.

164.   Bailey, P. S. The Reactions of Ozone with Organic Compounds. *Chem. Revs.* **1958**, *58*, 925–1010.

165.   Cha, Z. *Ozonation of Canadian Athabasca Asphaltene*; UMI microform: The University of Utah, Salt Lake City, Utah, 2009.

166.   Moschopedis, S. E.; Speight, J. G. The Oxidation of a Bitumen in Relation to Its Recovery from Tar Sand Formations. *Fuel* **1974**, *53*, 21–25.

167.   Moschopedis, S. E.; Speight, J. G.; Oxidation of A Bitumen. *Fuel* **1975**, *54*, 210–212.

168.   Campbell, P. G.; Wright, J. R. *Oxidation Products in an Oxygen-Blown Kuwait Asphalt*; National Bureau of Standards: Washington, D. C., 1964.

169.   Siddiquee, M. N.; de Klerk, A. Hydrocarbon Addition Reactions during Low-Temperature Autoxidation of Oil sands Bitumen. *Energy Fuels* **2014**, *28*, 6848−6859.

170.   Strausz, O. P.; Lown, E. M. *The Chemistry of Alberta Oil Sands, Bitumen and Heavy Oils*; Alberta Energy Research Institue (AERI): Calgary, AB, Canada, 2003, pp. 89–133.

171.   Kampschmidt, L. W. F.; Wibaut, J. P. On the Ozonization and the Ozonolysis of Naphthalene, 2,3-Dimethylnaphthalene, and 1,4-Dimethylnaphthalene in Connection

with the Reactivity of the Ring System. *Recueil des Travaux Chimiques des Pays-Bas* **1954**, *73*, 431–454.

172.   Mill, T.; Tse, D. S.; Loo, B.; Yao, C. C. D.; Canavesi, E. Oxidation Pathways for Asphalt. *Prepr. ACS Div. Fuel Chem.* **1992**, *37*, 1367–1375.

173.   Burger, J. G.; Sahuquet, B. C. Chemical Aspects of In-Situ Combustion – Heat of Combustion and Kinetics. *SPE J.* **1972**, *12*, 410–422.

174.   Fassihi, M. R.; Brigham, W. E.; Ramey, Jr. H. J. Reaction Kinetics of In-Situ Combustion: Part 1 – Observations. *SPE J.* **1984**, *24*, 399–407.

175.   Kisler, J. P.; Shallcross, D. C. Improved Model for the Oxidation Processes of Light Crude Oil. *Trans IChemE.* **1997**, *75*, 392–400.

176.   Mamora, D. D.; Brigham, W. E. Implications of Low-Temperature Oxidation in Kinetic and Combustion Tube Experiments. Presented at the 6th UNITAR International Conference on Heavy Crude and Tar Sands, Houston, TX, 1995.

177.   Moore, R. G.; Belgrave, J. D. M.; Mehta, S. A.; Ursenbach, M. G.; Laureshen, C. J.; Xi, K. Some Insights into Low Temperature In-Situ Combustion Kinetics. Presented at the 8th SPE/DOE Symposium in IOR, Tulsa, Oklahoma, 1992.

178.   Badamchi-Zadeh, A. *Use of CO2 in Vapex, Experimental and Modeling Study*; A Ph.D. Thesis, Department of Chemical and Petroleum Engineering, University of Calgary: Calgary, Alberta, Canada, 2013.

179.   He, L.; Li, X.; Wu, G.; Lin, F.; Sui, H. Distribution of Saturates, Aromatics, Resins, and Asphaltenes Fractions in the Bituminous Layer of Athabasca Oil Sands. *Energy Fuels* **2013**, *27*, 4677–4683.

180.   Peramanu, S.; Pruden, B. B.; Rahimi, P. Molecular Weight and Specific Gravity Distributions for Athabasca and Cold Lake Bitumen and Their Saturate, Aromatic, Resin, Asphaltene Fractions. *Ind. Eng. Chem. Res.* **1999**, *38*, 3121–3130.

181. Adegbesan, K. O.; Donnelly, J. K.; Moore, R. G.; Bennion, D. W. Liquid Phase Oxidation Kinetics of the Oil Sands Bitumen, Part 1: Experimental Investigation, and Part 2: Kinetic Models for In-Situ Combustion Numerical Simulation. *American Institute of Chemical Engineers Journal* 1986, *32*, 1242–1252.

182. Wallace, D.; Henry, D.; Takamura, K. A Physical Chemical Explanation for Deterioration in the Hot Water Processability of Athabasca Oil Sand due to Aging. *Fuel Sci. Technol. Int.* **1989**, *7*, 699–725.

183. Xu, H. H.; Okazawa, N. E.; Moore, R. G. In Situ Upgrading of Heavy Oil. *Journal of Canadian Petroleum Technology* **2001**, *40*, 45–53.

184. Bailey, P. S. *Ozonation in Organic Chemistry, Volume 2: Nonolefinic Compounds*; Academic Press: New York, 1982.

185. Jia, N.; Moore, R. G.; Mehta, S. A.; Ursenbach, M. G. Kinetic Modeling of Thermal Cracking and Low Temperature Oxidation Reactions. *Journal of Canadian Petroleum Technology* **2006**, *45*, 21–28.

186. Blokker, P. C.; Van-Hoorn, H. *Durability of Bitumen in Theory and Practice*; World Petroleum Congress: New York, USA, 1959.

187. Santagata, E.; Baglieri, O.; Tsantilis, L.; Dalmazzo, D . Evaluation of Self-Healing Properties of Bituminous Binders Taking into Account Steric Hardening Effects. *Construction and Building Materials* **2013**, *41*, 60–67.

188. Siddiquee, M. N.; de Klerk, A. Hydrocarbon Addition Reactions during Low-Temperature Autoxidation of Oilsands Bitumen. *Energy Fuels* **2014**, *28*, 6848−6859.

189. Traxler, R. N.; Schweyer, H. H. Increase in Viscosity of Asphalt with Time. *Proc. Am. Soc. Test Mater.* **1936**, *36*, 544–551.

190. Anslyn, E.; Dougherty, D. *Modern Physical Organic Chemistry*; University Science Books: Sausalito, CA, 2006.

191.   Atkins, P.; de Paula, J. *Physical Chemistry: 8th edition*; W. H. Freeman and Company: New York, 2006.

192.   Petersen, J. C. An Infrared Study on Hydrogen Bonding in Asphalt. *Fuel* **1967**, *46*, 295–305.

193.   Janoschek, R.; Weidemann, E. G.; Pfeiffer, H.; Zundel, G. Extremely High Polarizability of Hydrogen Bonds. *J. Am. Chem. Soc.* **1972**, *94*, 2387–2396.

194.   Simonescu, C. M. Application of FTIR Spectroscopy in Environmental Studies. In: *Advanced Aspects of Spectroscopy*; Farrukh, M. A. Eds.; InTech, 2012, pp. 49–84.

195.   Bart, J. C. J. *Plastics Additives: Advanced Industrial Analysis*; IOS Press: Amsterdam, Netherlands, 2006.

196.   Borrego, A. G.; Blanco, C. G.; Prado, J. G.; Díaz, C.; Guillén, M. D. ^{1}H NMR and FTIR Spectroscopic Studies of Bitumen and Shale Oil from Selected Spanish Oil Shales. *Energy Fuels* **1996**, *10*, 77–84.

197.   Jain, P. K.; Tyagi, O. S.; Singh, H. Physico-Chemical and Compositional aspects of Bitumen Bearing Crudes and Their Instrumental Characterization. *Petroleum Science and Technology* **1998**, *16*, 567–582.

198.   Nciri, N.; Song, S.; Kim, N.; Cho, N. Chemical Characterization of Gilsonite Bitumen. *J. Pet. Environ. Biotechnol.* **2014**, *5*.

199.   Woods, J. R.; Kung, D.; Kingston, D.; McCracken, T.; Koltlyar, L. S. Sparks, B. D.; Mercier, P. H. J.; Ng, S.; Moran, K. Comparison of Bitumens From Oil Sands with Different Recovery Profiles. *Petroleum Science and Technology* **2012**, *30*, 2285–2293.

200.   Nciri, N.; Song, S.; Kim, N.; Cho, N. Physicochemical Characterization of Asphalt Ridge Froth Bitumen and Petroleum Pitch. *International Journal of Chemical, Environmental & Biological Sciences (IJCEBS)* **2013**, *1*, 749–756.

201.   Siddiqui, M. N. Effect of Oxidation on the Chemistry of Asphalt and its Fractions. *Journal of King Saud University, Science* **2009**, *21*, 25–31.

202.   Timberlake, J. C. *Chemistry: An Introduction to General, Organic, & Biological Chemistry (11ᵗʰ Edition)*; Prentice Hall: LA, 2008.

203.   Nonhebel, D. C.; Walton, J. C. *Free Radical Chemistry: Structure and Mechanisms*; Cambridge University Press: London, 1974.

204.   Razumovskii, S. D.; Zaikov, G. E. *Ozone and Its Reactions with Organic Compounds*; Elsevier Science Ltd.: Amsterdam, **1984**.

205.   Razumovskii, S. D.; Zaikov, G. E. Kinetics and Mechanism of the Reaction of Ozone with Double Bonds. *Russ. Chem. Rev.* **1980**, *49*, 1163–1180.

APPENDIX A

APPENDIX A.1. Differential scanning calorimetry (DSC) of bitumen samples

Thermal analysis of Athabasca bitumen before and after 6 h ozonation at 140, 150 and 160 °C was conducted using differential scanning calorimeter as described in Chapter 3 (section 3.2.3.3). The total heat flow curves for Athabasca bitumen and ozonized bitumen samples after 6 h ozonation at 140, 150 and 160 °C were obtained by DSC and the analysis was triplicated for each sample. The obtained curves by DSC are presented in **Figure A.1**, **Figure A.2**, **Figure A.3** and **Figure A.4**.

Sensitivity of DSC is the ability of the DSC instrument to detect a weak transition from the background noise, and it depends on heating rate and sample weight. [1] In order to have an identical sensitivity in all the DSC measurements of the bitumen feed and ozonized bitumen products, the DSC test conditions were tried to be kept identical (sample weight and temperature method) in all the runs.

As it can be observed in the DSC curves, for the same sample there is a clear difference in the shape of the curves. These differences are thermal history dependent. Thermal history, including sample preparation technique, and thickness of the samples plays a direct role in the formation of the bitumen microstructure. [2][3]

The molecules of paraffinic and microcrystalline waxes which are two major types of waxes in bitumen will rearrange during storage and annealing at ambient temperature. Different conformations of the bitumen molecules will lead to energy changes. So different energy or heat flow peaks might be obtained by DSC for the same bitumen sample. [2][3][4][5][6][7][8]

Moreover, the bitumen sample has to be allowed to level out on the bottom of the crucible by placing the crucible horizontally for few minutes on a hot plate at temperatures around 100 °C before starting DSC analysis. After this, the sample should be annealed at ambient temperature for a minimum of 24 h. This is required to provide a proper contact between the bottom surface of the crucible and the bitumen sample. If the contact is not properly made between the bitumen sample and the aluminum crucible, the onset of the heat flow of the sample may give a signal in the DSC curve and create peaks that are not due to any thermal events to the bitumen sample but geometric changes. [3]

Consequently, very different images can be obtained depending on the preparation conditions and the aging or annealing time during storage. Also since bitumen shows aging due to oxidation and/or steric hardening, sample preparation procedure for DSC needs attention to avoid unrepeatability of the peaks. [3][9] So in general, different factors such as rearrangements of the bitumen molecules led to appearance of different heat flow peaks in the DSC curves of the same bitumen sample. Thus, the DSC curves for the bitumen feed and ozonized bitumen samples were difficult to interpret with certainty.

As it can be seen in **Figure A.1**, no noticeable thermal events can be observed in the DSC curves of Athabasca bitumen feed. The observed gradual step changes in **Figure A.2**, **Figure A.3** and **Figure A.4**, could suggest that some cracking and loss of material might have happened during ozonation. The measured onset temperature for these events has been reported in **Table A.1**.

As it can be observed in these figures, there are numerous random endothermic and exothermic thermal events in **Figure A.4** compared to **Figure A.2** and **Figure A.3** which could be an indication of more complexity of this product compared to the other ones. The normalized integrated peak area and onset temperature of the observed thermal events in all the aforementioned figures are mentioned in **Table A.1**.
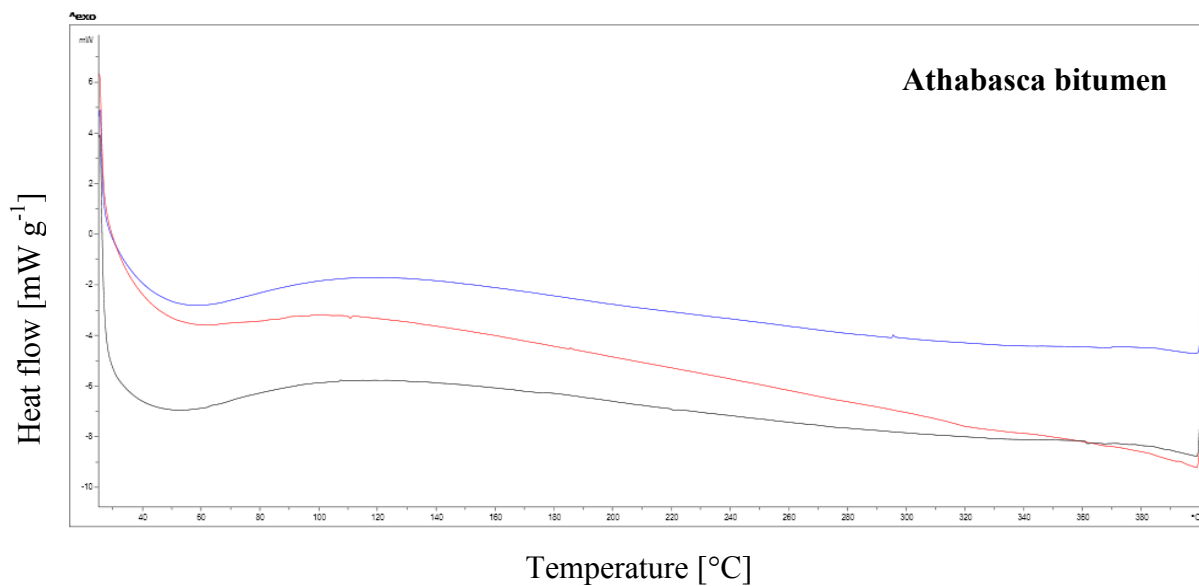
Figure A.1. Total heat flow curves obtained by DSC for original Athabasca bitumen
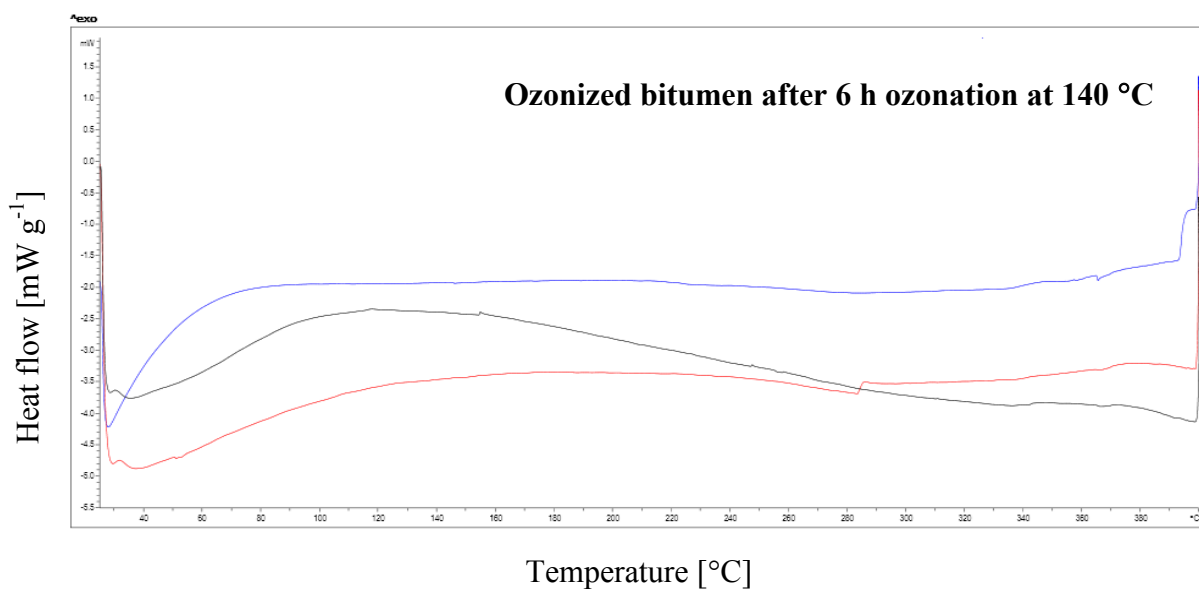
Figure A.2. Total heat flow curves obtained by DSC for ozonized bitumen after 6 h ozonation at 140 °C
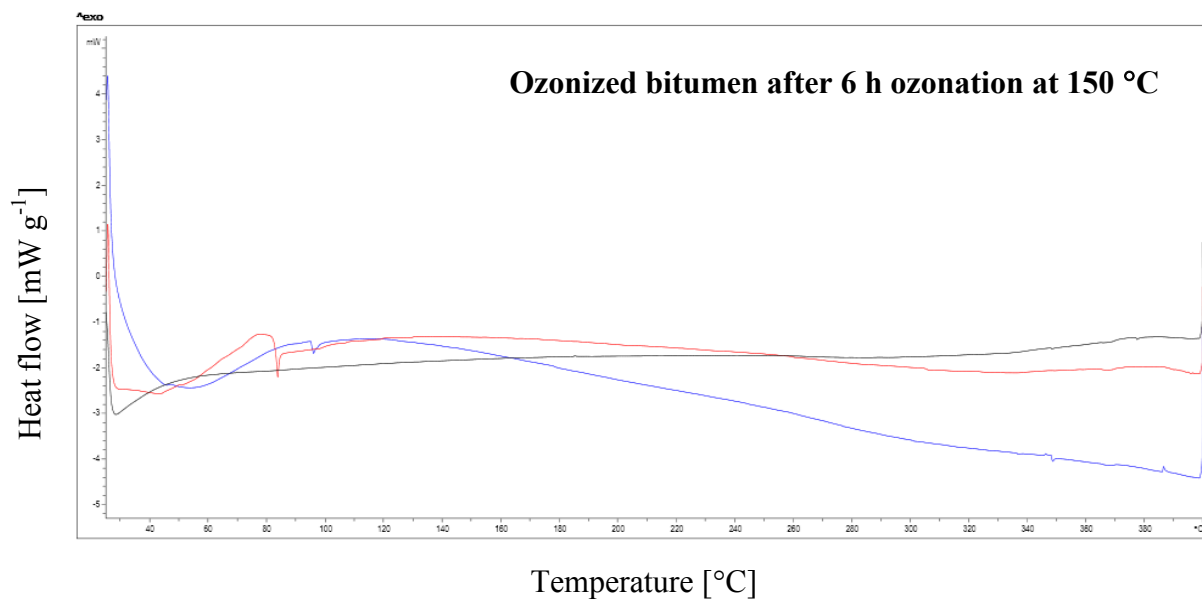
Figure A.3. Total heat flow curve obtained by DSC for ozonized bitumen after 6 h ozonation at 150 °C
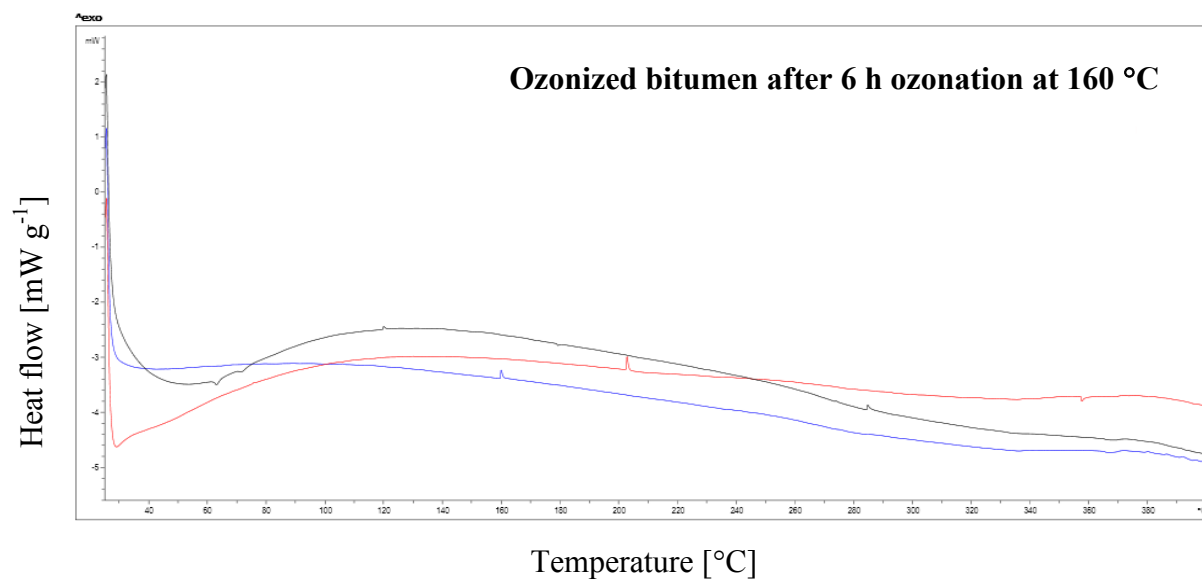
Figure A.4. Total heat flow curve obtained by DSC for ozonized bitumen after 6 h ozonation at 160 °C

Table A.1. Measured onset temperature and normalized integrated peak area obtained from DSC curves for ozonized Athabasca bitumen after 6 h ozonation at 140, 150 and 160 °C

Name	Colour of the curve in **Figure A.2** – **Figure A**.4	Type of Thermal Event	Onset Temperature [°C]	Normalized Integrated Peak Area [J g^{-1}]
Ozonized bitumen at 140 °C [**Figure A.2**]	Blue curve	Exothermic	28.64	-0.11
		Exothermic	154.25	-35.86e-03
		Exothermic	246.85	-13.94e-03
		Endothermic	254.76	+39.16e-03
		Step change	364.75	-
		Step change	369.24	-
	Red curve	Endothermic	29.64	-0.16
		Endothermic	50.85	+13.33e-03
		Step change	283.28	-
		Step change	285.27	-
		Step change	364.58	-
	Black curve	Endothermic	26.95	-
		Endothermic	357.57	+21.02e-03
		Endothermic	364.88	+0.12
Ozonized bitumen at 150 °C [**Figure A.3**]	Blue curve	Endothermic	27.35	-
		Step change	347.84	-
		Endothermic	376.92	+ 55.75e-03
	Red curve	Endothermic	43.63	+ 74.06e-03
		Endothermic	95.89	+ 0.42
		Endothermic	335.94	+ 17.62e-03
		Exothermic	345.44	- 24.33e-03
		Endothermic	347.93	+ 0.14
		Exothermic	385.73	- 75.68e-03
	Black curve	Endothermic	35.33	+ 0.72
		Exothermic	48.29	- 26.50e-03

		Endothermic	82.41	+ 1.99
		Step change	369.33	-
Ozonized bitumen at 160 °C [**Figure A.4**]	Blue curve	Endothermic	61.66	+ 0.14
		Endothermic	69.89	+ 0.11
		Exothermic	119.43	- 30.79e-03
		Endothermic	178.55	+ 16.41e-03
		Exothermic	273.03	- 10.09e-03
		Exothermic	284.13	- 74.94e-03
	Red curve	Exothermic	159.38	- 85.92e-03
	Black curve	Step change	28.14	-
		Exothermic	74.93	- 5.10e-03
		Endothermic	104.99	+ 6.89e-03
		Exothermic	202.03	- 94.35e-03
		Endothermic	356.91	+ 73.45e-03

APPENDIX A.2. References

1. Van-Ekeren, P. J.; Holl, C. M.; Witteveen A. J. A Comparative Test of Differential Scanning Calorimeters. *Journal of Thermal Analysis* **1997**, *49*, 1105–1114.

2. Das, P. K.; Kringos, N.; Wallqvist, V.; Birgisson, B. Micromechanical Investigation of Phase Separation in Bitumen by Combining AFM with DSC Results. *Road Mater Pavement Des* **2013**, *14*, 25–37.

3. Soenen, H.; Besamusca, J.; Fischer, H. R.; Poulikakos, L. D.; Planche, J. P.; Das, P. K.; Kringos, N.; Grenfell, J. R. A.; Lu, X.; Chailleux, E. Laboratory Investigation of Bitumen Based on Round Robin DSC and AFM Tests. *Materials and Structures* **2013**, *47*, 1205–1220.

4. Das, P. K.; Tasdemir, Y.; Birgisson, B. Evaluation of Fracture and Moisture Damage Performance of Wax Modified Asphalt Mixtures. *Road Materials and Pavement Design* **2012a**, *13*, 142–155.

5. Das, P. K.; Tasdemir, Y.; Birgisson, B. Low Temperature Cracking Performance of WMA With the Use of the Superpave Indirect Tensile Test. *Construction and Building Materials* **2012b**, *30*, 643–649.

6. Lu, X.; Langton, M.; Olofsson, P.; Redelius, P. Wax Morphology in Bitumen. *Journal of Materials Science* **2005**, *40*, 1893–1900.

7. Michon, L. C.; Netzel, D. A.; Turner, T. F.; Martin, D.; Planche, J. P. A ^{13}C NMR and DSC Study of the Amorphous and Crystalline Phases in Asphalts. *Energy Fuels* **1999**, *13*, 602–610.

8. Vargas-Nordcbeck, A.; Timm, D. H. Rutting Characterization of Warm Mix Asphalt and High RAP Mixtures. *Road Materials and Pavement Design* **2012**, *13*, 1–20.

9. Foreman, J.; Sauerbrunn, S. R.; Marcozzi, C. L. *Thermal Analysis and Rheology: Exploring the Sensitivity of Thermal Analysis Techniques to the Glass Transition*; TA Instruments Inc.: New Castle, D. E., 1995.

APPENDIX B

APPENDIX B.1. T-Test

For all the studied model compounds, the measured mean refractive index before and after ozonation is numerically different. As mentioned in Chapter 3 (section 3.3.4), in order to test the hypothesis that the parent model compounds and ozonized model compounds are associated with statistically different mean refractive indices, an independent samples' t-test at a 5% significance level was performed. The p-value was calculated for the refractive indices of the parent model compounds and ozonized model compounds. As it can be seen in **Table B.1**, the calculated p-value for the refractive indices of the model compounds measured at 20 and 60 °C is less than the significance level of 0.05 for all the studied compounds. It can be concluded that for all the compounds, the mean refractive index of the parent compound and the ozonized compound after 6 h ozonation at 130 °C is statistically different in all the cases at both measurement temperatures of 20 and 60 °C.

Table B.1. Calculated p-values for the refractive indices of the studied model compounds before and after 6 h ozonation at 130 °C

Name	P-value	
	At 20 °C	At 60 °C
Naphthalene	Not measured [a]	Not measured [a]
Ozonized naphthalene after 6 h ozonation at 130°C		
Tetralin	0.00	0.00
Ozonized tetralin after 6 h ozonation at 130°C		
Indane	0.00	0.00
Ozonized indane after 6 h ozonation at 130°C		
Indene	Not measured [a]	0.00
Ozonized indene after 6 h ozonation at 130°C		
Decalin	0.00	0.01
Ozonized decalin after 6 h ozonation at 130°C		
p-cymene	0.00	0.00
Ozonized p-cymene after 6 h ozonation at 130°C		
n-decane	0.00	0.00
Ozonized n-decane after 6 h ozonation at 130°C		
Thianaphthene	Not measured [a]	0.00
Ozonized thianaphthene after 6 h ozonation at 130°C		
Indoline	0.00	0.00
Ozonized indoline after 6 h ozonation at 130°C		
Indole	Not measured [a]	0.00
Ozonized indole after 6 h ozonation at 130°C		
Quinoline	0.00	0.00
Ozonized quinoline after 6 h ozonation at 130°C		
2,3-dihydrobenzofuran	0.00	0.00
Ozonized 2,3-dihydrobenzofuran after 6 h ozonation at 130°C		
2,3-benzofuran	0.00	0.00
Ozonized 2,3-benzofuran after 6 h ozonation at 130°C		

[a] P-value was not calculated because the refractive index was not measured.

The measured mean viscosity, penetration, refractive index, and the corresponding standard deviations for Athabasca bitumen feed, bitumen conditioned under nitrogen, ozonized bitumen, oxidized bitumen using oxygen and oxidized bitumen using air are presented in **Table B.2**. By comparison, the ozonized bitumen, oxidized bitumen using air and bitumen samples conditioned under nitrogen are associated with a numerically smaller viscosity and refractive index results and larger penetration results compared to the oxidized bitumen samples using oxygen at three different temperatures of 140, 150 and 160 °C. Once again an independent samples t-test at a 5% significance level was performed in order to test the hypothesis that the oxidized bitumen using pure oxygen, ozonized bitumen, oxidized bitumen using air and bitumen conditioned under nitrogen are associated with statistically different mean viscosity, penetrability and refractive indices.

Once the probability or p-value is calculated for all the samples, it is compared to the specified significance level of 0.05. The calculated p-values for viscosity, penetration and refractive indices of the samples are presented in **Table B.3**, **Table B.4** and **Table B.5** respectively. The calculated p-value for viscosity of the ozonized bitumen and oxidized bitumen using oxygen at 140 °C, and also oxidized bitumen using air at 150 °C and bitumen feed, and the calculated p-value for penetration of the ozonized bitumen and oxidized bitumen using oxygen at 140 and 150 °C, and also the bitumen conditioned under nitrogen at 140 and 150 °C and bitumen feed, and the calculated p-value for the refractive index of the bitumen conditioned under nitrogen at 140 and 160 °C and the bitumen feed is slightly more than 0.05. Therefore, for the aforementioned samples, there is no significant difference between the means ($p > 0.05$). However for all the other samples the p-value is less than 0.05. It can be concluded that the means of viscosity, penetration and refractive index are statistically different for all the other samples ($p < 0.05$).

Table B.2. The mean viscosity, penetration, refractive index and the corresponding standard deviations for Athabasca bitumen feed, bitumen conditioned under nitrogen, ozonized bitumen, oxidized bitumen using oxygen and oxidized bitumen using air

Name			Viscosity [Pa s]		Penetration [mm]		Refractive index [nD]	
			Mean	Standard deviation	Mean	Standard deviation	Mean	Standard deviation
Athabasca bitumen			2.67	0.01	2.70	0.10	1.5670	0.0000
Reaction temperature [°C]	140	Bitumen conditioned under nitrogen	2.63	0.02	2.50	0.10	1.5673	0.0002
		Ozonized bitumen	14.87	2.75	1.07	0.07	1.5711	0.0003
		Oxidized bitumen using oxygen	18.30	1.51	1.06	0.09	1.5721	0.0002
		Oxidized bitumen using air	5.66	0.70	1.96	0.05	1.5699	0.0004
	150	Bitumen conditioned under nitrogen	2.73	0.02	2.50	0.10	1.5676	0.0001
		Ozonized bitumen	16.51	1.98	1.00	0.13	1.5720	0.0003
		Oxidized bitumen using oxygen	29.51	5.87	0.96	0.09	1.5737	0.0004
		Oxidized bitumen using air	6.67	1.28	1.84	0.09	1.5708	0.0005
	160	Bitumen conditioned under nitrogen	2.76	0.01	2.43	0.12	1.5675	0.0003
		Ozonized bitumen	18.68	2.42	0.86	0.15	1.5732	0.0002
		Oxidized bitumen using oxygen	81.60	4.68	0.50	0.05	1.5765	0.0005
		Oxidized bitumen using air	8.03	0.77	1.47	0.05	1.5718	0.0003

Table B.3. Calculated p-values for viscosity of Athabasca bitumen, bitumen conditioned under nitrogen, ozonized bitumen, oxidized bitumen using oxygen and oxidized bitumen using air

P-value		Ozonized bitumen and oxidized bitumen using oxygen	Ozonized bitumen and oxidized bitumen using air	Oxidized bitumen using oxygen and oxidized bitumen using air	Ozonized bitumen and bitumen under nitrogen	Oxidized bitumen using oxygen and bitumen under nitrogen	Oxidized bitumen using air and bitumen under nitrogen	Ozonized bitumen and bitumen feed	Oxidized bitumen using oxygen and bitumen feed	Oxidized bitumen using air and bitumen feed	Bitumen under nitrogen and bitumen feed
Reaction temperature [°C]	140	0.15	0.02	0.00	0.02	0.00	0.02	0.02	0.00	0.02	0.00
	150	0.05	0.00	0.02	0.01	0.02	0.03	0.01	0.02	0.19	0.00
	160	0.00	0.01	0.00	0.01	0.00	0.01	0.00	0.00	0.01	0.00

Table B.4. Calculated p-values for penetration of Athabasca bitumen, bitumen conditioned under nitrogen, ozonized bitumen, oxidized bitumen using oxygen and oxidized bitumen using air

P-value		Ozonized bitumen and oxidized bitumen using oxygen	Ozonized bitumen and oxidized bitumen using air	Oxidized bitumen using oxygen and oxidized bitumen using air	Ozonized bitumen and bitumen under nitrogen	Oxidized bitumen using oxygen and bitumen under nitrogen	Oxidized bitumen using air and bitumen under nitrogen	Ozonized bitumen and bitumen feed	Oxidized bitumen using oxygen and bitumen feed	Oxidized bitumen using air and bitumen feed	Bitumen under nitrogen and bitumen feed
Reaction temperature [°C]	140	0.77	0.00	0.00	0.00	0.00	0.01	0.00	0.00	0.00	0.07
	150	0.42	0.00	0.00	0.00	0.00	0.00	0.00	0.00	0.00	0.07
	160	0.00	0.00	0.00	0.00	0.00	0.00	0.00	0.00	0.00	0.04

Table B.5. Calculated p-values for refractive indices of Athabasca bitumen, bitumen conditioned under nitrogen, ozonized bitumen, oxidized bitumen using oxygen and oxidized bitumen using air

P-value		Ozonized bitumen and oxidized bitumen using oxygen	Ozonized bitumen and oxidized bitumen using air	Oxidized bitumen using oxygen and oxidized bitumen using air	Ozonized bitumen and bitumen under nitrogen	Oxidized bitumen using oxygen and bitumen under nitrogen	Oxidized bitumen using air and bitumen under nitrogen	Ozonized bitumen and bitumen feed	Oxidized bitumen using oxygen and bitumen feed	Oxidized bitumen using air and bitumen feed	Bitumen under nitrogen and bitumen feed
Reaction temperature [°C]	140	0.00	0.00	0.00	0.00	0.00	0.00	0.00	0.00	0.00	0.10
	150	0.00	0.00	0.00	0.00	0.00	0.00	0.00	0.00	0.00	0.01
	160	0.00	0.00	0.00	0.00	0.00	0.00	0.00	0.00	0.00	0.09